Semi-preparative expression and purification of a recombinant glucocerebrosidase protein with a PTD4 transduction domain: a potential therapeutic strategy for neuronopathic Gaucher's disease.

by

Alexandria Taylor Jack
B.Sc., University of Victoria, 2009

A Thesis Submitted in Partial Fulfillment
of the Requirements for the Degree of

MASTERS OF SCIENCE

in the Department of Biology

Supervisory Committee

Semi-preparative expression and purification of a recombinant glucocerebrosidase protein with a PTD4 transduction domain: a potential therapeutic strategy for neurnopathic Gaucher's disease.

by

Alexandria Taylor Jack
B.Sc., University of Victoria, 2009

Supervisory Committee

Dr. Francis Choy, (Department of Biology)
Supervisor

Dr. Juergen Ehlting, (Department of Biology)
Departmental Member

Dr. Patrick Walter, (Department of Biology)
Departmental Member

Abstract

Supervisory Committee

Dr. Francis Choy, (Department of Biology)
Supervisor

Dr. Jeurgen Ehlting, (Department of Biology)
Departmental Member

Dr. Patrick Walter, (Department of Biology)
Departmental Member

Gaucher's disease (GD) is an autosomal recessive lysosomal storage disorder which is caused by a mutation in the gene encoding acid β-glucocerebrosidase (GBA, EC 3.2.1.45). Deficient activity in GBA leads to a wide variety of clinical phenotypes, including visceral symptoms such as hepatospenomegaly as well as neurological symptoms. Current enzyme replacement therapy is effective in treating visceral symptoms but cannot cross the blood-brain barrier to target neurological manifestations. Another drawback to current therapy is the high cost to patients due to present protein expression strategies. Recently, protein transduction domains, such as the synthetic PTD4 domain, have been proposed as a therapeutic strategy for drug delivery to the central nervous system. In the present study, we use an economical yeast expression system, *Pichia pastoris*, to produce a recombinant fusion protein GBA-PTD4, and semi-preparative hydrophobic interaction chromatography and gel filtration chromatography for purification. Results show that final preparations are near homogenous, with GBA-PTD4 accounting for approximately 76% of total protein and only one major contaminant. A cell line expressing GBA without a transduction domain was also created in anticipation of further cellular uptake studies. Future research will focus on large scale enzyme expression in fermentation systems and more direct purification methods such as immunoaffinity chromatography for better protein recovery.

Table of Contents

List of Tables

List of Figures

Abbreviations

4-MuGP	4- methyl-umbelliferyl-β-D-glycopyranoside
Afu	arbitrary fluorescence units
AOX	alcohol oxidase gene (*P. pastoris*)
AOX	alcohol oxidase protein (*P. pastoris*)
BBB	blood-brain barrier
β-Gal	β- galactosidase
BMGY	buffered glycerol-complex medium
BMMY	buffered methanol-complex medium
bp	base pair
BSA	bovine serum albumin
CHO	Chinese hamster ovary
CNS	central nervous system
CV	column volume
dH_2O	distilled water
DNA	deoxyribonucleic acid
dNTP	deoxy nucleotide triphosphate
DTT	dithiothreitol
EtBr	ethidium bromide
ERT	enzyme replacement therapy
GBA	acid β- glucocerebrosidase gene
GBA	acid β- glucocerebrosidase protein
GD	Gaucher's disease
GFC	gel filtration chromatography
GH-A	glycoside hydrolase A
HIC	hydrophobic interaction chromatography
HIS4	histidine dehydrogenase gene (*P. pastoris*)
HIV TAT	human immunodeficiency virus transactivator of transcription
HK	hexokinase
IAC	immunoaffinity chromatography
IPTG	isopropyl-β-D-thiogalactopyranoside
kb	kilobase
kDa	kiloDalton
LB	Luria-Bertani
mAb	monoclonal antibody
MD	minimal dextrose
MM	minimal methanol
mRNA	messenger RNA
Mut^+	methanol utilization plus

Mut^S	methanol utilization slow
OD	optical density
PBST	phosphate-buffered saline
PEG	polyethylene glycol
PCR	polymerase chain reaction
PTD	protein transduction domain
PVDF	polyvinylidene fluoride
REN	restriction endonuclease
SDS-PAGE	sodium dodecyl sulphate polyacrylimide gel electrophoresis
SRT	substrate reduction therapy
U	units
UV	ultraviolet
YPD	yeast extract peptone dextrose medium
X-gal	bromo-chloro-indolyl-galactopyranoside

Acknowledgments

First and foremost, I would like to thank my supervisor, Dr. Francis Choy, for sparking my interest in genetics early on in his Biology 230 class, then later during my final undergraduate year when I worked as a directed studies student before beginning my graduate program. His continued support and encouragement have helped me to improve my critical thinking skills and gain confidence in the scientific field. Also, thank you to my committee members Dr. Patrick Walter and Dr. Jürgen Ehlting for your helpful insights and suggestions during committee meetings, especially in the final months of my program. I would also like to thank our collaborators in Dr. Terry Pearson's lab for providing the monoclonal antibody analysis and their expertise in the area, as well as those at the Pacific Forestry Centre for providing us with access to their fermentation system.

I had a great deal of help and support developing the laboratory skills involved in this research. Thanks first of all to my predecessor, April Goebl, for spending so much time introducing me to the basic procedures and creating the yeast cell line construct that served as the basis for my work. To all the Choy lab members past and present, including Lin Sun, Geoff Morris, Rebecca Jantzen, Sarah Truelson, Michael McLean, Valerie Taylor and Laura Sutherland, thank you for all the troubleshooting help, support, and friendship that has made this experience truly a pleasure. In addition, I would like to thank Dr. Graeme Roche for his troubleshooting help. Thank you also to the undergraduate students who have helped with this project, Vincent Li, Leo Smyth, Sam Abhar and Glynis Byrne.

Lastly, thank you to my family and friends, who have proved to me that good company and conversation is the ultimate stress reliever and is essential while completing graduate studies. Also, thank you to Tyler Stene for his enthusiasm and welcome distractions. In addition, I would like to thank everyone who reads and learns from this thesis; my ultimate hope is that my work will have a lasting effect on future researchers in the field.

Chapter 1 Introduction

1.1 Gaucher's disease

1.1.1 Gaucher's disease classification and overview of clinical symptoms

Gaucher's disease (GD) is the most common lysosomal storage disorder, with a frequency of 1 in 100,000 in the general population, and a higher frequency of 1 in 855 individuals in populations of Ashkenazi Jewish descent (Guggenbuhl, *et al*. 2008). GD is an autosomal recessive disorder which is often the consequence of a single mutation in the gene encoding the metabolic housekeeping enzyme glucocerebrosidase (GBA), which catalyzes the hydrolysis of the lipid glucocerebroside. The accumulation of lipid substrate resulting from the metabolic defect causes a highly heterogeneous patient population (Jmoudiak and Futerman 2005).

Although the clinical progression of GD can vary widely and symptoms are considered to be a spectrum due to genetics and other contributing factors, patients are generally classified into three different subtypes based on their neurological involvement (Elstein *et al*. 2001). Type I, or non-neuronopathic GD, is the more common and less severe of the three because of the patients' lack of CNS symptoms. The peripheral symptoms for patients with Type I GD are highly heterogeneous, but commonly seen symptoms include hepatosplenomegaly, thrombocytopenia, anaemia, and various manifestations of skeletal disease. Severity of symptoms can vary from mild, where little to no treatment is needed, to more severe, where lifelong treatment is necessary. With current treatments for Type I GD, patients can generally live a healthy, normal lifestyle.

Type II and Type III GD, or acute neuronopathic and sub-acute neuronopathic respectively, are the more severe forms of the disease as they involve manifestations of the CNS. Type II is generally considered the infantile form, with symptoms showing before the age of 2 with aggressive progression; this generally leads to fatality within 2 years of disease onset (Pastores 2010). Type III, the juvenile form, can still present itself within the first 2 years of life, but is characterized by a slower disease progression and a greater heterogeneity in the symptoms. Limited psychomotor development can ensue with these conditions, as well as other neurological complications such as seizures, oculomotor apraxia, spasticity and dysphagia (Pastores 2010; Elstein *et al*. 2001). Unlike Type I GD, there are currently no clinical treatments for patients suffering with the debilitating CNS complications of types II and III GD.

1.1.2 Gaucher's disease at the DNA level

Gaucher's disease is caused by a mutation in the gene encoding for the enzyme GBA which affects its activity. These mutations can range in severity, from slight inhibition of GBA function to a completely dysfunctional enzyme. Heterozygous carriers of GD often show no symptoms, and homozygous patients display a wide variety of clinical complications (Zuckerman *et al*. 2007).

The functional *GBA* gene locus is located on chromosome 1, band q21, and it's 11 exons and 10 introns that span 7.6 kB in length (Hruska *et al*. 2008; Beutler and Gelbart 1996). There is a pseudogene located 16kB downstream which has a 96% sequence homology with its functional counterpart, despite being 1.9 kB shorter because of several

Alu repeats in the intronic sequence in the latter. The pseudogene is believed to be the result of a duplication of this region of chromosome 1, a theory strengthened by the fact that the downstream gene for metaxin also has a pseudogene 16 kB downstream (Hruska *et al*. 2008). The high sequence identity between *GBA* and the non-functional pseudogene encourages the possibility of recombination events between these two loci.

Hruska, *et al*. (2008) report over 250 mutations in *GBA* that have been found to date; these include a variety of missense mutations, nonsense mutations, mutations in splice sites, and recombination events with the pseudogene. Some mutations are more common than others, for example, there are 4 mutations that account for over 90% of the GD occurrences in the Ashkenazi Jewish population and 70% in the non- Jewish, Caucasian population (Mao *et al*. 2001). These mutations are N370S, L444P, 84GG and IVS2 + 1 G>A (two missense mutations, an insertion and a splice site mutation, respectively) (He and Grabowski 1992; Hruska *et al*. 2008). The N370S and L444P point mutations were the first mutations for GD described (Tsuji *et al*. 1988) and are still considered to be the most prevalent mutations among patients (Hruska *et al*. 2008), making them the first target for mutation screening. One interesting point is that the L444P mutation is present in the wild type pseudogene, and its occurrence in the functional gene could possibly be due to a recombination event as well as a point mutation (Hruska *et al*. 2008).

Although all of these mutations have the ultimate effect of reduced GBA enzyme activity, they operate by different mechanisms. Ohashi *et al*. (1991) investigated this by artificially creating and expressing cDNA for six mutant GBA enzymes, including the mutant genes for the N370S and L444P variants. They found that while the L444P GBA

tended to be an unstable protein, the N370S GBA was expressed normally; however, the N370S mutant did not interact as efficiently with its activator protein, saposin C. These different mechanisms are what lead to the variability in GBA function with different mutations, and consequently different outcomes for disease progression. There have been some inferences made about mutations being associated with certain phenotypes; for example, N370S is generally associated with the less severe forms of GD while the L444P mutation in homozygous form is commonly thought to have a more severe phenotypic outcome (Hruska *et al*. 2008; Jmoudiak and Futerman 2005). However, these are generalizations, especially in cases of compounding heterozygosity. As a result, while mutation analysis of GD patients can be a useful tool to predict the clinical course of the disease, it is most certainly enhanced when used in combination with other predictive methods such as biochemical analysis and monitoring of symptom progression.

1.1.3 Gaucher's disease at a biochemical level

Glucocerebrosidase is a β-acid hydrolase enzyme; it has a total of 498 amino acid residues and upon proper glycosylation is 63-67 kDa in size (Durand *et al*. 1997; Berg-Fussman *et al*. 1993). After expression and glycosylation in the ER, GBA is packaged in the Golgi and targeted to the lysosome, though its targeting mechanism remains largely unknown (Futerman and Van Meer 2004; Jmoudiak and Futerman 2005). The acidic conditions in the lysosome create an optimal pH for GBA activity.

GBA belongs to the glycoside hydrolase A (GH-A) clan of proteins, a group suggested to be derived from a common ancestor, which share a general homology within

the active site (Durand *et al*. 1997; Dvir *et al*. 2003). GH-A enzymes all adopt a $(\alpha/\beta)_8$ TIM barrel in their active domain, which lines up the nucleophile and proton donor, both glutamic acid residues, on the C-terminal ends of two of the β strands (Durand *et al*. 1997; Dvir *et al*. 2003). The X-ray crystal structure of GBA was first elucidated by Dvir *et al*. (2003), and its catalytic domain (Domain III), was shown to have these properties. In the active site, Glu 340 acts as a nucleophile, while adjacent Glu 258 acts as a proton donor (Phenix *et al*. 2010). Its other two domains, I and II, although not involved in catalytic activity, have been implicated as important factors in the binding of both substrate and activator peptide saposin C (Atrian *et al*. 2008). See Supplementary Figure 1for a depiction of the GBA structure.

Although this housekeeping enzyme is expressed across all human cell types, Doll and Smith (1993) experimented with an artificial GBA substrate to suggest that GBA expression can be differentially regulated, with differences in expression over 50 fold between various cell lines. For example, their results show that fibroblasts and brain derived cell lines had extremely high GBA activity whereas cell lines such as epithelial or monocytes had moderate activity and lymphoblasts had very low activity comparatively. This study confirmed previous theories about mRNA level expression regulation, but also suggests that GBA expression can be controlled at the level of protein synthesis as well. Knowledge of regulation of GBA expression could have value when investigating new therapeutic strategies.

Glucosylceramide is the natural lipid substrate for GBA; it consists of a two-tailed ceramide molecule attached to glucose via a β-glycosidic linkage by the enzyme glucosylceramide synthase (Koltun *et al*. 2011). It is found in abundance within animal

cell membranes, and GBA is required within lysosomes during membrane digestion and turn over (Cox 2001). This process is important because not only does it provide building blocks for other biosynthetic pathways (for example, ceramide can be further broken down into single fatty-acyl chains), but also ceramide itself has been implicated as a crucial regulator molecule in cellular processes such as cell cycle arrest and stress responses (Kitatani *et al*. 2008). Recycling of ceramide for use in signalling pathways has been termed the "salvage pathway".

Mutations which cause decreased function of GBA lead to the build up of glucosylceramide within the lysosomes of cells, especially those belonging to the mononuclear phagocyte system (Cox 2001). Enlarged cells that are engorged with lipids take on a characteristic wrinkled appearance. Termed "Gaucher cells", they are considered the hallmark of Gaucher disease.

1.1.4 Pathophysiology of Gaucher's disease

The effectiveness of current GD treatments involving substrate reduction and enzyme replacement in ameliorating symptoms serve as evidence towards the build up of glucosylceramide being responsible for the clinical manifestations of this disease. The mass of lipid accumulated in Gaucher patients accounts for less than 2% of the total gain in tissue weight in the visceral organs (Cox 2001), which leads to the understanding that there is some underlying mechanisms of pathogenesis in GD that remain unclear. There are, however, some proposed theories.

One theory that has been extensively investigated is the suggestion that the altered state of macrophages, the main cell type affected by GD, may be a factor in the progression of physiological symptoms (Jmoudiak and Futerman 2005). Macrophages are not only responsible for phagocytising cellular debris and invasive pathogens, the mononuclear phagocyte system plays a fundamental role in the elicitation of immune responses through a complex secretome (Alberts *et al*. 2002; Cox 2001). Although Gaucher cells have historically been considered functionally inert due to the excessive amount of lipid they contain (Boven *et al*. 2004), it stands to reason that inappropriate activation could lead to downstream effects that cause clinical symptoms associated with GD. For example, in some studies Gaucher patients have shown to have increased serum concentrations of cytokines such as IL-6 and IL-10, which act to aid in inflammatory responses. This alteration in inflammatory responses may contribute to some of the widespread skeletal manifestations seen within the patient population (Jmoudiak and Futerman 2005). In addition, increased serum levels of pro-inflammatory cytokines TNFα and IL-1β have also been detected among patient groups, although conflicting data inhibits any conclusion at this point. Current investigations into this matter involve analyzing changes in global gene expression in Gaucher mouse models (You-Hai Xu *et al*. 2011), and may lead to understanding some important implications in differential disease progression in the future.

Like that of visceral symptoms, neurological disease progression in Type II and III GD is yet to be fully understood. Upon autopsy of brain tissue from type II and III GD patients, Kaye *et al*. (1986) observed the presence of Gaucher cells within CNS tissue, and Cabrera-Salazar *et al*. (2010) speculate that accumulation of lipid substrate leads to

neuronal degradation, although this mechanism remains unclear. Pelled *et al*. (2005) conducted investigations which lead them to discover correlations between glucocerebroside accumulation and agonist-induced release of calcium via ryanodine receptors in human brain tissue; they postulated that changes in calcium homeostasis may be a factor in the connection between Gaucher cells and neuronal cell death. Increased understanding of these underlying mechanisms could assist in the development of novel treatment strategies. Current work in our lab focuses on reprogramming of human fibroblasts back to pluripotent stem cell status, to eventually be alternatively differentiated into neuronal cells. The aim of this research is to be able to reprogram fibroblasts obtained from GD patients and differentiate them into neurons, for an *in vitro* model of GD which would answer more questions about neuronal disease progression.

1.1.5 Current treatments

Enzyme replacement therapy

Investigation into enzyme replacement therapies (ERTs) for sphingolipid storage disorders began in the 1970's, when HexA, the enzyme deficient in Tay Sachs disease, was isolated from human urine and intravenously administered to an infant (Johnson *et al*. 1973). This treatment was unsuccessful over the long term, but started a new avenue of research for lysosomal storage diseases. Eventually, it was discovered that proteins for testing enzyme replacement therapies could be isolated from human placenta, and among the enzymes collected was GBA to treat GD (Brady 2003). Shortly after trials began with ERT for GD, it was determined that the enzyme could be targeted to macrophages by the removal of terminal oligosaccharides from complex oligosaccharide chains to expose

mannose-6-phosphate sugars, which can then bind to mannose-6-phosphate receptors present on the external membrane of macrophages to induce endocytosis (Brady 2003; Sato and Beutler 1993). GBA purified from human placenta extracted and further modified to expose mannose residues was marketed by Genezyme Corp. as Ceredase™ in 1991 and became a widely used treatment for GD. The extraction of enzymes from human tissues is not without its limitations (Grabowski *et al*. 1995). First of all, there is the limit of how much placenta tissues is available for enzyme extraction, and secondly, there is the risk of transmission of infectious diseases. To that end, a new form of ERT was developed, using recombinant GBA expressed in a mammalian Chinese hamster ovary system. Cerezyme™ (Genezyme Corp.) was approved for treatment use in 1994, and continues to be a popular choice in treatment for this disease (Brady 2003; Hollak *et al*. 2010). Comparisons of effectiveness between Ceredase™ and Cerezyme™ conducted by Grabowski *et al*. (1995) concluded that there is no significant difference in symptom amelioration between natural and recombinant GBA enzymes, and these studies led to the discontinued use of the natural enzyme therapy (Wraith 2006). Effectiveness and safety of the treatment was further reinforced by the Gaucher registry in the early 2000's (Weinreb *et al*. 2002) with a large patient base being studied over 2-5 years of treatment.

Although it is widely in use today, there are some drawbacks to enzyme replacement therapy in GD. First, there is the cost of treatment; since ERT is not a cure but a lifelong treatment, patients generally require intravenous infusions of Cerezyme™ every two weeks (Hollak *et al*. 2010), and Beutler (2006) reports that for the average GD patient receiving ERT the cost will be $200, 000 USD annually. This is attributable to the high cost of maintaining the mammalian expression system with expected quality control

standards, and the relatively low patient base over which to spread the production costs. The high expense of ERT for GD patients can cause an extreme effect on the health care economy (Beutler 2006).

Another drawback to ERT comes from the enzyme's inability to cross that blood brain barrier, which results in ineffective alleviation of the neurological symptoms associated with Types II and III (Schueler *et al*. 2002). Pardridge (2006) reports that over 98% of large macromolecular drugs, including recombinant proteins, are not able to treat neurological symptoms due to their inability to penetrate the endothelium of brain capillaries. This represents a major hurdle in drug development for GD and other lysosomal storage disorders which cause impaired neurological functioning.

Substrate reduction therapy and other potential therapeutic options

There is a second form of treatment on the market today for GD patients; miglustat (marketed as Zavesca® by Acetelion Pharmaceuticals since 2002) is a form of substrate reduction therapy (SRT) (Pastores and Barnett 2003). Originally developed as an anti-viral therapy, it was found that even though its anti-viral capacity was not impressive, this synthetic N-alkylated iminosugar could inhibit the enzyme glucosylcerebroside sythase (Moyses 2003). This is the enzyme that catalyzes the addition of a glucose head group to ceramide, the product being the substrate for GBA. This provides an alternative treatment for patients who are unsuitable or unable to receive ERT treatment. There are some side effects to SRT, namely the gastrointestinal effects associated with sugar accumulation in the intestinal lumen and the resulting osmotic imbalance (Moyses 2003). Since SRT has not proven to be as efficient as ERT in improving clinical symptoms, and also is only able to slow production of

glycosylceramide but has no effect on existing build-up of lipid, this therapy is often prescribed in concert with ERT (Aerts *et al*. 2006).

Investigations into alternative therapies for GD are continuing; two potential therapeutic strategies that have been proposed are small molecule chaperones and gene therapy. Small molecule chaperones have been shown to assist with proper folding of enzymes in the endoplasmic reticulum, therefore increasing activity (Zheng *et al*. 2007). Molecular chaperones are generally competitive inhibitors of GBA that can bind in the active site. Also under investigation is gene therapy, where the gene for GBA is delivered to the patient via a viral vector (Rahim *et al*. 2011). Gene therapy is of special interest for alleviating the neuronal symptoms that cannot be treated with ERT and SRT. The use of protein transduction domains, such as the native HIV-TAT transduction domain and PTD4, a synthetic transduction domain, is another avenue of therapy which is currently under investigation. These may be able to transport therapeutic enzymes across the blood brain barrier. This investigation is focussed on exploring a recombinant PTD4 fusion protein as a therapeutic strategy for Types II and III GD.

1.2 *Pichia pastoris* as a potential expression system

The mammalian Chinese hamster ovary (CHO) expression system is currently utilized to produce therapeutic recombinant GBA (Hollak *et al*. 2010). The CHO expression system has been used in past years to produce a number of useful therapeutic proteins because of several advantages that this technique offers, such as extensive characterization, inherent mammalian post-translational modifications, and

industrialization (Durocher and Butler 2009; Sethuraman and Stadheim 2006). In the case of GBA, CHO expression systems are indeed effective for mass production of an enzyme with as much therapeutic potential as that from natural sources. Unfortunately, this system is highly laborious and costly, as well as being difficult to manipulate with regards to glycosylation of recombinant proteins produced (Sethuraman and Stadheim 2006). To this end, therapy for GD could benefit from an alternative expression system which produces an enzyme with comparative efficiency to that produced with CHO, without the disadvantages in production.

The methylotropic yeast *Pichia pastoris* has the potential to be an alternative expression system for GBA. Initially developed in the 1970's as a method of using methanol as a source of protein for animal feed (Macauley-Patrick *et al*. 2005), it has since been recognized as an effective, inducible expression system, and has been used for the expression of many recombinant proteins, such as β-galactosidase, human epidermal growth factor and human insulin-like growth factor (Cregg, Vedvick, and Raschke 1993). There are several advantages that make *P. pastoris* a particularly desirable organism for recombinant protein expression. For example, it is easily manipulated at a genetic level, making cloning as simple as in widely used prokaryote systems (Cereghino *et al*. 2002; Daly and Hearn 2005). Another advantage is that it has a fast growth rate and can be scaled up from shake flask cultures to fermentation systems, making it suitable for large scale production of recombinant proteins (Cereghino *et al*. 2002). Also, it's ability to make post-translational modifications appropriate for human proteins make it possible for manufacturing therapeutic recombinant enzymes, whereas this fails in prokaryotic systems such as *E. coli* which do not have the ability to make N-linked glycosylations.

A key factor in making recombinant proteins with *P. pastoris* is that there is the potential for strong inducible promoters due to the fact that the genes required for methanol metabolism are only engaged when methanol is present as a carbon source (Macauley-Patrick *et al*. 2005). The most frequently used of all promoters in this genome is that of the alcohol oxidase (AOX) gene. The enzyme alcohol oxidase is responsible for the first step in the methanol metabolic pathway, oxidizing methanol to formaldehyde and hydrogen peroxide (Cereghino and Cregg 2000). While the transcription of this enzyme is essentially non-existent in the presence of alternative carbon sources (glucose, glycerol, or ethanol), when grown with limiting amounts of methanol, AOX contributes to 30% or more of the total protein within the cell (Cereghino and Cregg 2000; Higgins and Cregg 1998).

There are two genes for alcohol oxidase in the *P. pastoris* genome, *AOX I*, which is more actively transcribed, and *AOX II* which yields approximately 10-20 times less alcohol oxidase activity (Macauley-Patrick *et al*. 2005). This brings about multiple scenarios when inserting recombinant DNA behind the *AOX I* promoter. If *AOX I* is not disrupted by gene insertion, the yeast strain will show wild type growth on methanol, denoted the Mut^+ phenotype; however, if *AOX I* is disrupted during genetic cloning, the yeast will have to rely on the weaker *AOX II*, significantly slowing down the metabolism of methanol (Mut^S phenotype) (J. L. Cereghino and Cregg 2000; Cregg *et al*. 1989). Either phenotype can be useful for expression, depending on the recombinant protein in question.

When expressing human recombinant glycoproteins, a eukaryotic expression system is crucial in most cases, because prokaryotic systems do not have the ability to

perform N-linked glycosylation (Daly and Hearn 2005). Glycosylation patterns are not only important for proper protein folding, and consequentially protein functionality, but also for protein clearance *in vivo* (Hamilton and Gerngross 2007); therefore choosing the right organism for expression of therapeutic enzymes in critical. This is why mammalian expression systems such as CHO are a useful tool, because the wild type glycosylation patterns are similar to that in humans. Glycosylation patterns in mammalian expression systems, however, are not always congruent with what is needed for the particular enzyme that is being produced. As mentioned, recombinant GBA currently used for therapy of GD is further altered after expression in CHO to expose mannose residues for targeting to macrophages (Brady 2003). This is done by enzymatic removal of the terminal sialic acids that are the result of mammalian glycosylation, without removing these residues GBA would be cleared by the hepatocytes of the patient instead of being targeted to the cells of interest. This second step in processing is required because the CHO system is difficult to manipulate with regard to glycosylation patterns (Sethuraman and Stadheim 2006).

Initial attempts to produce functional GBA from *P. pastoris* in our lab yielded disappointing results, with recombinant GBA being difficult to characterize due to a limited functionality and stability of the enzyme (Sinclair 2001). It was later realized that this was the result of post-translational modification patterns inherent in yeast which are not conducive to proper functioning of human GBA. Initial N- linked glycosylation occurring in the ER is the same for yeast and mammals, in the golgi, however, yeast tend to hypermannosylate their N-linked glycans whereas in mammals complex glycans are formed by trimming mannose residues and the addition of galactose and sialic acid

(Hamilton and Gerngross 2007). Vervecken *et al*. (2004) devised a way to produce a *P. pastoris* strain with humanized N-glycosylation patterns using the simple knock-in cloning strategy that is used for the addition of genes for production purposes. In this strain, the gene for Och1p, the α-1,6-mannosyltransferase responsible for initiating hypermannosylation in yeast is disrupted, and the introduction of the gene for ER-retained α-1,2-mannosidase and two other chimeric glycosyltransferases conferred the addition of complex glycans mimicking that of mammalian proteins (although non-sialylated). This humanized strain of yeast has been used in our lab for the production of a functional GBA fusion protein (Goebl 2010).

1.3 Treatment of GD neurological symptoms

1.3.1 The blood brain barrier

The blood brain barrier (BBB) is the dynamic partition between the CNS tissue and the microvasculature that is important for the physiological maintenance of the neurological tissue. In their review of the BBB, Cardoso *et al*. (2010) suggest four distinct functions: maintenance of homeostasis in the CNS, protection from the peripheral environment, constant nutrients supply using specific transport systems, and finally a localized immune response. In other words, the BBB provides a shield for the CNS to protect it from outside molecules which are potentially toxic to neurological tissue, while being selectively permeable to essential nutrients. While these mechanisms are important for mammalian CNS function, they create a barrier for drug delivery to the neurological tissues as well; an increased understanding of the anatomy and biochemistry of the BBB

will further investigations into how to overcome it to establish therapeutic strategies to alleviate neurological symptoms in diseases such as GD.

The BBB neurovascular unit is composed of multiple components: endothelial cells, the endothelial basement membrane, glial cells and pericytes (Cardoso *et al*. 2010; Ballabh *et al*. 2004). Each of them has a role to play in the maintenance of BBB function. The endothelial cells of the CNS are of great importance to the function of the BBB, and differ from those found in other organs; their lack of fenestrations and limited pinocytosis prevent the transcellular passage of large polar molecules (Ballabh, *et al*. 2004). Another crucial part of the BBB anatomy is the intercellular tight junctions. Tight junctions make up the major barrier to paracellular pathways; those present within the neurovascular unit have less pore-like discontinuities than those found in the periphery, lending to their role as blockades for the BBB (Dallasta *et al*. 1999). Tight junctions are made up of integral proteins: claudins, which form the primary seal between the cells, and occludins, which serve to regulate the permeability of the tight junctions (Ballabh, *et al*. 2004). Tight junctions are not stationary structures, but can undergo rapid assembly and disassembly to regulate paracellular pathways. Changes in permeability have been shown with both physiological and pathological signals (Cardoso *et al*. 2010; Chen and Liu 2011).

Strong intercellular junctions and limited pinocytosis in cells themselves raises the question of how the brain receives any of the important molecules needed for proper functioning. Very small hydrophilic molecules (<500 Da) can diffuse through the intercellular tight junctions, but this mode of crossing the BBB is quite limited (Chen and Liu 2011). In contrast, lipid soluble molecules such as O_2, CO_2, alcohol and steroid hormones can simply diffuse through the membranes of endothelial cells to cross the

BBB (Chen and Liu 2011; Ballabh *et al*. 2004). Any other molecules have to rely on specific transporters which create the selectively permeable nature of the brain. For example, glucose and amino acids utilize protein carriers that are stereo-specific and in some cases use ion-concentration gradients for transport (Mann, *et al*. 2003; ElAli and Hermann 2011). Other large, water-soluble proteins, such as insulin and transferrin, utilize receptor-mediated endocytosis to cross the BBB (Ballabh, *et al*. 2004; Pardridge 2006).

1.3.2 Potential strategies for neurological drug delivery

There are current investigations into strategies to overcome the BBB to treat neurological symptoms associated with lysosomal storage diseases such as GD. Cabrera-Salazar *et al*. (2010) studied the effects of direct intracerebroventricular injections of GBA into type II GD mouse models; they reported that GBA was globally distributed in the brain within 1 hr post-injection, and mice given three daily treatments during the first 3 days of life showed nearly wild type levels of glucocerebroside and decreased neuronal degradation compared to controls. Although intracerebroventricular injections may not be practical for therapeutic treatment in GD patients, this research does indicate that GBA delivered to the CNS may alleviate neurological symptoms. There are current theories for potential strategies for drug delivery to the brain that are more practical for therapeutics; these include, but are not limited to, molecular Trojan horses, gene therapy, and protein transduction domains.

Molecular Trojan horses take advantage of the endogenous receptor-mediated endocytosis at the BBB. Reviews by Pardridge (2006) and Chen and Liu (2011) explain that if a molecule to be delivered to a cell is specifically directed towards an endogenous receptor, that molecule will be taken up by the vesicles formed. This can be done in one of two ways, either by fusing the recombinant protein molecule to the peptide which is recognized by the receptor, or fusing it to a monoclonal antibody directed towards the receptor. The advantage to the latter is that the binding of the recombinant enzyme does not have to necessarily inhibit endogenous binding of protein, and is therefore not as likely to affect normal functioning of the BBB (Pardridge 2006). Zhang and Pardridge (2005) used this method to deliver active β-Galactosidase (β-Gal, 116 kDa) from intravenous injections to mouse brain tissue using an antibody to the transferrin receptor. Their experiment provided evidence that this technique could be used to deliver large, active enzymes to CNS tissue.

Gene therapy has also been considered as a potential therapeutic for lysosomal storage disorders; they often result from a single genetic defect, which makes them excellent candidates, and gene therapy may be a technique that would help with the treatment of both visceral and CNS symptoms (Sands and Davidson 2006; Cheng and Smith 2003). Success with treating animal models in the past has been seen in experiments injecting genes encoding for functional enzymes present in a viral vector directly into CNS tissue (Cheng and Smith 2003). The downside to treating with genetic material is that when administered intravenously it is subjected to endo/exonuclease degradation and consequently cannot cross cell barrier, especially that of the BBB (Boado 2007). A potential method to avoid this would be to use synthetic

polyethyleneglycol (PEG) liposomes to encapsulate gene products. Boado (2007) describes delivery of a β-Gal expression cassette to rhesus monkey brains utilizing these synthetic liposomes, which include some PEG molecules that are conjugated to insulin receptor monoclonal antibodies; this technique utilizes both gene therapy and Trojan horse delivery (termed Trojan horse liposomes).

1.3.3 Protein transduction domains

Protein transduction domains (PTDs) are yet another potential therapeutic strategy that could be used to treat the neurological symptoms of GD. Investigation of protein transduction domains didn't arise until Frankel and Pabo (1988) and Green and Loewenstein (1988) independently discovered the unique ability of the TAT protein produced by human immunodeficiency virus (HIV) to easily traverse cell membranes in culture; this protein is a trans-activator of transcription of HIV genes. Fawell *et al*. (1994) investigated the potential of the HIV TAT to enhance transduction of heterologous proteins across cell membranes; they were able to show that the C-terminal end of the TAT protein conjugated with β-Gal or horse radish peroxidise was able to traverse the membranes of multiple different cell types *in vitro* as well as in a mouse model. Further investigations identified a small basic domain to be responsible for protein transduction (the PTD) (Park *et al*. 2002). Crucial investigations carried out by Schwarze *et al*. (1999) investigated how PTD techniques could be applied to therapeutics by creating a fusion protein with the TAT-PTD and β-Gal. They showed that intraperitoneal administration of

the fusion protein in mouse models resulted in a strong signal of β-Gal activity in brain areas 4 hrs after injection compared to control mice injected with β-Gal without a PTD.

After Schwarze *et al*. (1999) gave strong evidence supporting the potential therapeutic value of PTDs, investigations into how to optimize the transduction potential of the TAT-PTD ensued. Ho *et al*. (2001) developed a series of synthetic PTD's, all variations of the amino acid composition of TAT-PTD, in an attempt to optimize the structure. One synthetic molecule, PTD4, was shown to have an increase in transduction across mammalian cell membranes both *in vitro* (33X increased potential) and *in vivo* (5X increase in potential). The PTD4 has optimized placement of its arginine residues which according to Ho *et al*. (2001) stabilizes the core alpha helix of the peptide and consequentially enhances protein transduction. Although this structure optimization lends some insight into how this peptide traverses cell membranes, ultimately the PTD's mechanism remains to be elucidated. Some evidence points towards the positively charged PTD interacting with anionic glycosaminoglycans present at the surface of the cell membrane, especially heparin sulphate (Simon *et al*. 2009; Duchardt *et al*. 2007). Investigations by Duchardt *et al*. (2007) indicate that PTDs can act either through endocytic pathways or with an endocytosis- independent mechanism. Their research suggests that high concentrations (> 5μM) of exogenous protein supports the latter, and that heparinase treatment of cell membranes inhibits this method of uptake.

1.4 Project overview

This investigation will attempt to optimize the expression and purification of a recombinant fusion protein GBA-PTD4 using a *P. pastoris* expression system. The *P. pastoris* cell line expressing this protein was constructed previously in our lab and used for small scale experimental purification trials. I will use a semi-preparative hydrophobic interaction chromatography column for initial purification, which will allow me to purify at least 10X the amount of crude medium previously used for small scale trials. Gel filtration chromatography will be explored as a second purification step. Purified GBA-PTD4 can be used in the future to study *in vitro* and *in vivo* cellular uptake of recombinant protein, giving an estimation of therapeutic value. In anticipation of these future studies, I will also begin construction of a cell line expressing recombinant GBA without a transduction domain (GBA- only construct) to use in the future as a negative control.

Chapter 2 Materials and Methods

2.1 Shake-Flask *P. pastoris* cell culture

P. pastoris glycerol stocks stored at -80ºC were streak plated on histidine-deficient minimal dextrose (MD) plates (1.34% (w/v) yeast nitrogen base, 2% (w/v) dextrose, $4x10^{-5}$% (w/v) biotin, 1.5% (w/v) agar) and incubated at 30ºC for 3-4 days (plates stored at 4ºC for several uses). One colony was used to inoculate 25 ml of buffered glycerol-complex medium (BMGY; 1% (w/v) yeast extract, 2% (w/v) peptone, 100 mM sodium citrate, pH 5.5, 1.34% (w/v) yeast nitrogen base, $4x10^{-5}$% (w/v) biotin, 1% (v/v) glycerol) and incubated at 28ºC, shaking at 200 rpm for 16-18 hours, or until an OD_{600} of 2-6 was reached. The culture was then scaled up by inoculating 750 ml BMGY with 2 ml of small *P. pastoris* culture. These large cultures were incubated at 28ºC shaking at 200 rpm for 16-18 hours, or until an OD_{600} of 2-6 was reached. Large cultures were centrifuged at 3000xg and cells were suspended in 150 ml buffered methanol-complex medium (BMMY, 1% (w/v) yeast extract, 2% (w/v) peptone, 100 mM sodium citrate, pH 5.5, 1.34% (w/v) yeast nitrogen base, $4x10^{-5}$% (w/v) biotin, 0.5% (v/v) methanol) for Mut^S clones, and to an OD_{600} of 1 for Mut^+ clones, and incubated at 26ºC shaking at 200 rpm to begin induction. Induction was carried out for 48 hours, with 1% methanol being added to each culture after 24 hours. At the 48 hour time point, cultures were centrifuged again at 3000xg and crude media was collected and stored at -80ºC and *P. pastoris* cells were discarded. Each week began with fresh small scale cultures, until enough crude media was obtained for protein purification (3-4L).

2.2 GBA Purification

2.2.1 HIC purification

A 50 ml HPLC Custom Pack column (BioRad) was packed with Phenyl Sepharose High Performance (Amersham Bioscience). For each purification run, the column was first rinsed 2-4 column volumes (CV) of filter degassed distilled water, then equilibrated with 5 CV filter-degassed Buffer B (50 mM citric acid, 0.1 M NaCl, pH 5.5) proceeded by 5 CV filter-degassed Buffer A (50 mM citric acid, 0.1 M NaCl, 1.45 M $(NH_4)_2SO_4$, pH 5.5) at a flow rate of 250 ml/hour at 4ºC.

Crude *P. pastoris* media harvested at 48 hours was taken out of the -80ºC freezer and thawed completely before the addition of a reducing agent (10 mM of either dithiothreitol (DTT) or β-mercaptoethanol). Ammonium sulphate was added to crude media to a concentration of 1.45 M and media was placed on an orbital shaker with agitation until all the salt had dissolved. Media was centrifuged at 6088xg then filter-degassed. Prepared media was loaded onto the equilibrated column at flow rates varying from approximately 100-200 ml/hour. Media loading usually took 24 hours or longer, because of the large volumes used.

Following loading, column was washed with 4 CV of Buffer A at a flow rate of 250 ml/hour. This flow rate was used through the remainder of the desalting gradient; all buffers pumped into the column throughout the purification run were filter-degassed. A stepwise desalting gradient was used starting with Buffer A at 4ºC, 5 CV of each of the following was run through the column: Desalting 1 (50 mM citric acid, 0.1 M NaCl, 1.0 M $(NH_4)_2SO_4$, pH 5.5), Desalting 2 (50 mM citric acid, 0.1 M NaCl, 0.5 M $(NH_4)_2SO_4$,

pH 5.5), Buffer B, distilled water. Throughout desalting gradient, fractions of 16.67 ml flow-through were collected and kept at 4ºC.

GBA elution was done with one of either cholate or ethylene glycol. For cholate elution, the column was set up to an Atka Prime FPLC system (Amersham Biosciences) previously cleaned and filled with distilled water. A continuous gradient of 0-2% cholic acid was undergone over a 400 ml volume at a flow rate of 4.5 ml/ minute, and a continuous UV readout was collected and saved using PrimeView software. Fractions of 6.5 ml were collected and stored at 4ºC.

Ethylene glycol elution was done with stepwise increases in concentration, with flow rate varied to compensate for increasing viscosity and back pressure; all ethylene glycol buffers contained 20 mM sodium citrate. Approximately 4 CV of 20% ethylene glycol was pumped through column (collecting 10 ml fractions) before switching to 37.5%. After 2 CV of 37.5% ethylene glycol, the column was given a short incubation period of 3-4 hours at 4ºC before continuing with another 2 CV. The pump was detached briefly from the column in order to fill all tubing with 55% ethylene glycol, and 1 CV was pumped onto the column before leaving it for an overnight incubation at 4ºC. Following the incubation approximately 4 CV was pumped through the column, collecting 4 ml fractions.

All fractions were analyzed for activity with an artificial substrate 4-methyl-unbelliferyl-β-D-glycopyranoside (4-MUGP, Sigma-Aldrich Canada). Protein content of fractions could be determined by reading the absorbance at 280 nm with a UV spectrophotometer (Beckman Coulter™, DU® 530). Fractions which were suspected of containing GBA were combined into several pools, amicon and/or centricon concentrated

(depending on sample volume), and further analyzed with SDS-PAGE silver staining, immunoblotting, and activity with the natural lipid substrate. Column was stored in 0.02% sodium azide at 4ºC between uses.

2.2.2 GFC purification

A pre-packed HiLoad Superdex 200 gel filtration column (GE Healthcare) was equilibrated with 1 CV of each of the following filter-degassed buffers for HIC samples eluted with ethylene glycol: low ionic (100 mM sodium citrate, 50 mM NaCl, pH 5.5), equilibration 1 (100 mM sodium citrate, 150 mM NaCl, 15% ethylene glycol pH 5.5), equilibration 2 (100 mM sodium citrate, 150 mM NaCl, 35% ethylene glycol pH 5.5), and running buffer 1 (100 mM sodium citrate, 150 mM NaCl, 55% ethylene glycol, pH 5.5). For HIC samples eluted with cholate, the column was equilibrated with the following degassed buffers: low ionic, equilibration 1, and running buffer 2 (100 mM sodium citrate, 150 mM NaCl, 20% ethylene glycol, pH 5.5). All buffers were pumped through the column at 6 ml/hour throughout equilibration and run, equilibration started at room temperature but with addition of running buffer the column was put into fridge, where it remained at 4ºC for the remainder of the run.

HIC purified samples with similar protein profiles were combined and centricon concentrated to approximately 1 ml. Protein samples were dialyzed with centricon into appropriate running buffer if needed. Samples were then centrifuged at 13000xg for 20 minutes at 4ºC before being injected onto the column through use of a sample loop. Running buffer was pumped through the column while collecting 2 ml fractions.

Fractions were analyzed for activity with 4-MUGP substrate and absorbance at 280 nm could be measured with a UV spectrophotometer (Beckman Coulter™, DU® 530).

2.3 Protein Analysis

2.3.1 Enzyme activity assays

Activity analysis of post-purification fractions was analyzed with the artificial fluorometric substrate 4-MUGP. Ten µl of purified or partially purified enzyme sample was added to a reaction mixture of 3.5 mM 4-MUGP, 0.03M citrate buffer pH 5.5, 0.1% w/v sodium taurocholate and incubated at 37ºC for 30 minutes. After incubation, addition of 0.2M glycine buffer, pH 10.5 stopped the reaction. Fluorescence was measured using a Sequoia-Turner Model 450 Digital fluorometer (Turner Designs, Sunnyvale, CA).

Samples known to contain high concentrations of GBA could be assayed using the natural lipid substrate. 40 µl of concentrated enzyme sample was added to 1 mg/ml C_8-glucosylceramide (Avanti Polar Lipids Inc., Alabaster, AL) in 0.04M sodium citrate buffer pH 5.5, 0.8% sodium taurocholate and 0.1% Triton X-100™. Reactions were incubated for 4 hours shaking at 37ºC. To stop the reaction, samples were boiled for 5 minutes, then centrifuged at 13000xg for 15 minutes at 4ºC. Supernatent was mixed with 10 volumes of hexokinase (HK) reagent (Sigma-Aldrich Canada) and incubated for 10 minutes at 37ºC. This enzyme reacts with glucose released by previous reaction, and produces NADH. The NADH released was assessed by taking the absorbance at 340 nm with a UV spectrophotometer (Beckman Coulter™, DU® 530) and this is directly proportional to glucose generated by GBA enzyme.

2.3.2 SDS-PAGE protein analysis

Protein samples were run on SDS-PAGE gels consisting of a 10% (v/v) tris-glycine resolving layer and a 4% (v/v) tris-glycine stacking layer. Samples were prepared by mixing with 3X SDS sample buffer (NEB) containing 42 mM dithithreitol, and boiling for 5 minutes. NaOH (1 M) was used to adjust the pH of samples before they were centrifuged for 5 minutes at 13000xg. Gels were resolved on a Mini-Protean® Tetra Cell electrophoresis unit (BioRad) and a Precision Plus dual color marker (BioRad) or a pre-stained protein marker (NEB) was used to estimate sample protein molecular masses.

2.3.3 Silver stain analysis

Silver stain analysis was used for visualization of protein bands on SDS-PAGE gels. Gels were placed in fixative (50% v/v ethanol, 5% v/v glacial acetic acid) and microwaved for 90 seconds. Gels were then placed in wash solution (50% v/v ethanol) and microwaved for 90 seconds, then in sensitize solution (0.02% w/v sodium thiosulfate) and microwaved 90 seconds. After rinsing gels in distilled water for 90 seconds at room temperature, they were stained with 0.2% (w/v) silver nitrate at room temperature, shaking for 20 minutes. After staining, gels were rinsed for 90 seconds at room temperature with distilled water before being developed in a solution of 0.04% (v/v) formaldehyde and 2% (w/v) sodium carbonate for as long as necessary. Developing was stopped with 5% (v/v) glacial acetic acid at room temperature with agitation for 5 minutes.

2.3.4 Western blot analysis

After separating protein samples on SDS-PAGE, proteins were transferred to BioTrace™ polyvinylidene fluoride (PVDF) membranes (Pall Corporation) at 10V overnight or at 100V for 1 hr in 10% v/v methanol transfer buffer (25 mM tris-HCL, 0.2 M glycine) using a Mini Trans-Blot Cell apparatus (BioRad). After transfer, each of the following steps was performed at room temperature with gentle agitation. Membrane was first washed of transfer buffer in phosphate-buffer saline and 0.2% v/v Tween 20 (PBST), and then blocked in 5% (w/v) skim milk in PBST for 1 hour. After being washed of blocking reagent, membrane was incubated for 2 hours with monoclonal mouse anti-GBA antibody (mAb) H00002629-M01 (Abnova Corporation, Taipei City, Taiwan) diluted 1/1000 or 1/3000 times in PBST. Primary antibody was removed with 3 washes in PBST for 5 min each. Membrane was then incubated with secondary goat anti-mouse horseradish peroxidise conjugated (Thermo Scientific, Waltham, MA) at 1/1000 dilution in blocking reagent for 1 hr, and washed as above. Blotted membranes were reacted with SuperSignal® West Dura extended duration substrate (Pierce, Rockford, IL) for 5 min before exposure to CL-X Posure™ film (Pierce) for times varying from 5 sec to overnight, and visualized using a Kodak X-OMAT 2000A Processor.

2.4 Custom antibody analysis

2.4.1 ELISA analysis

Six ascites fluid samples containing custom monoclonal antibodies were obtained from Abmart (Shanghai, China). Our collaborators in Dr. Terry Pearson's lab at the

University of Victoria performed ELISA testing on each antibody. ELISA 96 well plates (Becton-Dickinson, Mississagua, ON) were coated with crude induction medium from either GBA-PTD4 *P. pastoris* cultures or vector-only *P. pastoris* medium so that each well contained approximately 1 μg of protein. Plate was allowed to dry overnight at 37˚C. Skim milk diluted to 3% in PBS was added to each well and plate was incubated for 1hr at 37˚C. The plate was washed 3X with PBST before ascites fluid diluted in PBST with 1% skim milk was added to each of the wells. Initial dilution of ascites was 1/400 and increased exponentially. The plate was incubated for 1 hr at 37˚C before being washed with PBST 3X for 10-15 minutes each. Caltag goat-anti mouse IgG/IgM Alk-Phos (Life Technologies, Burlington, ON) was diluted 1/2000 with PBST with 2% skim milk and added to each well. Plate was incubated for 1 hr at 37˚C and washed as was done previously. The substrate (pill dissolved in diethanolamine buffer) was added to the plate and incubated 15-30 minutes at room temperature in the dark. Absorbance at 405 nm was read on the ELISA reader.

2.4.2 Immunoprecipitation

Immunoprecipitation was carried out to assess whether the ascites fluid samples would recognize fold GBA-PTD4 in *P. pastoris* crude medium. This procedure was done by our collaborators in Dr. Terry Pearson's lab. Fifty microlitres of goat anti-mouse IgG Dynabeads (Invitrogen, Oslo, Norway) were pelleted and rinsed with sterile, cold PBS and then resuspended in ascites fluid diluted 1/100 with PBS. Ascites and beads were mixed by end-to-end tumbling overnight at 4˚C. Beads were then removed from diluted

ascites fluid and rinsed three times with sterile PBS before being suspended with 1 ml crude GBA-PTD4 *P. pastoris* medium. Tubes were mixed again with end-to-end tumbling overnight at 4˚C. Beads were pelleted and washed three times with 1 ml PBS/0.03% CHAPS ([3-cholamidopropyl-dimethylammnoio]-1-propanesulfonate). Fifty microlitres of 2X SDS samples buffer was added to beads and boiled for 15 minutes to release bound proteins. Samples were loaded onto an SDS-PAGE gel and gel run followed by transfer and western blot was carried out.

2.5 Construction of a GBA-only construct

2.5.1 Cloning Details

The construct pPIC9K-*GBA* was made from amplification of *GBA* from an existing pPICZα-*GBA* construct (April Goebl, University of Victoria, Victoria, BC). See Figure 2.1 for pPIC9K details. *GBA* cDNA sequence (provided by Dr. Ernest Beutler, The Scripps Research Institute, La Jolla, CA) in this construct as well as the pPIC9K-*GBA*-PTD4 construct used in protein expression/purification studies started with the codon that encoded the first amino acid of the mature-polypeptide, found in exon 3 of human genomic DNA sequence. Amplification of *GBA* was done with primers PFwd and PRvs with tails containing restriction endonuclease (REN) sequences *EcoRI* and *NotI* respectively; reaction contained 1.5 mM $MgSO_4$, 0.25 mM dNTPs, 1X Pfx amplification buffer (Invitrogen), 0.4 µM of each of the custom primers PFwd and PRvs, and 0.5 units Platinum Pfx polymerase (Invitrogen). See Table 2.1 for custom primer sequences. Amplification was performed using a S100™ Thermal Cycler (BioRad) with an initial

denaturation of 94˚C for 5 min, 35 cycles of 94˚C for 1 min, 60˚C for 1 min, and 72˚C for 1.5 min, and a final elongation of 72˚C for 5 min.

Table 2.1. Custom oligonucleotide primers used for PCR amplification of GBA. Primers introduced *EcoRI* and *NotI* restriction sites (in bold print) flanking the gene to aid in cloning into pPIC9K expression vector. Extra base pairs were added outside of the restriction sites to aid in restriction digest.

Primer name	Primer Sequence	Orientation
PFwd	**5'-** ATAA**GAATTC**GCCCGCCCCTGCATCC	Sense
PRvs	**5'-** TATATT**GCGGCCGC**TCACTGGCGACG	Anti-sense

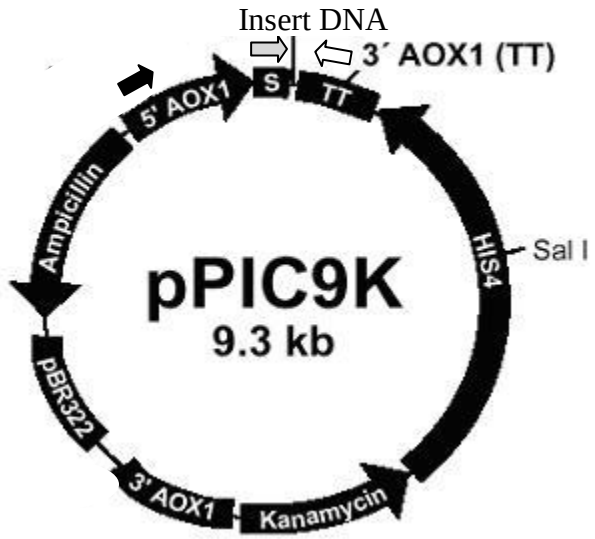

Figure 2.1. Schematic representation of the pPIC9K vector indicating insertion site of recombinant DNA.

Arrows indicate vector specific primer binding sites: dark arrow 5' AOX forward, grey arrow α-secretion forward, white arrow 3' AOX reverse. For sequences of vector specific primers see Supplementary Table 1. α- secretion signal indicated by S, termination of transcription signal indicated by TT. Also included are ampicillin and kanamycin resistance genes, as well as the HIS4 gene which allows growth of yeast on histidine deficient medium. Image adapted from pPIC9k vector manual (Invitrogen).

PCR products were run alongside a 1 kB DNA standard (New England Biolabs, NEB, Beverly, MA) on a 1.5% (w/v) agarose gel and stained in 0.5 µg/mL ethidium bromide (EtBr) for visualization using a EpiChemi^3 Darkroom UV imager and LabWorks software (UVP BioImaging Systems). PCR products were purified following a protocol from a Qiaquick® PCR purification kit (Qiagen, Mississauga, ON).

PCR products were A-tailed in preparation for ligation into pGEM-T vector, reaction included 1X Thermopol Reaction Buffer (NEB), 2.5 mM $MgCl_2$, 0.2 mM dATPs, and 5 units Taq Polymerase (NEB). Reaction was incubated for 20 min at 70˚C. Construct was then T/A ligated into pGEM®-T vector (Promega, Madison, WI) according to the manufacturers' protocol to create a pGEM-T-EcoRI-*GBA*-NotI construct. Ligation products (2 µl) were used to transform competent DH5α *E. coli* cells (Invitrogen) using heat shock treatment according to the manufacturers' protocol. SOC medium (2% (w/v) tryptone, 0.5% (w/v) yeast extract, 10 mM NaCl, 2.5 mM KCl, 10 mM $MgCl_2$, 20 mM glucose, pH 7.0) was used for cell recovery before transformed cells were plated on Luria-Bertani broth (LB; 1% (w/v) tryptone, 0.5% (w/v) yeast extract, 0.1 M NaCl, pH 7.5, 1.5% (w/v) agar) containing 0.4 mM isopropyl-beta-D-thiogalactopyranoside (IPTG), 0.02 mg/ml 5-bromo-4-chloro-3-indolyl-beta-D-galactopyranoside (X-Gal) (Invitrogen), and 0.08 mg/ml ampicillin (Sigma-Aldrich Canada). Plates were incubated overnight at 37˚C and blue-white screening was used to identify transformants containing PCR inserts. White colonies were screened using PCR with custom made primers PFwd and PRvs, the reaction mixture contained 3.75 mM $MgCl_2$, 1X Thermopol Reaction buffer (NEB), 0.25 mM dNTPs, 0.75 µM of each of the primers, and 1 unit Taq polymerase (NEB). PCR was performed using a S100™ Thermal

Cycler (BioRad) under the following conditions: initial denaturation of 94˚C for 5 min, 35 cycles of 94˚C for 1 min, 60˚C for 1 min, 72˚C for 2.5 min and a final elongation of 72˚C for 7 min. Products were resolved on a 1.5% (w/v) agarose gel alongside a 1 kb DNA ladder (NEB) and stained with EtBr for visualization as above.

Selected cultures with PCR products of appropriate size (2 kB) had plasmid DNA isolated using QIAprep® Miniprep kit (Qiagen) according to the manufacturers' protocols. Subsequent confirmation of ligation was obtained by digesting isolated plasmid with 1 U/µl EcoRI(NEB) and 1 U/µl NotI (NEB) (reaction contained 1X NEB EcoRI buffer and 1X BSA) for 3.5 hrs at 37˚C. Digestion products were run on a 1.5% agarose gel with a 1 kB DNA ladder (NEB) and stained with EtBr for visualization as above. Confirmed ligations were sent to Eurofins MWG Operon (Huntsville, AL) for sequencing and DNA sequence data was analyzed using BioEdit alignment tool.

The pPIC9K vector was digested with 1 U/µl EcoRI (NEB) and 1 U/µl NotI (NEB) (with 1X NEB EcoRI buffer and 1X BSA) at 37˚C for 3 hrs. pGEM-T-EcoRI-*GBA*-NotI digested as above to create EcoRI-GBA-NotI insert was ligated into digested plasmid with 1X Rapid Ligation buffer (Promega) and 400 U T4 DNA ligase with ratios of both 3:1 insert to vector and 2:1 insert to vector (incubated at 16˚C overnight) to create a pPIC9K-EcoRI-*GBA*-NotI construct. Ligations were used to transform DH5α *E. coli* competent cells (Invitrogen) as above. Blue-white screening and colony PCR using custom primers PFwd and PRvs was carried out as above to test for clone which contained vector with inserted DNA. Miniprep of selected clones was done using QIAprep® Miniprep kit (Qiagen) according to the manufacturers' protocols and confirmation of ligation was carried out by a double digest as described above.

Confirmed ligations were again sent to Eurofins MWG Operon (Huntsville, AL) for sequence confirmation and analyzed as above.

2.5.2 *Pichia pastoris* transformation

A YA208 *P. pastoris* cell line (humanized GS115 strain) was induced into a competent state for transformation. Ppic9K-*GBA* plasmid was linearized by digestion with either BglII (for promotion of Mut^S phenotype) or Sac I (for promotion of Mut^+ phenotype). Sac I digest utilized 1X Digestion Buffer 1 (NEB) and 1X BSA with 30 U SacI. BglII digests contained 1X Digestion Buffer 3 (NEB) and 30 U BglII. All digestions were carried out at 37˚C overnight. Five to ten µg linearized plasmid was used to transform 80 µl electrocompetent humanized *P. pastoris* strain GS115 with pGlycoSwitchM5 (Vervecken *et al*. 2004) (obtained from Dr. Contreras, Department of Molecular Biology, Ghent University, Belgium). Gap cuvettes (0.2 cm) and a Gene Pulser™ electroporation apparatus was used with settings at 2.5 kV, 25 µFD capacitance, and 200 Ω resistance). Cells were rescued post-electroporation with 1 hr incubation at 30˚C in 1M sorbitol. Transformants were plated on histidine-deficient MD plates for selection of clones with at least one integrant.

2.5.3 Multiple copy integration and Mut^S/ Mut^+ phenotype determination

Clones with multiple integration events were selected via increased resistance to Geneticin® (Invitrogen). Transformants on MD plates were collected according the

pPIC9K manual, by suspending cells in sterile dH_2O on plates and collecting (at this point transfected cells could be frozen at -80˚C in 15% glycerol for stocks to be analyzed at a later time). Cells were then plated on increasing concentrations of Geneticin®, from 0- 0.75 mg/ml onYPD agar plates (1% (w/v) yeast extract, 2% (w/v) peptone, 2% (w/v) dextrose, 1.5% (w/v) agar). Clones which grew well on 0.75 mg/ml Geneticin® were used for further study.

Multiple copy integration clones were then tested for methanol utilization phenotype. Cells were suspended in dH_2O and plated on both MD medium and minimal methanol (MM) medium (1.34% (w/v) yeast nitrogen base, 0.5% (v/v) methanol, $4x10^{-5}$% (w/v) biotin, 1.5% (w/v) agar) and incubated at 30˚C. Relative growth on MD and MM medium was scored after approximately 48 hours. All clones were predicted to grow well on MD medium, but growth on MM medium would be slower in clones with the Mut^S phenotype.

2.5.4 Amplification of insert from *P. pastoris* genomic DNA.

Genomic DNA was isolated from selected clones by 2 hr 30˚C incubation of cells with 2 U of zymolyase (Seikagaku Corporation, Tokyo, Japan) for cell lysis followed by submersion in liquid nitrogen. PCR amplification mixture contained 5 µl cell lysate, 1X Thermopol Reaction buffer (NEB), 2.5 mM $MgCl_2$, 0.25 mM dNTPs, 0.3 µM of each vector specific primer (5’ AOXI forward and 3’ AOXI reverse), and 1 U Taq Polymerase (NEB). PCR was carried out with S100™ Thermocycler (BioRad) under the following conditions: initial denaturation 94˚C for 5 min, 30 cycles of 94˚C 1.5 min, 58˚C for 1.5

min, 72˚C for 2 min and a final elongation at 72˚C for 5 min. PCR products were separated on a 1.5% agarose gel alongside a 1kB DNA ladder (NEB or BioBasic). Gels were stained and visualized as above. Mut^S clones would contain one PCR product, the inserted transgene, Mut^+ clones however would also have the endogenous *P. pastoris AOXI* gene amplified by the 5' *AOXI*/ 3' *AOXI* primer set. To this end, a nested PCR was carried out using 3-5 µl PCR product as template and α-secretion signal vector specific forward primer in conjunction with 3' *AOXI* reverse primer. PCR reaction for the nested amplification was the same as described for amplification from genomic DNA above. PCR was carried out under the following conditions: initial denaturation 94˚C for 5 min, 30 cycles of 94˚C 1.5 min, 56˚C for 1.5 min, 72˚C for 2 min and a final elongation at 72˚C for 5 min. Separation and visualization for agarose gels was completed as above. PCR products were either gel extracted or purified using QIAquick® PCR Purification Kit (Qiagen). Samples were sent to Eurofins MWG Operon (Huntsville, AL) for sequence confirmation.

Chapter 3 Results

3.1 Expression of GBA-PTD4 in large scale *P. pastoris* shake-flask cultures

Shake-flask cultures were used to produce GBA-PTD4 protein in harvested *P. pastoris* crude induction medium. To verify the presence of GBA-PTD4, proteins from crude medium both non-concentrated and 10X concentrated were separated with SDS-PAGE and probed with GBA specific monoclonal antibody (Figure 3.1). Non-concentrated and 10X concentrated medium from pPIC9K only negative control cell line was western blotted alongside GBA-PTD4 cell line. Two cultures of both cell lines were analyzed. Figure 3.1 shows that GBA is present in induction medium from GBA-PTD4 cell line but absent in medium from pPIC9K only negative control. This is verification of previous work done in our lab (Goebl 2010).

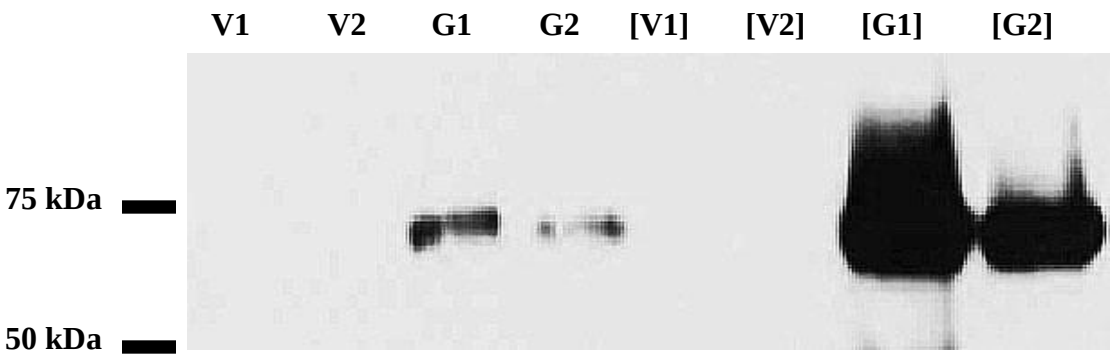

Figure 3.1 Western blot of crude *P. pastoris* induction medium of both GBA-PTD4 and pPIC9K vector only cell lines.
Proteins from both non-concentrated and 10X concentrated samples (denoted with [ ]) were separated by SDS-PAGE analysis prior to immunoblot using an anti-GBA mAB (Abnova, H00002629-M01). Two cultures of each cell type were analyzed (GBA-PTD4 cultures G1 and G2, pPIC9K vector only cultures V1 and V2).

3.2 Hydrophobic interaction chromatography

Crude *P. pastoris* induction medium was purified using two separate purification steps. The first step, hydrophobic interaction chromatography, utilized a step-wise desalting gradient, and one of either a continuous cholate detergent gradient or a stepwise ethylene glycol gradient.

The step-wise desalting gradient went from 1.45 M ammonium sulphate to 0 M ammonium sulphate, followed by a water wash. Figure 3.2 shows the protein elution during this gradient as measured by a UV spectrophotometer at 280 nm. Each defined peak of protein corresponds to a step-wise decrease in the ammonium sulphate concentration, and proteins present in each are predicted to have increasing hydrophobic properties according to their pattern of elution. Natural lipid substrate activity analysis

(Figure 3.4) confirm minimal elution of GBA during this gradient as a result of its highly hydrophobic nature. A high peak in 4-MuGP activity is witnessed during this gradient which spans the 0.5 M and 0 M steps (Figure 3.3). Since 4-MuGP is not specific to GBA in that it can act as a substrate for any β-glucosidase, this large peak in activity can be attributed to an endogenous yeast β-glucosidase. Figure 3.4 shows GBA activity of this peak with the natural lipid substrate; an activity of 6.34 nmols glucose/hr/ml in the desalting gradient was significantly smaller than the highest activity seen in pooled fractions from the cholate gradient, which was 18.40 nmols glucose/hr/ml.

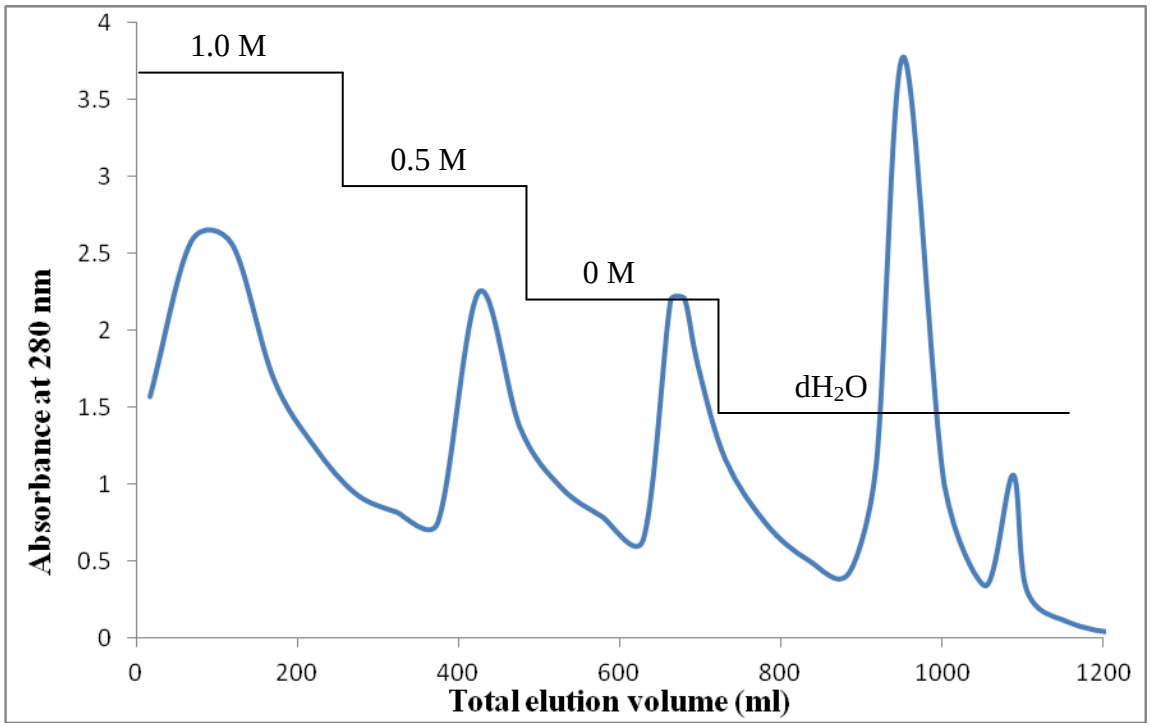

Figure 3.2. Protein elution profile of a desalting gradient from a hydrophobic interaction chromatography column loaded with crude *P. pastoris* media.
Starting ammonium sulphate concentration was 1.45 M, and stepwise decreases in ammonium sulphate were applied every 250 ml, to 1.0 M, 0.5 M, O M, then finally a dH_2O wash. 16.67 ml fractions were collected and absorbance at 280 nm read with a Beckman-Coulter DU® 530 UV spectrophotometer.

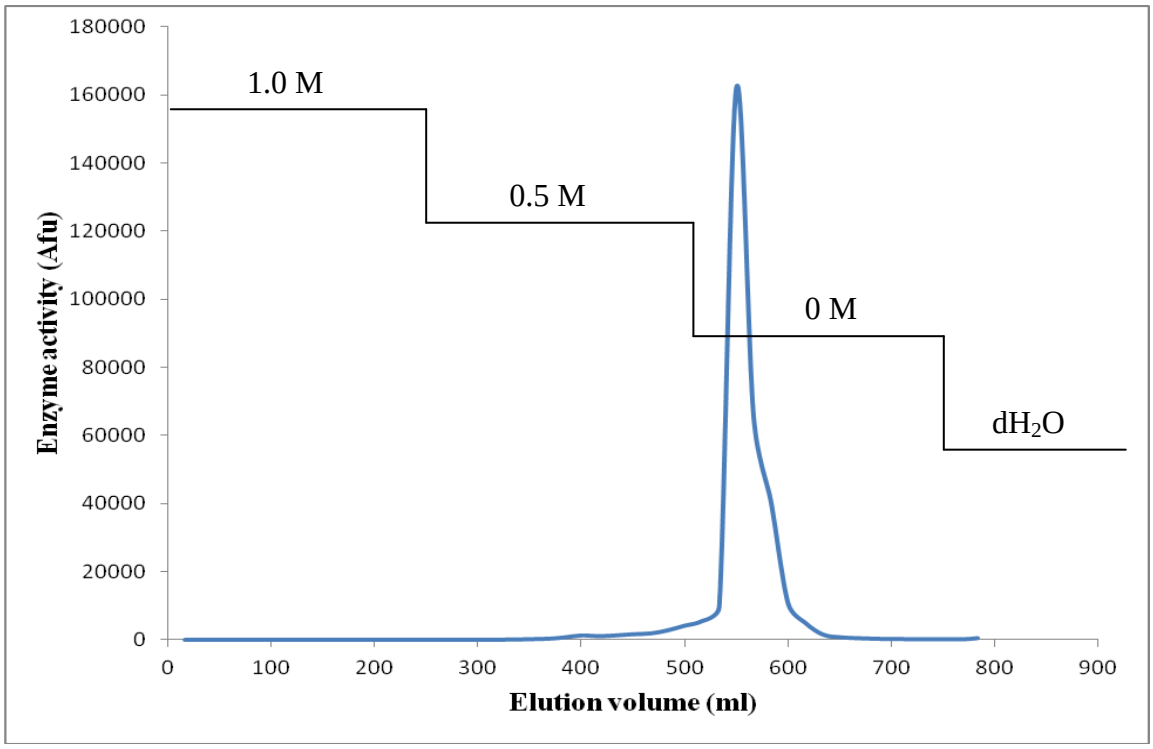

Figure 3.3. 4-MuGP activity profile of a desalting gradient from a hydrophobic interaction chromatography column loaded with crude *P. pastoris* media.

Starting ammonium sulphate concentration was 1.45 M, and stepwise decreases in ammonium sulphate were applied every 250 ml, to 1.0 M, 0.5 M, O M, then finally a dH_2O wash. 16.67 ml fractions were collected and each was analyzed for fluorogenic activity. Large peak in activity present at approximately 550 ml elution volume is due to elution of endogenous *P. pastoris* β-glucosidases.

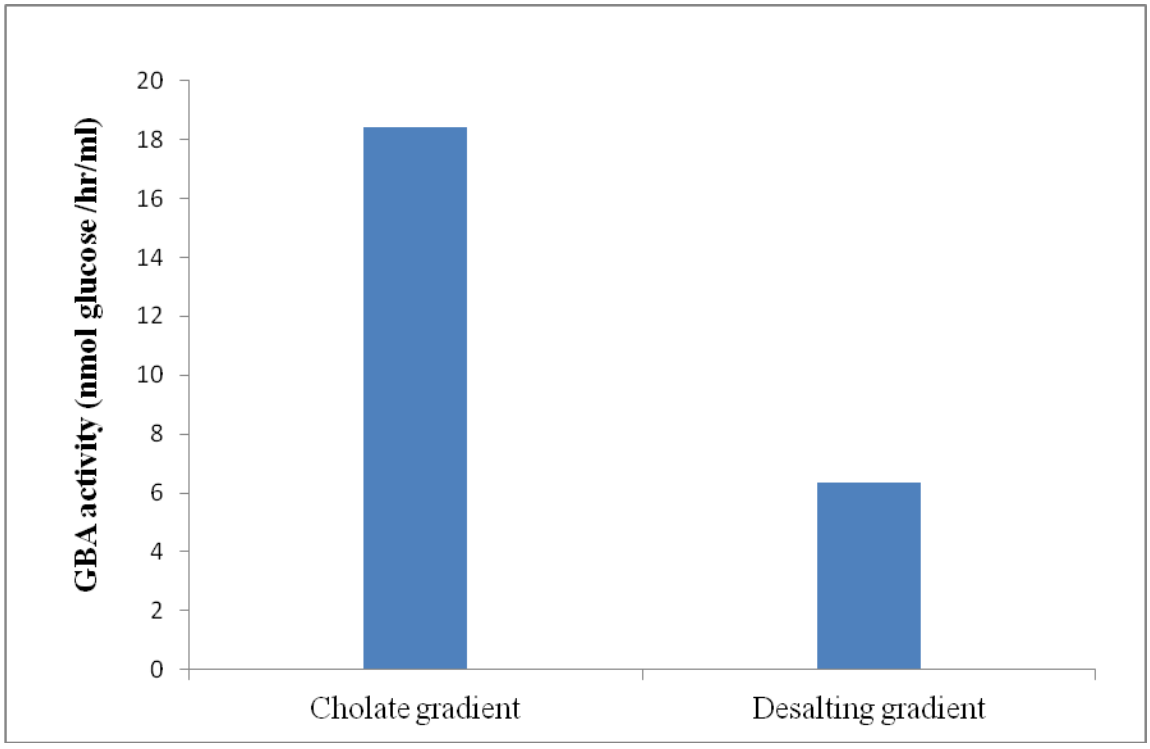

Figure 3.4. Natural lipid substrate assay of pooled fractions from hydrophobic interaction chromatography purification of *P. pastoris* crude induction medium.
Pools with highest activities in both the cholate and desalting gradient are shown. Concentrated enzyme samples were incubated with C_8-glucosylceramide (Avanti Polar Lipids) for 4 hr prior to HK reagent reaction. Activity in nmol glucose/hr/ ml for each fraction before concentration was calculated.

A continuous cholate gradient from 0- 2% was initially utilized to elute GBA from the HIC column. This method generally had good resolution of eluted hydrophobic proteins and GBA was knocked off the column generally in a small volume of approximately 15-20 ml, although the protein preparation still had many contaminants (not shown).

The problem encountered with this method was the aggregation of GBA enzyme upon being subjected to the detergent nature of the cholate solution. The aggregates could

be detected in the western blots of partially purified preparations (samples 1, 2 and 3) as in Figure 3.5 **(a)**, where a small amount of protein separated by SDS-PAGE would cause significant smearing in each of the protein lanes. The aggregation of enzyme creates difficulties later in the size exclusion purification step.

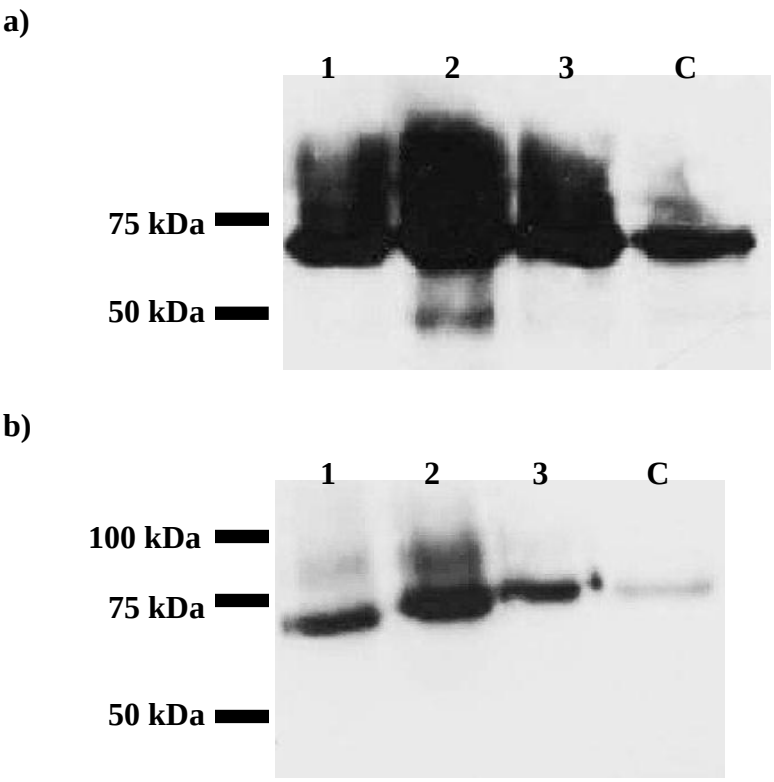

Figure 3.5. Immunoblot of concentrated fractions after a hydrophobic interaction chromatography purification of GBA-PTD4 from *P. pastoris* crude induction medium. **a)** Fractions collected after HIC with cholate elution were tested for 4 MuGP activity, and peaks 1, 2 and 3 were pooled and concentrated. Separation of proteins in all pooled fractions and concentrated crude medium (C) by SDS-PAGE was followed by immunoblot using an anti-GBA mAB (Abnova, H00002629-M01). **b)** Fractions collected after HIC with ethylene glycol elution were tested for 4 MuGP activity, and peaks 1, 2 and 3 were pooled and concentrated. Separation of proteins and immunoblot for each of the three pooled fractions and crude medium (C) were carried out as in (a). A dual-color protein marker (BioRad) was run on SDS-PAGE and transferred to membrane for size identification. GBA specific band can be seen in both (a) and (b) at approximately 67 kDa.

To avoid protein aggregates, ethylene glycol was investigated as a potential elution agent using stepwise increases in concentration from 0% (water wash) to 55%. An optimized elution of GBA utilizing this method included a 4 hr incubation of the column in 37.5% ethylene glycol to elute contaminating proteins slightly less hydrophobic than GBA, and column incubation overnight with 55% ethylene glycol to elute GBA in a concentrated volume. Figure 3.7 and Figure 3.8 depict the protein elution pattern and the 4-MuGP activity assay, respectively, of the fractions eluted during the stepwise ethylene glycol gradient. Figure 3.7 shows that there is a resolved peak of protein elution directly after the 4 hour incubation with 37.5% ethylene glycol. There is no corresponding peak in activity seen in Figure 3.8, which indicates that these are contaminating proteins. There is a large spike in absorbance at 280 nm and activity with the 4-MuGP following the overnight incubation. This overnight incubation was crucial to the resolution of GBA elution for this gradient. Figure 3.5 (b) shows the effect that ethylene glycol had on the aggregation of GBA. GBA specific bands are much cleaner than in (a), indicating that the majority of GBA is in its monomeric form. Figure 3.6 shows all protein species present within the partially purified preparation. Many species can be seen in each of the pooled and concentrated fractions although there is a clear reduction in the heterogeneity as compared to the crude medium sample. A significant band approximately the size of GBA is present in each of the samples; this corresponds to the GBA specific band seen in Figure 3.5 (b).

Table 3.1 shows an estimation of the total GBA-PTD4 recovery after HIC as being 1.17% that of the crude induction medium. This was measured after all

concentration and analysis steps. A total of approximately 10 mg GBA-PTD4 was recovered in this particular purification run.

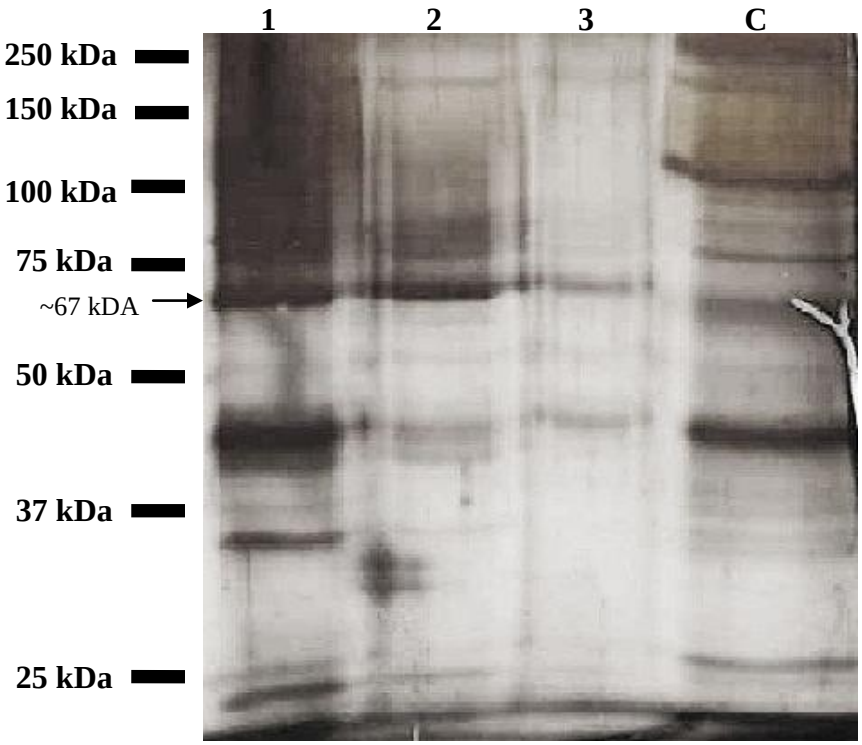

Figure 3.6. Silver stain of concentrated fractions after a hydrophobic interaction chromatography purification of GBA-PTD4 from *P. pastoris* crude induction medium.
Fractions collected after HIC with ethylene glycol elution were tested for 4 MuGP activity, and peaks 1, 2 and 3 were pooled and concentrated. Proteins were separated by SDS-PAGE as well as concentrated crude medium (C) before being stained with silver nitrate. A dual-color protein marker (BioRad) was run on SDS-PAGE for size identification. A strong protein band is present at approximately 67 kDa which is predicted to be GBA-PTD4.

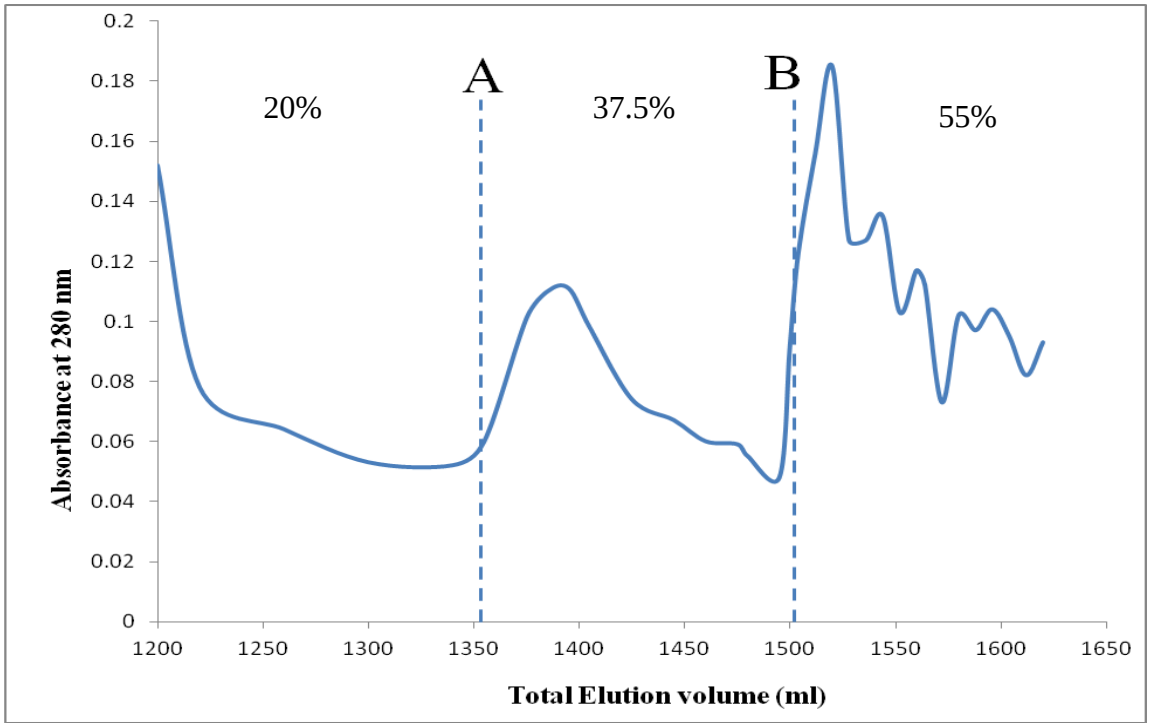

Figure 3.7. Protein elution profile of a stepwise ethylene glycol gradient from a hydrophobic interaction chromatography column following a desalting gradient where column was loaded with crude *P. pastoris* media.

Increases in ethylene glycol were applied to the column every 200 ml, starting with 20%, 37.5%, and finally 55%. Volume of fractions was 10 ml and 5 ml during 20% and 37.5% elution respectively, and 4 ml during 55% elution. A: 3 hr column incubation at 4˚C with 37.5%. B: overnight column incubation at 4˚C with 55% ethylene glycol. Absorbance at 280 nm read with a Beckman-Coulter DU® 530 UV spectrophotometer.

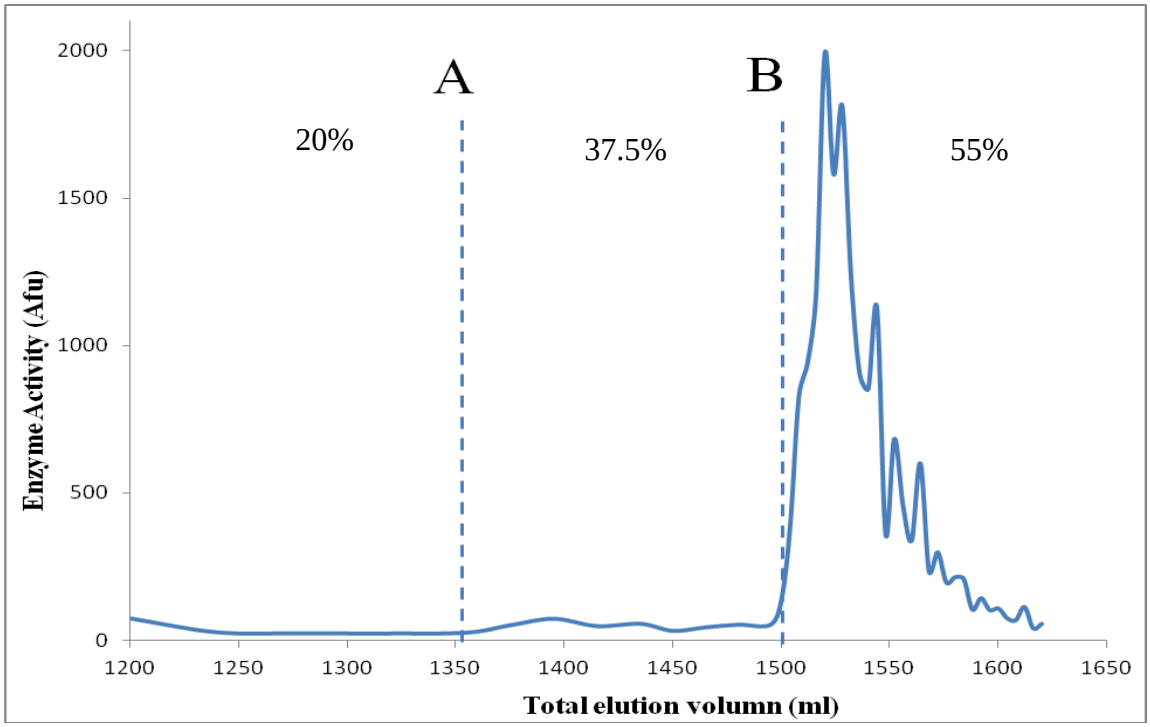

Figure 3.8. 4-MuGP activity profile of a stepwise ethylene glycol gradient from a hydrophobic interaction chromatography column following a desalting gradient where column was loaded with crude *P. pastoris* media.

Increases in ethylene glycol were applied to the column every 200 ml, starting with 20%, 37.5%, and finally 55%. Volume of fractions was 10 ml and 5 ml during 20% and 37.5% elution respectively, and 4 ml during 55% elution. A: 3 hr column incubation at 4˚C with 37.5%. B: overnight column incubation at 4˚C with 55% ethylene glycol. Fluorescence of each fraction was measured using a Sequoia-Turner Model 450 Digital fluorometer.

Table 3.1. Estimation of purification yield of HIC as determined by immunoblot band intensity comparison.

Crude induction medium and concentrated post-HIC pooled samples were run on an SDS-PAGE and transferred to a PVDF membrane to be probed with a GBA specific mAB (Abnova, H00002629-M01). A near-homogenous GBA preparation was used as a standard and Image J software was used to calculate band intensity on the resultant western blot.

Sample	Total GBA (mg)	Yield (%)
Crude *P. pastoris* media GBA-PTD4 (3L volume)	915.70	100
Post- HIC GBA-PTD4	10.71	1.17

The peak in activity using the fluorogenic substrate that was present in the desalting gradient of the HIC elution had much higher amplitude than that present in the ethylene glycol gradient. This suggested that most, if not all, of the non-specific β-glucosidases present in the medium were eluted in those fractions. To prove this theory, an HIC purification was undergone with 800 ml pPIC9K only negative control medium. Figure 3.9 shows the 4-MuGP profile of the entire HIC elution. The desalting gradient mimicked that of the GBA-PTD4 purification trials, with a single large peak of activity present at 500-600 ml total elution volume. There was, however, no peak in fluorogenic activity during the ethylene glycol gradient after either column incubations. Activity did not rise above 25 Afu, which we considered to be baseline.

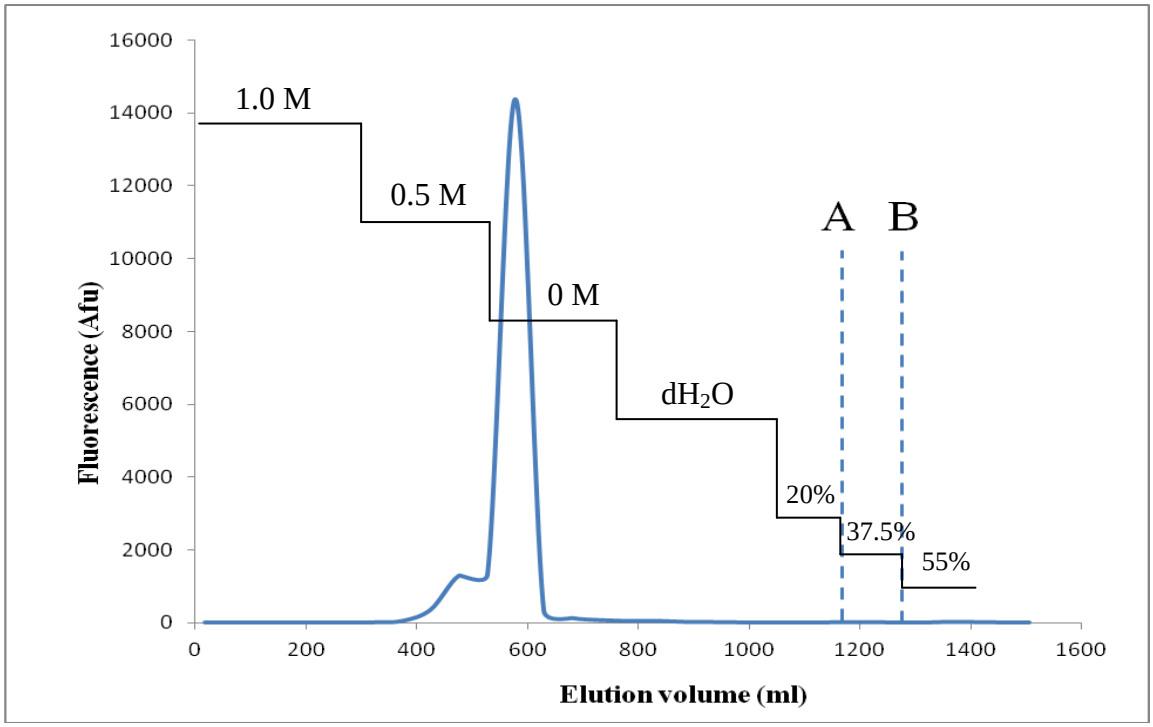

Figure 3.9. 4-MuGP activity profile of a stepwise ethylene glycol gradient from a hydrophobic interaction chromatography column where column was loaded with crude pPIC9K *P. pastoris* media.

Desalting gradient and ethylene glycol gradient were conducted in the same manner as GBA-PTD4 purification runs. 800 ml crude medium was loaded onto the column. Volume of fractions during desalting was 17 ml where volume during ethylene glycol gradient was 10 ml. A: 2 hr column incubation at 4˚C with 37.5%. B: overnight column incubation at 4˚C with 55% ethylene glycol. Fluorescence of each fraction was measured using a Sequoia-Turner Model 450 Digital fluorometer.

3.3 Gel Filtration Chromatography

The second purification step, utilizing a gel filtration chromatography column, was carried out after both types of hydrophobic interaction chromatography. Figure 3.10 and Figure 3.11 show the 4 MuGP enzyme activity profiles of elution after cholate partially purified enzyme was injected into the GFC column, and ethylene glycol partially purified enzyme injection, respectively. In Figure 3.10, a number of peaks of protein activity can be seen coming out of the column starting at approximately 55 ml and finishing at approximately 82 ml. Western blot confirms that the protein in these fractions are GBA (not shown) and the previous negative control run (Figure 3.9) confirms that non-specific glucosidases were separated from GBA during the hydrophobic interaction chromatography. Aggregation of enzyme would explain why it is eluted from the size exclusion column at various points instead of as one unit. Peaks in activity in fractions from this purification step are much lower (approximately 800 arbitrary fluorescence units) than those during hydrophobic interaction chromatography. It is possible that this can be attributed to loss of product through handling of enzyme during concentration and analysis, and the fact that it does not elute at one point from column. Area analysis of graphical profile using ImageJ software show that approximately 30% of GBA enzyme eluted in the major peak at approximately 68-72 ml total volume. Figure 3.11 shows the 4 MuGP enzyme activity profile from gel filtration chromatography of ethylene glycol partially purified enzyme. Here, the enzyme eluted in one peak with a broad base, starting at approximately 42 ml and finishing at approximately 62 ml. The earlier elution of GBA in this case is most likely due to the increased amount of ethylene glycol in the running buffer causing decreased interactions between the enzyme and the column.

The fact that there is one major peak instead of multiple peaks indicates that there is less aggregation of protein in partially purified preparation. Although the volume where enzyme is eluted is not that much smaller than with cholate partially purified preparation (approximately 25 ml versus approximately 20 ml), the peak of enzyme activity is larger (1100 Afu versus 800 Afu, indicating that more of the GBA is being eluted at the same time. This finding is also confirmed by approximate area calculation using ImageJ software; this analysis indicates that the major peak contributes to approximately 50% of the total GBA eluted from the GFC column following ethylene glycol HIC, whereas the largest peak in the GBA purification following cholate HIC contributes to approximately 30%. The increased concentration of ethylene glycol may also have a stabilizing affect on the GBA enzyme, making it a more appropriate solvent for enzyme analysis.

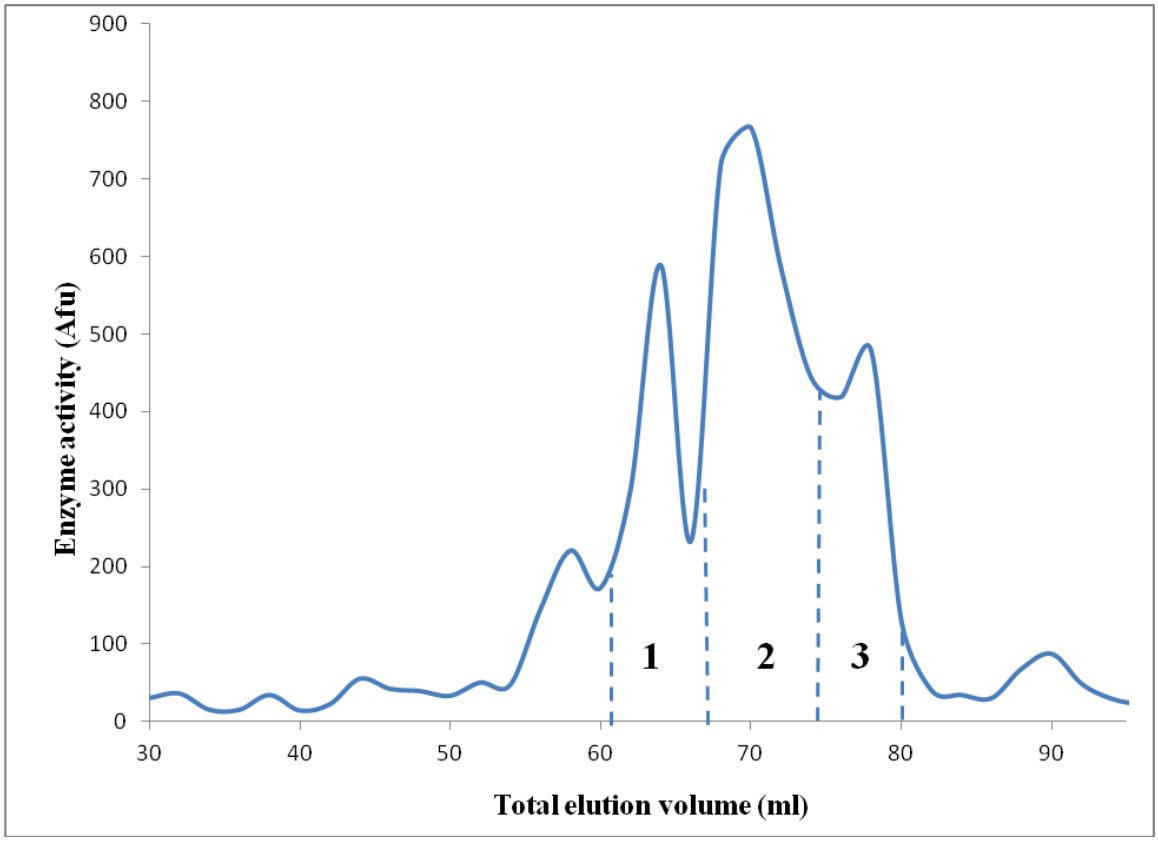

Figure 3.10. 4-MuGP activity profile from a gel filtration chromatography column injected with GBA partially purified from an HIC cholate gradient.

Elution buffer contained 15% ethylene glycol and fraction volume was 2 ml. Fluorescence of each fraction was measured using a Sequoia-Turner Model 450 Digital fluorometer. Pooled and concentrated fractions 1, 2 and 3 are indicated.

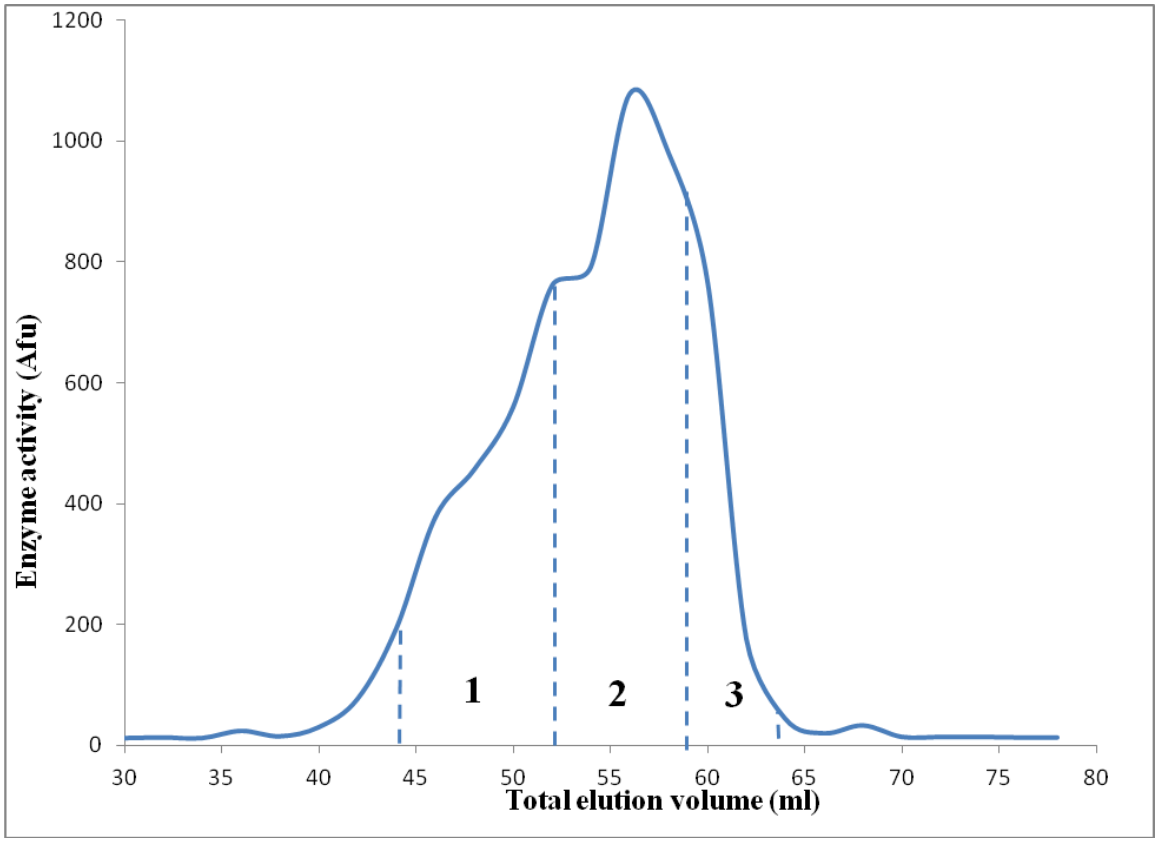

Figure 3.11. 4-MuGP activity profile from a gel filtration chromatography column injected with GBA partially purified from an HIC ethylene glycol gradient.
Elution buffer contained 55% ethylene glycol and fraction volume was 2 ml. Fluorescence of each fraction was measured using a Sequoia-Turner Model 450 Digital fluorometer. Pooled and concentrated fractions 1, 2 and 3 are indicated.

Silver stains of purified enzyme fractions also indicate that the gel filtration chromatography with ethylene glycol partially purified enzyme preparations is superior to that with cholate. Figure 3.12 shows a silver stain of purified enzyme after cholate HIC and GFC. The multiple major bands indicate that there are still a few significant contaminating species, and there is a diluted band at approximately the size of GBA.

These samples do not have GBA as the major protein species. Figure 3.13 shows that of purified enzyme after ethylene glycol HIC and GFC. Here, the strongest protein band is approximately the size of GBA, indicating that it is the major protein species. There is also a significant band at a slightly lower size, indicating that another protein was co-purified with GBA. Depending on what this protein species is, this may or may not have an effect on downstream therapeutic uses. Measurement of band intensities with ImageJ software gives a rough estimation of percentage of protein composition made up by GBA in each sample; GBA band accounts for 62% of the protein in sample 1, 76% of the protein in sample 2, and 70% of the protein in sample 3. This estimation was based on comparing the intensities of the two major protein bands, all other protein bands have either been eliminated during this purification procedure or significantly diluted. Comparison of Figure 3.12 and Figure 3.13 indicates that partial purification using ethylene glycol before gel filtration chromatography gives a better final enzyme preparation that is very near homogenous.

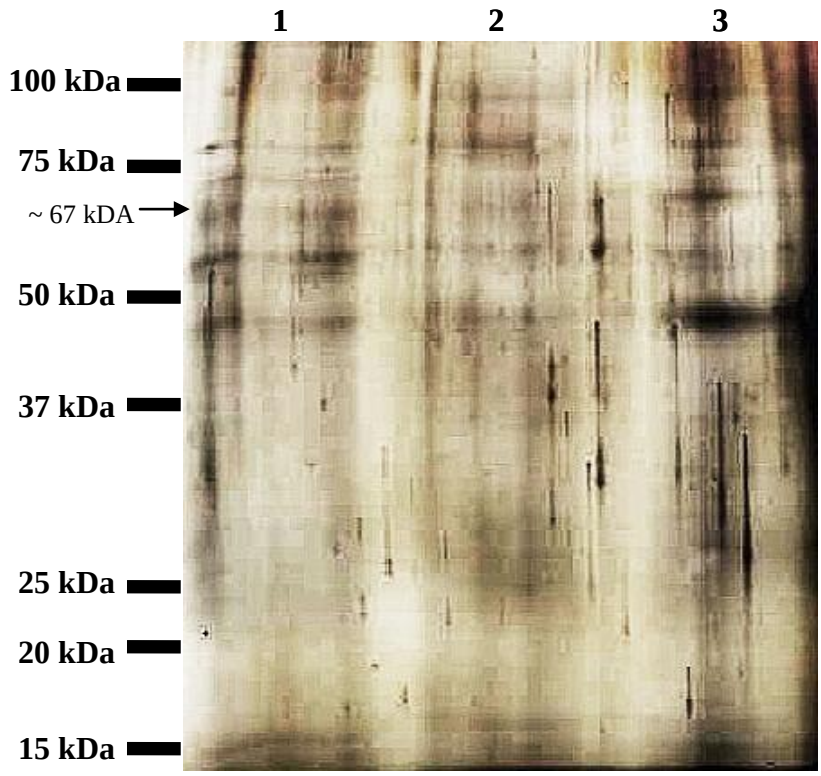

Figure 3.12. Silver stain of concentrated fractions after second purification step using a gel filtration chromatography column following partial purification with cholate HIC elution. 4-MuGP activity analyses were done on each 2 ml fraction eluted from the column and peaks were pooled and concentrated into samples 1, 2, and 3. Protein separation was achieved through SDS-PAGE before staining with silver nitrate. A dual-color protein marker (BioRad) was run on SDS-PAGE for size identification. A concentrated partially purified sample was run as well, but stained too darkly to see (not shown). A minor protein species is seen at the approximate size of GBA (approximately 67 kDa).

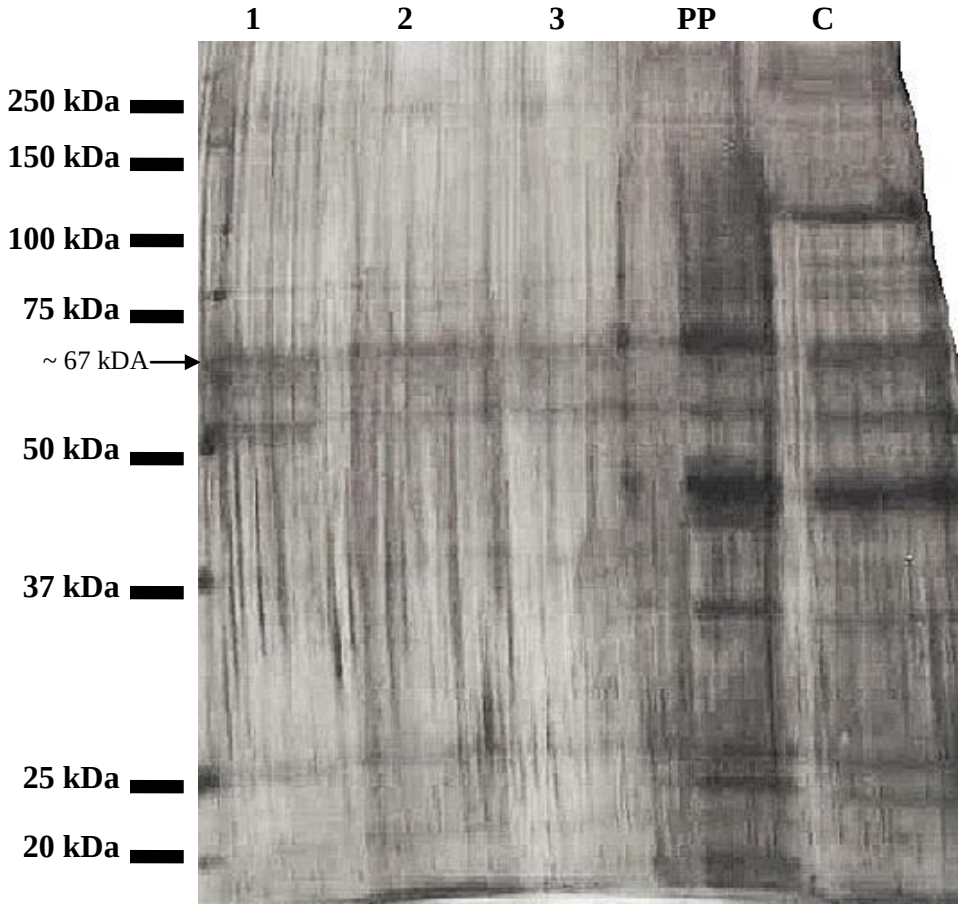

Figure 3.13. Silver stain of concentrated fractions after second purification step using a gel filtration chromatography column following partial purification with HIC with an ethylene glycol elution.

4-MuGP activity analyses were done on each 2 ml fraction eluted from the column and peaks were pooled and concentrated into samples 1, 2 and 3. Protein separation was achieved through SDS-PAGE before staining with silver nitrate. A dual-color protein marker (BioRad) was run on SDS-PAGE for size identification. Concentrated partially purified sample (PP) as well as concentrated crude medium (C) run on SDS-PAGE as well. A major protein species is present at the approximate size of GBA (approximately 67 kDa).

Western blot of concentrated samples was used to confirm the presence of GBA (Figure 3.14). Long exposure of film revealed presence of smaller amounts of GBA in sample 1 (not shown). Sample 2 had a large concentration of GBA as this was taken from the very peak of activity.

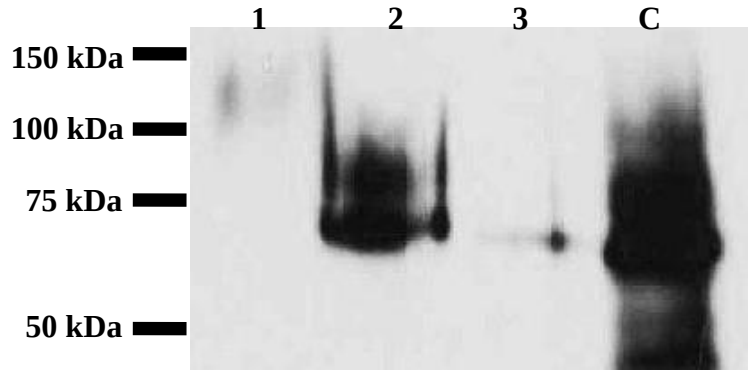

Figure 3.14. Western blot of concentrated fractions after second purification step using a gel filtration chromatography column.
Concentrated enzyme partially purified using ethylene glycol HIC was inejected into column, and 4-MuGP activity analyses were done on each 2 ml fraction eluted from the column and peaks were pooled and concentrated. Protein separation of pooled fractions 1 and 2, as well as crude medium (C) was achieved through SDS-PAGE before transfer to a PVDF membrane and probing with anti-GBA mAb (Abnova, H00002629-M01). A dual-color protein marker (BioRad) was run on SDS-PAGE for size identification. A strong band of appropriate size for GBA was seen in sample 2, with a fainter one in sample 3. Sample 1 did not have enough enzyme to be picked up with this short of exposure, but longer exposure revealed a small amount of enzyme product (not shown).

An estimation of total GBA-PTD4 recovery of the GFC purification step was done with immunoblot band intensity comparison and is shown in Table 3.2. The GFC step yielded approximately 6.9% of the total HIC purified GBA-PTD4 that was loaded onto the GFC column, a total of approximately 500 μg. This analysis was done after all concentration and analysis steps.

Table 3.2. Estimation of purification yield of GFC as determined by immunoblot band intensity comparison.
HIC purified GBA-PTD4 and concentrated post-GFC pooled samples were run on an SDS-PAGE and transferred to a PVDF membrane to be probed with a GBA specific mAB (Abnova, H00002629-M01). A near-homogenous GBA preparation was used as a standard and Image J software was used to calculate band intensity on the resultant western blot.

Sample	Total GBA (mg)	Yield (%)
HIC purified GBA-PTD4	7.65	100
Post- GFC GBA-PTD4	0.53	6.90

3.4 Analysis of custom monoclonal antibodies

Six samples of mouse ascites fluid were obtained from Abmart (Shanghai, China) and screened for affinity and specificity towards GBA-PTD4. ELISA screening of the antibodies using both GBA-PTD4 *P. pastoris* medium and vector-only medium indicated the strength of affinity of each antibody to the antigen as well as non-specific binding.

Figure 3.15 shows the antibody activity against crude medium containing GBA-PTD4, where a strong signal can be seen at the initial dilution of 1/400. The signal drops off rapidly with increasing dilutions of the ascites fluid, which does not correlate with Abmart's predicted titre of 128K against the peptide epitope. The strong signal at higher dilutions, however, shows promise for further downstream analysis.

The monoclonal anti-GBA antibodies from Abmart were sent to us as ascites fluid as opposed to a purified form, for this reason, it was possible that some of the signal seen in the ELISA analysis was due to non-specific antibody activity. A negative control ELISA using vector-only *P. pastoris* medium was performed to assess this. Figure 3.16 shows that although there was antibody activity using the negative control antigen, this was decreased in comparison to the GBA-PTD4 antigen. Sample 425-3 showed the highest non-specific activity, where the absorbance with the negative control was approximately 2.7 compared with GBA-PTD4 which had an absorbance of approximately 4.5. The other ascites samples showed activity of 1.5 or less with the negative control antigen, in the range of a 3-4X decrease in antibody activity.

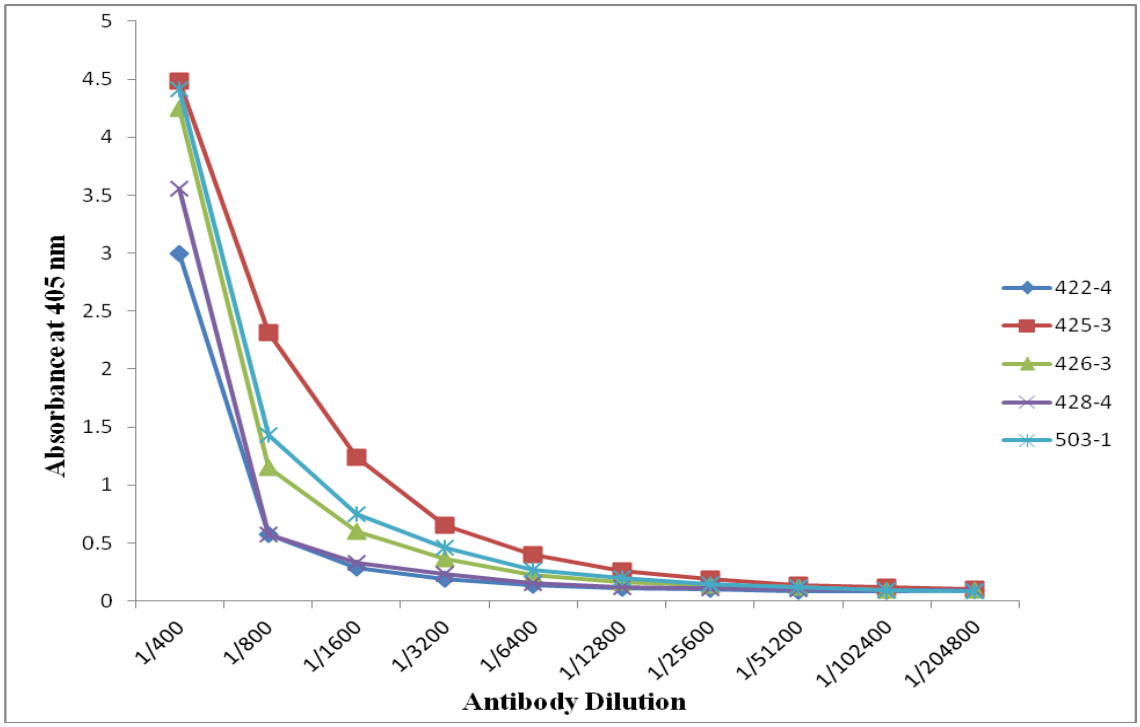

Figure 3.15. ELISA reading of antibody activity against GBA-PTD4 *P. pastoris* crude medium.

Five different ascites fluid samples (the first shipment: 422-4, 425-3, 426-3, 428-4, 503-1) were tested against GBA-PTD4 in crude medium. Antibody dilution started at 1/400 and was increased exponentially. A secondary goat-anti mouse IgG/IgM Alk-Phos antibody was used to confer a signal on the ELISA reader at a wavelength of 405 nm.

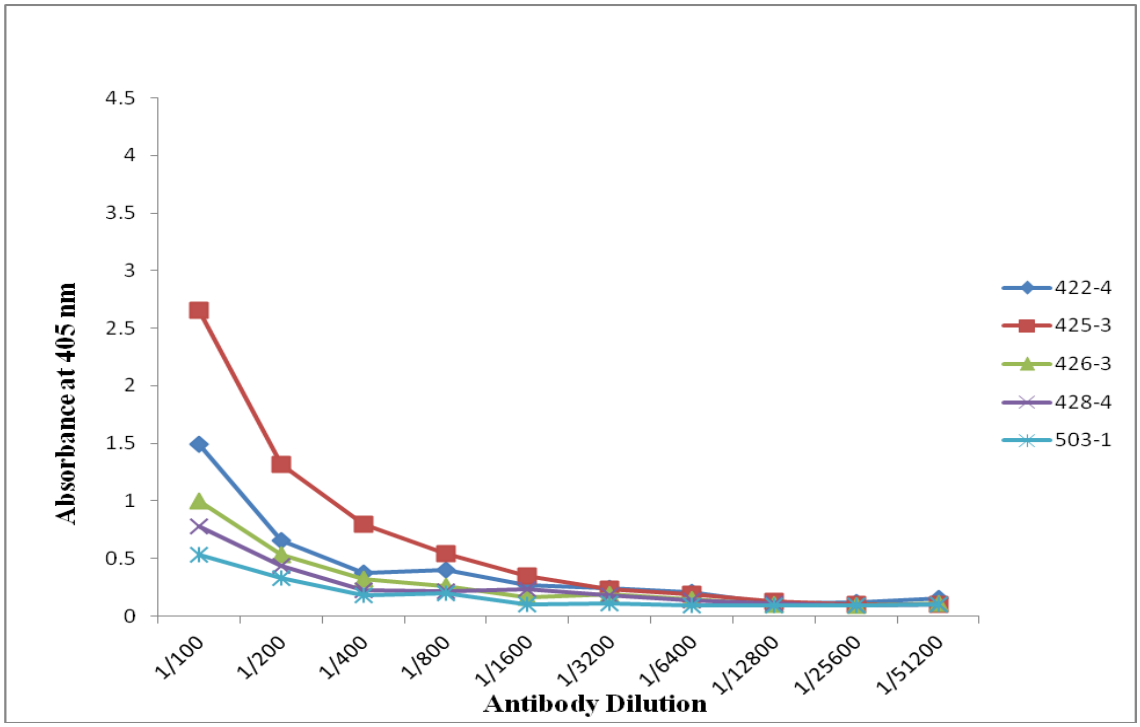

Figure 3.16. ELISA reading of antibody activity against vector-only *P. pastoris* crude medium.

Five different ascites fluid samples (the first shipment: 422-4, 425-3, 426-3, 428-4, 503-1) were tested against GBA-PTD4 in crude medium. Antibody dilution started at 1/400 and was increased exponentially. A secondary goat-anti mouse IgG/IgM Alk-Phos antibody was used to confer a signal on the ELISA reader at a wavelength of 405 nm.

SDS-PAGE analyses as well as western blots using GBA-PTD4 crude medium as the sample probing with custom monoclonals were also performed to test each of the antibodies against denatured antigen. Ascites from 503-1 and 426-3 showed no signal against the antigen on the membranes whereas ascites sample 425-3 had such high background that the whole membrane showed as dark signal. Ascites fluid 422-4 showed a high background initially similar to sample 425-3, but upon further washing of the membrane and an immediate exposure a single band was present (Figure 3.17 **a**). This band however was slightly larger than the expected GBA product (just under 100 kDa

instead of around 67 kDa). When ascites fluid 428-4 was used for a western blot showed two bands, one approximately 67 kDa and one approximately 100 kDa (Figure 3.17 **c**). The ascites fluid 526-2 bound to a single protein species, but similar to 428-4 this species was slightly larger than what was expected from previous western blots, where the signal for GBA was approximately 67 kDa (Figure 3.17 **b**). The pure monoclonal mouse anti-GBA antibody purchased from Abnova was used as a positive control, since this had proven to work well in past western blots. This blot showed a band of expected size, as well as some smaller bands indicating the protein degradation products (Figure 3.17 **d**).

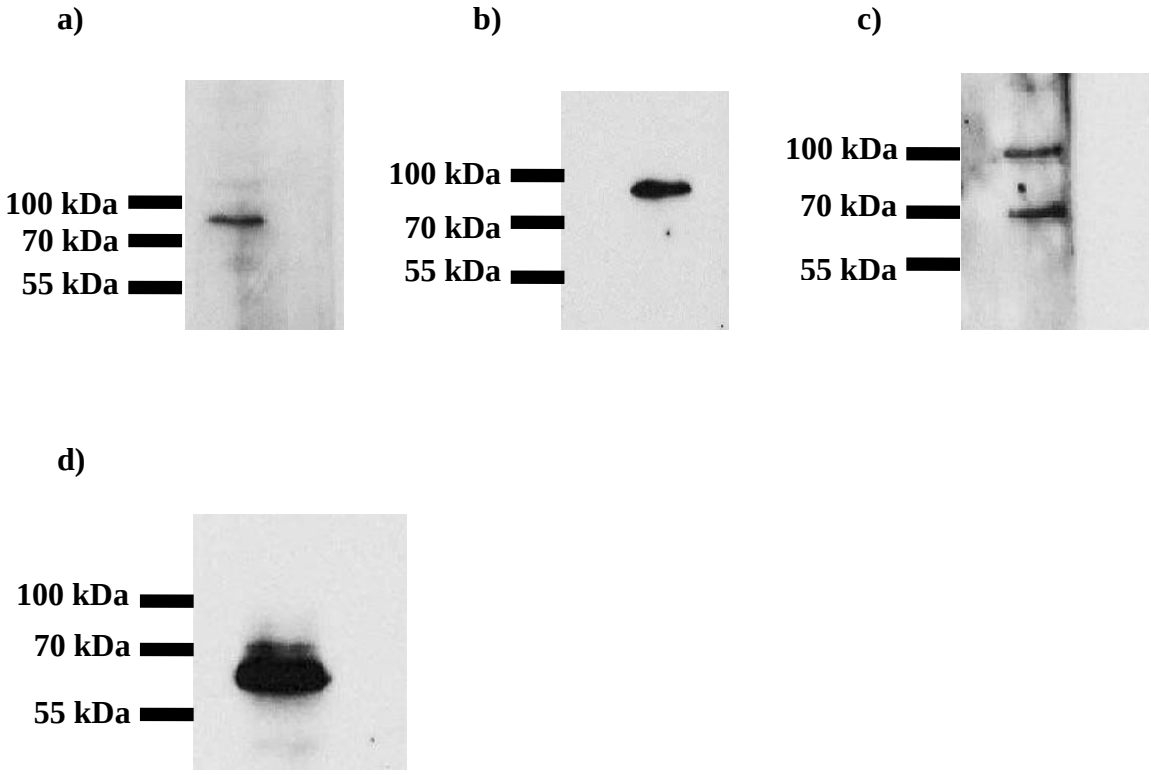

Figure 3.17. Western blot analyses of ascites fluid using crude GBA-PTD4 *P. pastoris* medium as the antigen.

Proteins from crude GBA-PTD4 medium were separated using SDS-PAGE analysis and transferred to a PVDF membrane. Ascites samples 422-4 **(a)**, 526-2 **(b)**, 428-4 **(c)** and positive control monoclonal from Abnova **(d)** were used to probe membranes as the primary antibody, and secondary goat anti-mouse was used to amplify the signal. Samples were not all run on the same gel, but a protein standard was run alongside each to estimate band size. Abnova monoclonal and 428-4 had bands at approximately 67 kDa. A second, larger band was present in 428-4, and larger bands (~ 100 kDa) were present in 422-4 and 526-2.

In order to assess whether the ascites fluid samples 422-4, 428-4, 526-2 would recognize the folded recombinant protein as well as the denatured amino acid sequence, an immunoprecipitation experiment (aka "pull down experiment") was done using magnetic beads and crude GBA-PTD4 medium. Separated primary antibody and antigen were run on SDS-PAGE and a western blot was performed with each respective ascites fluid sample. The blots are shown in Figure 3.18. Bands just above the 55 kDa marker represent the heavy-chain of the antibodies, which is present in every sample. The pure mouse monoclonal from Abnova (membrane 1) used as a positive control for western blots does not show any other protein signal, indicating that this antibody is not suitable for recognition of folded GBA. Immunoprecipitation with each of the ascites fluid samples 422-4, 428-4, 526-2 (membranes 2, 3 and 4, respectively) enriched a protein which is approximately 67 kDa in size. The similarity in size to the heavy-chain of the antibody makes it difficult to separate, but upon close inspection of the exposed film, it is apparent that there are two bands present. Efforts to confirm that this protein is GBA-PTD4 are currently underway, and include repetition of the immunoprecipitation experiment followed by excision of the ~67 kDa band from the SDS-PAGE gel for identification using mass spectrophotometry.

These results indicate that one or more of the commercial antibodies generated by Abmart may bind to both denatured and folded recombinant GBA-PTD4 present in crude *P. pastoris* medium. Upon confirmation of this, these antibodies can be generated in larger quantities using the mouse hybridoma cell lines; this would enable our lab to attempt immunochromatography for the purification of GBA-PTD4.

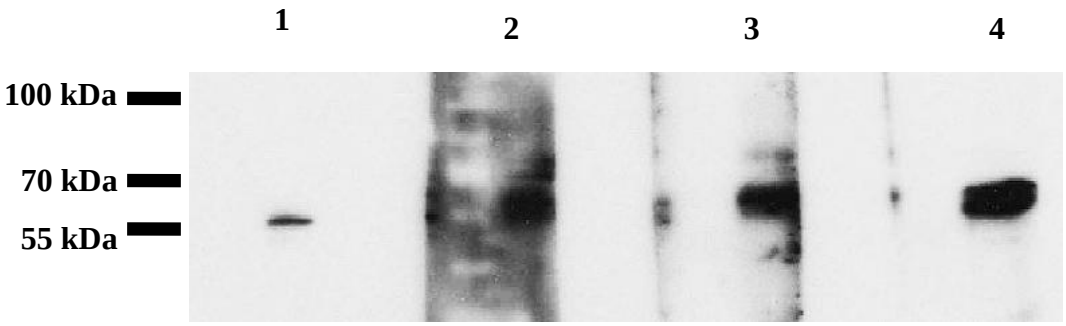

Figure 3.18. Western blot showing the results of the immunoprecipitation experiment with selected commercial antibodies and crude GBA-PTD4 *P. pastoris* medium as the antigen.

Magnetic beads coated with goat anti-mouse antibody were combined with sample ascites fluid initially and then combined with crude GBA-PTD4 medium. Beads were separated from mixture and primary antibodies and antigens were removed and separated by SDS-PAGE before being transferred to a PVDF membrane. Each membrane was probed with the same antibody as was used in the immunoprecipitation. Membrane 1 represents the pure Abnova mouse monoclonal, membranes 2, 3, and 4 are samples 422-4, 428-4, and 526-2 respectively. There is one band at just above 55 kDa present in all samples which represents antibody heavy-chain, membranes 2,3 and 4 also have a band present at approximately 67 kDa, the size of GBA.

3.5 Construction of *GBA*-only cell line

3.5.1 Construction of expression vector

Amplification of the *GBA* gene was followed by A-tailing and A/T ligation into the pGEM-T vector. After amplification of this vector by transformation of DH5α *E. coli* cells, double digestion was used to confirm successful ligation (Figure 3.19 **a**) as well as sequence confirmation to determine that the transgene was error free. Digested insert was then ligated into the pPIC9K expression vector in preparation for *P. pastoris* transfection. Again, double digestion (Figure 3.19 **b**) was used to confirm successful ligation of

amplified vector, and sequence was confirmed to be error free. For each digestion, a product of approximately 1.5 kB corresponding to *GBA* was detected along with vector products, approximately 3 kB for pGEM-T and approximately 9.3 kB for pPIC9k. Non-digested, circular plasmids were run alongside digestion products, which corresponded roughly to expected sizes, although slight deviation from the expected was allowed based on abnormal sieving of circular DNA in agarose gels.

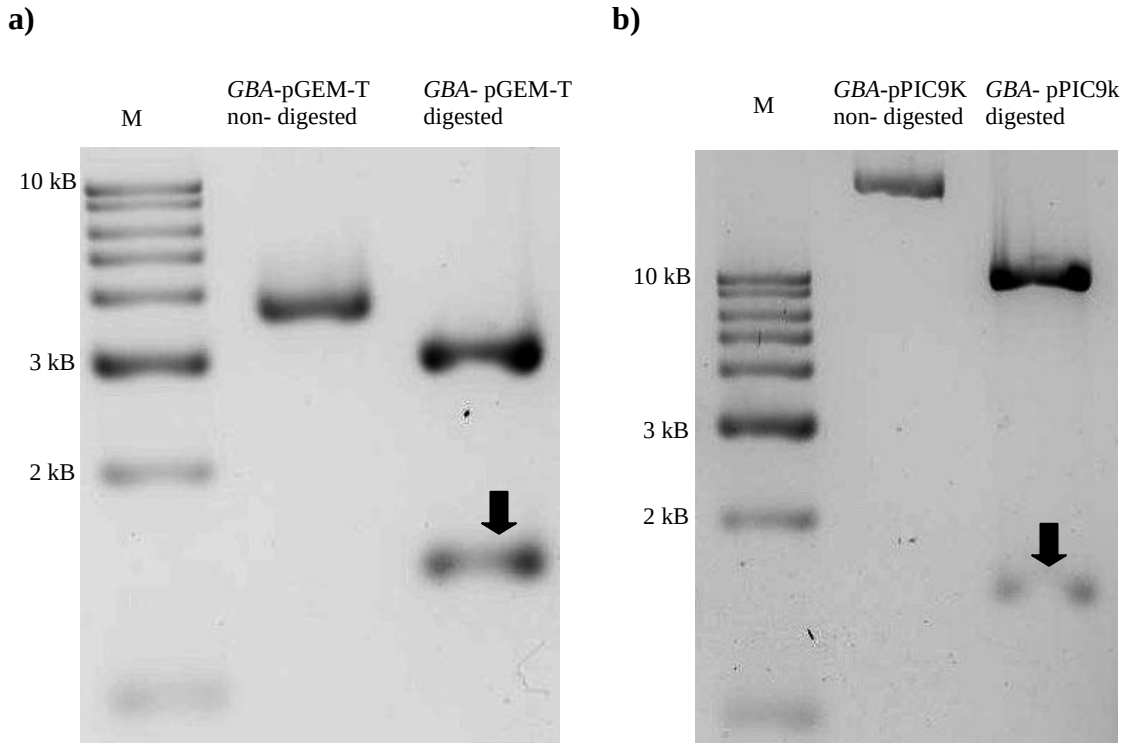

Figure 3.19. Agarose gel of EcoRI and NotI digested *GBA*-pGEM-T (a) and *GBA*-pPIC9k (b) expression vectors created for construction of *GBA*- only cell line.
Arrows indicate products which are the expected size of *GBA* insert (1.5 kB). Larger products of digestion are of expected sizes for each vector (3 kb and 9.3 kB for pGEM-T and pPIC9K respectively). Non- digested, circular plasmids with inserted *GBA* were run alongside digestion products. M denotes 1 kB DNA marker (NEB).

3.5.2 Transfection of *P. pastoris* and Mut^{+}/ Mut^{S} phenotype characterization

Expression vectors with confirmed error free insertions of *GBA* were used to transfect a humanized GS115 *P. pastoris* cell line. Clones which had been successfully transfected were selected on histidine deficient plates before being screened for multiple-copy insertions on increasing concentrations of geneticin. Clones which showed resistance to 0.75 mg/ml were further tested for presence of *GBA* within the *P. pastoris* genome by direct yeast PCR using vector specific primers which annealed to 5' *AOXI* (sense) and 3' *AOXI* (anti-sense). Figure 3.20 shows an example of a direct yeast PCR amplification with products run on an agarose gel. For some clones, one product can be seen by amplifying with these primers which corresponds to the approximate size of 2 kB expected for *GBA* amplification (1.5 kB for *GBA* + 0.5 kB vector amplification). These clones can be designated with the Mut^{S} genotype, since it appears as if the endogenous *P. pastoris* AOXI gene is not being amplified, indicating it has been replaced by the expression cassette during transfection. Some clones, on the other hand, have two products amplified by the 5' *AOXI*/ 3' *AOXI* primer set. These clones can be designated with the Mut^{+} genotype, since the endogenous *AOXI* gene appears to be present. Amplified genomic DNA from GBA-PTD4 *P. pastoris* cell line (Mut^{S}) has one band at approximately 2 kB present, while that amplified from non-transfected *P.pastoris* cells has only a 2.2 kB band present, which represents *AOXI*.

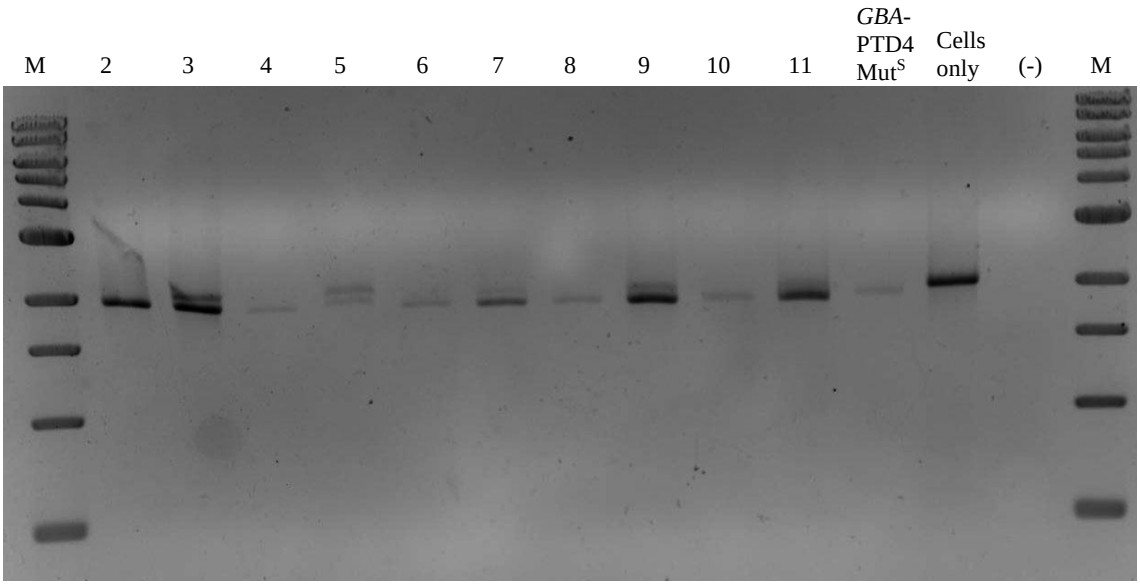

Figure 3.20. Agarose gel of direct yeast PCR amplification of *GBA*-pPIC9K from *P. pastoris* transformants using 5' *AOXI*/ 3' *AOXI* vector specific primer set.
M denotes 1 kB DNA marker (NEB). Lanes numbered 2-11 contain PCR products from various selected transformants. Genomic DNA from *GBA*-PTD4 *P. pastoris* cell line previously determined to be Mut^S was also amplified along with untransfected *P. pastoris* (cells only). A negative control (-) for the PCR was also run on the agarose gel. The smaller band at approximately 2 kB in all clones represents amplified *GBA*-pPIC9K. The larger band resolved in 3, 5,7 and 9 (approximately 2.2 kB) represents endogenous *AOXI* gene amplified in Mut^+ clones.

Confirmation of Mut^S/Mut^+ status was also done phenotypically by looking at comparative growth on methanol medium. Transformants were grown on plates with either dextrose or methanol as a carbon source. Comparison of growth at approximately 48 hrs revealed that all clones grew very well on dextrose medium. Growth on methanol medium was slightly slower for all clones, but there were some clones with noticeably stunted growth while using methanol as a carbon source. Most of the clones had appreciable growth on both dextrose and methanol, and these could be confirmed as Mut^+

phenotype. There were generally fewer clones in each selection which showed the Mut^S phenotype by displaying comparatively slower growth on methanol. Figure 3.21 **(a)** and **(b)** shows an example of methanol utilization phenotype screening of a selection of *P. pastoris* transformants.

a) **b)**

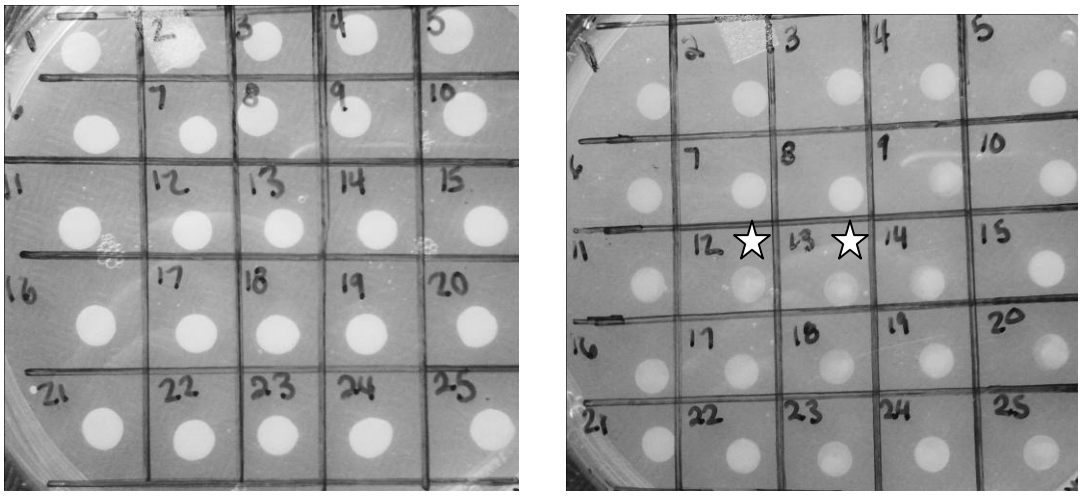

Figure 3.21. Phenotypic screening of *P. pastoris* transformants by plating on dextrose agar media (a) and methanol agar media (b) to determine Mut^+ and Mut^S integrants.
Of these 25 selected clones, the two denoted with a star showed noticeably slower growth on methanol medium, and therefore are likely to be Mut^S integrants.

3.5.3 Trial GBA expression studies

Selected Mut^+ and Mut^S clones were grown in large scale cultures to observe relative GBA expression levels. GBA was detected in non-concentrated crude medium from both clones through western blot (Figure 3.22). There was a stronger band present in the Mut^S crude medium compared with the Mut^+, indicating a higher GBA expression level in this clone. Higher expression also seems to lead to a higher amount of protein degradation, as there is the presence of a smaller protein band which is also detected by the GBA mAb.

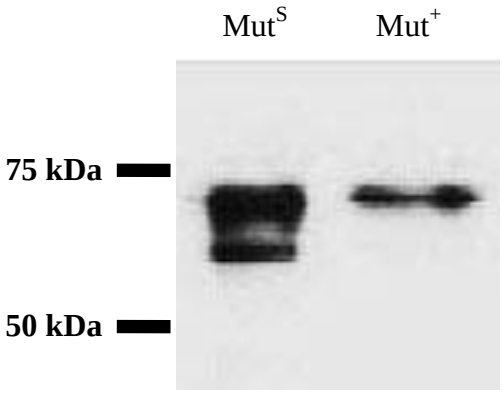

Figure 3.22. Immunoblot showing relative GBA expression levels of a selected Mut^S and Mut^+ cell line.

Proteins in non-concentrated crude medium were separated using SDS-PAGE and transferred to a PVDF membrane to be probed with an anti-GBA mAb (Abnova, H00002629-M01). A dual-color protein marker (BioRad) was run on SDS-PAGE for size identification. A strong GBA signal was detected at the approximate size of GBA (67 kDa) in crude medium from both clones, although the Mut^S clone had a stronger band. The smaller protein band indicates some GBA degradation.

Chapter 4 Discussion

4.1 GBA-PTD4 partial purification by HIC

4.1.1 HIC principles and desalting gradient

Initial purification of GBA-PTD4 from *P. pastoris* induction medium was done through hydrophobic interaction chromatography. Endogenous GBA is highly associated with the lysosomal membrane, and therefore has a high degree of hydrophobicity which makes it a good candidate for HIC purification (Dvir *et al*. 2003; Furbish *et al*. 1977). The principles of HIC are reviewed separately by Queiroz, *et al*. (2001) and Roettger and Ladisch (1989). At high salt concentrations, interactions between proteins and a weakly hydrophobic solid matix are promoted. Decreasing salt concentrations gradually in the running buffer weakens the interactions, eluting proteins in the order of their increasing hydrophobicities; this is termed "the salting out effect". Ammonium sulphate is reportedly one of the best salting out agents for use in HIC, as both the NH_4^+ cation and the SO_4^{2-} anion promote strong initial retention of proteins.

The desalting gradient depicted in Figure 3.2 and Figure 3.3 allows for separation of many endogenous *P. pastoris* proteins which are less hydrophobic than the GBA enzyme. Small scale HIC purification trials performed previously in our lab indicate that an initial ammonium sulphate salt concentration of 1.45M is optimal for protein retention (Goebl 2010). The ability of ammonium sulphate to precipitate proteins in solution makes optimal concentration of salt in loading buffer an important consideration (Jiang, *et al*.

2004). A concentration too low will not produce the desired amount of protein retention on the column, but too much salt could precipitate recombinant enzyme.

Initially, a continuous desalting gradient was utilized for protein elution in small scale trial procedures. A continuous gradient is desirable because of the high degree of resolution of protein peaks. This method required use of an Atka Prime FPLC system (Amersham Biosciences), which had a high degree of back-pressure. Upon scaling up of this procedure to a semi-preparative level, a 50 ml HIC custom packed column (BioRad) was used instead of the 5 ml pre-packed column (HiTrap™ Phenyl HP, GE Healthcare) used previously. A larger column allowed loading of at least10X more crude medium during each run, but made protein loading and elution difficult using the automated FPLC equipment; this is why a step-wise desalting gradient was utilized during large scale purification runs. For a step-wise gradient, an FPLC pump with one intake valve was used, which created a lower back pressure than the automated system. Over multiple runs, the desalting gradient was well characterized and highly reproducible. Figure 3.2 shows the protein elution pattern during the step-wise desalting gradient; with each decrease in salt concentration a new protein peak is eluted from the column. It is speculated that each peak contains a mixture of endogenous *P. pastoris* proteins which are secreted into the induction medium, and proteins present in the same elution peak will have relatively similar hydrophobicities based on background knowledge of HIC theory. Characterization of each of the proteins eluted is unnecessary in the scope of this project.

A large peak in activity with the 4-MuGP substrate was seen during the desalting gradient protein elution (Figure 3.3). Figure 3.4 shows the calculated GBA activity with the natural lipid substrate in both the desalting gradient and the cholate gradient; this

assay shows that the desalting gradient contains approximately one third of the amount of active GBA enzyme that the cholate gradient contains (6.34 nmol glucose/ml/hr and 18.40 nmol/glucose/ml/hr, respectively). We postulate that the small amount of GBA-PTD4 being eluted in the desalting gradient is due to incidental weakening of hydrophobic interactions between GBA-PTD4 and the column matrix when large amounts of contaminating endogenous *P. pastoris* proteins are eluted.

The large peak in activity present in the desalting gradient has been attributed to β-glycosidases which are endogenous to *P. pastoris* and will also cleave the artificial substrate. Mattanovich *et al*. (2009) conducted a thorough investigation on the *P. pastoris* secretome and found that 38% of secreted proteins were predicted to have glycosidase function. As more information on the *P. pastoris* secretome is uncovered, it may be possible in the future to directly inhibit these non-specific glucosidases in order to decrease the background activity levels in the crude induction medium to develop a method to get an accurate GBA activity estimation by 4-MuGP analysis.

4.1.2 Elution of GBA-PTD4 from HIC column

Cholate elution

For proteins with a high hydrophobicity, such as GBA, a desalting gradient is not enough to disrupt the interactions between the protein and the column matrix; for these conditions where milder methods are ineffective, additives can be introduced to enhance protein elution (Queiroz, *et al*. 2001). Two of the common reagents used to elute highly hydrophobic proteins are detergents such as cholate, and water-miscible alcohols such as

ethylene glycol. Both have been used as an elution agent in the purification of GBA in past experiments.

Previous attempts to purify GBA-PTD4 in our lab utilized a continuous cholate gradient to elute GBA from a pre-packed 5 ml HIC column (Goebl 2010). According to this study, a cholate detergent was an effective way to displace GBA from the hydrophobic matrix, and peaks in activity were seen in both the water wash and beginning of the cholate gradient.

Upon scaling up the procedure to a semi-preparative level using a custom-packed 50 ml HIC column and 10X the amount of crude medium, a cholate gradient also worked to elute GBA in a highly resolved peak from the column (not shown). Ionic detergents are successful in displacing bound proteins by competing for ligands on the hydrophobic matrix (Queiroz, *et al*. 2001; Shukla *et al*. 2002); Wetlaufer and Koenigbauer (1986) describe the successes of a cholate derivative ionic detergent, 3-[(3-cholamidopropyl)dimethylammonio]-l-propane sulfonate (CHAPS), to displace proteins from hydrophobic columns with varying elution patterns, making it appropriate for high resolution chromatography.

Although we had success collecting partially purified GBA-PTD4 with a cholate gradient there was a noticeable aggregation of the protein in the preparations, as is shown in the western blot in Figure 3.5 **(a)**, where the protein can be detected as a smear instead of in its monomeric form. The aggregation was irreversible, as dialyzation of the protein samples did not appear to have a significant effect and just added to the loss of enzyme due to increased handling. Im, *et al*. (1990) reported a similar aggregation affect when attempting to use cholate to solublize a membranous G-coupled protein receptor.

Detergents such as cholate are amphipathic, and have been reported to form micelles above a critical micelle concentration (CMC) (Chattopadhyay and Harikumar 1996). Because of the hydrophobic nature of GBA, we speculate that it may become incorporated in the hydrophobic centers of the micelles forming from the detergent molecules, as this would explain the aggregation seen in the protein preparations. It is possible that the increased concentration of cholate (between 1 and 2%) needed to elute GBA-PTD4 from the semi-preparative column was over the CMC, so as to create micelles in these enzyme samples where in past experiments there was no formation of aggregates. Also, the increased concentration of protein could have an effect on the CMC, since it has been reported that this concentration can fluctuate according to many different variables (Wetlaufer and Koenigbauer 1986). Although this method would be considered successful in that GBA-PTD4 was efficiently eluted and partially purified from much of the endogenous *P. pastoris* proteins, enzyme aggregates decrease the efficiency of our second purification step, which involves size exclusion. To this end, we sought to find a different procedure for initial purification that would approximate the efficiency of the cholate gradient but yield a monomeric enzyme preparation.

Ethylene glycol elution

Ethylene glycol is another frequently used elution agent in HIC protein purification as it can compete for ligand binding and decrease hydrophobic interactions between proteins and the column matrix (Queiroz, *et al*. 2001; Ray 1969). Among water-miscible alcohols, ethylene glycol is particularly advantageous as an elution agent because it is a very mild denaturant; proteins are stable in moderate concentrations of

ethylene glycol (up to approximately 50%) and even in its pure form or at extremely high concentrations of 80-90% there is minimal unfolding of some proteins (Nemethy and Ray 1971). Ethylene glycol has been used in the purification of GBA with a number of different affinity columns, including HIC. Furbish *et al*. (1977) used an ethylene glycol gradient from 30-80% to displace placental (native) GBA from an HIC column, with GBA eluting at approximately 60% ethylene glycol. Grabowski and Dagan (1984) purified native GBA using substrate affinity chromatography as one purification step, where they report that most of the GBA enzymatic activity is seen within fractions eluted between 40-60% ethylene glycol. Ethylene glycol has also been used to elute native GBA from an immunoaffinity column, where 90% ethylene glycol was optimal for disruption of GBA binding to monoclonal antibody, and did not interfere with enzyme activity (Aerts *et al*. 1986). An added bonus of using ethylene glycol is that it has been reported to have a stabilizing effect on the GBA enzyme. Both Grabowski and Dagan (1984) and Aerts *et al*. (1986) describe enzyme stability at freezing temperatures of -20˚C (for approximately 50% ethylene glycol) or 0˚C (for 90% ethylene glycol) upon storage for several weeks to a year. Ethylene glycol has freezing temperatures much below that of water or other aqueous solutions such as cholate: ethylene glycol freezes at -13˚C in its pure state, and below -45˚C when it's at approximately 60% concentration; in this way, it provides protection of the protein by minimizing loss of activity due to freeze/thawing that is required for enzyme storage in cholate. Because of the successes in elution and storage of GBA in ethylene glycol in past literature, it was a likely candidate for experiments in our own laboratory.

An initial purification trial with ethylene glycol used stepwise increases in ethylene glycol concentration from 0% in the water wash, then 4%, 8%, 12%, 20%, 30%, 40% and finally 50%. Activity analysis of each of the fractions using the fluorogenic substrate indicated that 50% ethylene glycol was sufficient to elute GBA-PTD4 from the column, but the resolution using this method was poor, as we did not see a sharp peak of enzyme elution but rather a slow diffusion off the column. The enzyme came out in various peaks over approximately 400 ml of 50% ethylene glycol buffer, which not only affected the purity of the sample but also made concentration a long process which reduces the activity of the enzyme due to excessive handling. Furbish *et al*. (1977) used a decyl-agarose column and a linear gradient of ethylene glycol for HIC purification of native human GBA enzyme. Perhaps the continuous gradient of ethylene glycol was essential to their success in obtaining a high degree of resolution; however, due to the high back pressure created by increased concentrations of ethylene glycol and our equipment limitations, optimizing the stepwise gradient was the best option for our purification procedures.

During this trial run, we noticed that following an overnight column incubation in 50% ethylene glycol (mandatory due to the length of the procedure) there was a significant increase in protein elution. We concluded that for this particular procedure, incubation of the column with increased ethylene glycol would promote better resolution and did not appear to have a detrimental effect on protein activity. Figure 3.7 and Figure 3.8 show the protein elution pattern and fluorogenic activity, respectively, from an HIC elution with 2 column incubations, four hours incubation with 37.5% ethylene glycol and overnight incubation with 55% ethylene glycol. The initial incubation serves to elute

more proteins which are less hydrophobic than GBA and consequently improve the purity of the resulting enzyme preparations. Protein elution patterns in Figure 3.7 show a resolved peak in protein elution following this incubation, while the activity profile (Figure 3.8) shows no increase in fluorogenic activity, indicating that this concentration of ethylene glycol is not sufficient to produce the elution of GBA-PTD4. The second incubation was meant to displace more hydrophobic proteins such as GBA. Previous trials which indicated that 50% ethylene glycol was just enough to promote the dissociation of GBA-PTD4 from the column prompted us to use a 55% buffer as well as an overnight incubation, to ensure the removal of the entire amount of enzyme that had been retained on the column in as little volume as possible. This concentration of ethylene glycol for GBA elution is in keeping with other past experiments, where similar concentrations have been used successfully for GBA purification (Furbish *et al*. 1977). The sharp peak in activity following the incubation indicates that this method was successful in the collection of GBA-PTD4. To confirm that this peak in activity was due only to GBA-PTD4 and not in part by other non-specific glucosidases present in the medium, a negative control HIC run was carried out. Figure 3.9 shows the 4-MuGP activity profile of an HIC run (both desalting gradient and ethylene glycol gradient) with pPIC9K only crude *P. pastoris* medium. The same profile as the GBA-PTD4 crude medium run was seen in the desalting gradient, however, a peak in activity was not seen following overnight incubation of the column with 55% ethylene glycol. This indicated that the activity seen in fractions during the ethylene glycol gradient are due to GBA-PTD4, and other non-specific glycosidases have been separated from the recombinant protein with this purification step.

The large peak in protein elution following the incubation shows that there are likely many proteins of approximately the same hydrophobicity as GBA which are also displaced from the column in 55% ethylene glycol; this is confirmed by the many proteins shown by SDS-PAGE and silver stain analysis (Figure 3.6). A significant reduction of proteins present can be detected in the HIC partially purified preparations compared with that of the crude induction medium, lending to the effectiveness of HIC with ethylene glycol elution as an initial step in purification of GBA-PTD4. A major band in the silver stain is present at the appropriate size for GBA, and correlates with the GBA specific band seen after western blot analysis (Figure 3.5 **b**). This indicates that although there are many contaminating proteins at this stage in the purification, GBA-PTD4 has a major presence in the heterogeneous protein mixture. Comparisons between western blot analyses after a cholate elution and ethylene glycol elution are presented in Figure 3.5 **(a)** and **(b)**. A decrease in smearing upon SDS-PAGE protein separation leads us to believe that use of ethylene glycol as an elution agent does not have the protein aggregation affect that cholate appears to have under these conditions. GBA-PTD4 appears to be in a monomeric form, which is optimal for proceeding with size exclusion purification.

Protein yield was calculated based on band intensity comparisons in an immunoblot. The approximate yield of GBA-PTD4 after an HIC purification run was quite low, at 1.17% that of GBA-PTD4 present in crude medium loaded onto the column (Table 3.1). We predict that there is a major loss of protein during the concentration steps that is unavoidable with this procedure. Partially purified enzymes need to be amicon concentrated, centricon concentrated, or both, depending on the volume of the sample.

Another point of GBA-PTD4 loss during the procedure is the desalting gradient, where some GBA activity is detected due to incidental disruption of binding to the column matrix (Figure 3.4). Initially, we thought that another point of loss may be initial retention, where the column was not able to bind all GBA-PTD4 present in the crude medium. Low activity seen in 4-MuGP assay of various fractions of post-binding medium ruled out this possibility. The semi-preparative column is able to absorb all of the GBA-PTD4 and non-specific β-glycosidases within at least 3 L of crude induction medium.

The amount of protein obtained from this purification step, 10 mg, is still over 10X more protein collected during smaller scale HIC purification steps, which was less than 1 mg. Despite the low yield of this purification, using a semi preparative column is still an effective way to scale-up GBA-PTD4 partial purification.

4.2 GBA-PTD4 Purification by GFC

After separating recombinant GBA-PTD4 from endogenous *P. pastoris* proteins using differences in hydrophobicity, further enzyme purification was established using size exclusion chromatography with a gel filtration column. Gel filtration chromatography was utilized by Grabowski and Dagan (1984) as a second purification step for native GBA after HIC analysis.

Gel filtration chromatography was used to further purify enzyme preparations obtained from both cholate and ethylene glycol HIC elution; Figure 3.10 and Figure 3.11 show the enzymatic activity of eluted fractions using the 4-MuGP substrate of cholate

HIC/GFC purified and ethylene glycol HIC/GFC purified samples respectively. When this purification step was undergone using cholate partially purified preparation as the sample, activity analysis determined that GBA-PTD4 was not eluted as a single protein peak, rather as various peaks over approximately 30 ml buffer. We surmised that aggregation of the enzyme creates many different sized particles depending upon the volume of the cholate micelles, which leads to multiple peaks in protein activity upon size exclusion chromatography elution. Also, silver stain analysis of GFC purified preparations show many prominent protein species but there is not a significant band apparent at the expected size of GBA (Figure 3.12). Although the purity of GBA-PTD4 is much higher in these preparations as compared to HIC partially purified GBA-PTD4, the purified fractions were not homogenous nor did they have monomeric GBA-PTD4 as the major species.

Decreased aggregation of protein due to using ethylene glycol for HIC elution had the potential to improve GFC purification studies. Having the protein predominantly in its monomeric form and not associated with cholate micelles was predicted to replace the multiple peaks of enzyme elution through size exclusion with one major peak of active protein. Figure 3.11 shows the enzyme activity of elution fractions with 4-MuGP substrate from GFC purification using ethylene glycol partially purified GBA-PTD4 as a sample; in this elution, only one protein peak with a broad base is seen, compared to the multiple peaks seen with this procedure following cholate HIC elution. The elution volume with which GBA activity is present is slightly decreased using ethylene glycol samples as compared to cholate samples (approximately 25 ml compared with 20 ml), and the quality of fractions is improved. Upon observation of activity profile in Figure

3.11 and area calculations using ImageJ software, approximately 50% of the GBA-PTD4 is being eluted as the major part of the peak at the 55-60 ml total elution volume mark, as compared to approximately 30% in the major peak seen in Figure 3.10. The maximum peak in activity was also higher for the post-ethylene glycol sample, at 1100 Afu compared to 800 Afu in the post-cholate sample. We attribute these improvements to the decreased aggregation seen in the post-ethylene glycol HIC samples through the western blots, which would mean a greater percentage of the GBA-PTD4 protein would be of identical size (in monomeric form) and therefore will elute from a size exclusion column in a smaller volume and with higher resolution. Another difference noted between GFC runs with samples of post-cholate HIC and post-ethylene glycol HIC was the point at which the entire GBA activity peak was eluted from the column; in the post-cholate run negligible enzyme activity was detected in fractions before approximately 55 ml total elution volume, whereas in the post-ethylene glycol run GBA appeared to begin elution at approximately 45 ml total elution volume. This can be explained by the difference in ethylene glycol concentration of the running buffers, which was substantially less in the post-cholate run (15%) than the post-ethylene glycol run (55%). The enzyme was already dissolved in 55% ethylene glycol after the HIC purification in the latter, and because of its apparent stabilizing properties and anti-freeze ability it was determined that the increased concentration should be maintained during GFC purification. Because ethylene glycol minimizes mild hydrophobic interactions between proteins and purification matrices (Queiroz, *et al*. 2001; Ray 1969), an increased concentration would decrease the weak, non-specific interactions between proteins in the partially purified sample and gel

filtration column, making all proteins elute at an earlier volume than with the standard 15% ethylene glycol concentration in the running buffer.

An improvement on the extent of purification following GFC can be detected through silver stain analysis; Figure 3.12 and Figure 3.13 show a comparison of silver stain analyses of GFC purified preparations using cholate HIC partially purified GBA-PTD4 as a sample and ethylene glycol HIC partially purified GBA-PTD4 as a sample. While GBA-PTD4 does not appear to be the major product after cholate HIC and GFC purification steps, there is a marked improvement with the ethylene glycol HIC and GFC purification. The strongest band in each of the samples is approximately 67 kDa, the size of GBA, which also corresponds to the approximate size of the GBA specific band seen through western blotting (Figure 3.14). There is a slightly smaller protein product; since the protein is close in size to GBA-PTD4 as shown by SDS-PAGE analysis, we believe that it is an endogenous protein from *P. pastoris* that is co-purified with GBA-PTD4 during size exclusion purification. This protein is likely to share similar hydrophobic properties with GBA as well, since it must have been co-purified with GBA-PTD4 during hydrophobic interaction purification, although this cannot be confirmed as this protein has yet to be identified. Band intensity analysis with ImageJ software was utilized to compare the relative amounts of these two major products within each of the GFC purified samples and get a rough quantification of GBA-PTD4 purity (Figure 3.13 silver stain image was used for this estimation); calculated intensities estimated that GBA-PTD4 was the most pure in sample 2, where the predicted GBA protein band accounted for 76% of the protein in the sample, followed closely by 70% and 63% in samples 3 and 1 respectively. Although the unidentified *P. pastoris* protein is a significant by-product of

purification, it still makes up a small amount of the total protein content, especially in samples 2 and 3 out of the three GFC purified pooled and concentrated fractions. The implications of contamination of this protein in GBA-PTD4 preparations cannot be fully elucidated without knowledge of what the protein is and its properties. Certainly if recombinant GBA-PTD4 expressed in *P. pastoris* were used for therapeutics the full characterization of this contaminant protein and a method of removal would be essential. Because of the characteristics it shares with GBA, namely size and hydrophobicity, a different method of purification may need to be employed either in concert with the two described here or as a replacement method; perhaps the substrate affinity chromatography or immunoaffinity chromatography used in previous studies to purify the native enzyme should be explored (Grabowski and Dagan 1984; Aerts *et al*. 1986). Other protein bands produced by the silver stain are faint, indicating that these trace contaminants are present in a very low concentration. Judging by the various sizes of the proteins observed by SDS-PAGE analysis, there is the possibility that these are protein contaminates from buffers or equipment used throughout the purification procedure rather than *P. pastoris* proteins co-purified along with GBA-PTD4.

The approximate recovery of this step was calculated by band intensity comparisons in immunoblot analysis, and was 6.9% of the amount of HIC-partially purified GBA loaded onto the GFC column (Table 3.2). A total of approximately 500μg of GBA-PTD4 was collected, as compared with 5 μg (approximately 2% recovery) collected from a GFC following small scale HIC purification done previously in our lab (Goebl 2010). We believe that handling and concentration of enzyme samples contribute significantly to the low percentage of recovery.

As mentioned previously, ethylene glycol seems to have a stabilizing effect on our enzyme samples, and previous reports indicate that storage at temperatures of 0 to -20˚C in various concentrations of ethylene glycol kept GBA intact and active for at least several weeks (Grabowski and Dagan 1984; Aerts *et al*. 1986). We found that once GBA-PTD4 was in a near homogenous state, enzyme activity dropped rapidly, even with the addition of a reduction agent to keep disulfide bonds intact. Previous work with native GBA enzyme for therapeutic uses has indicated that the addition of human serum albumin to final preparations increases the stabilization of GBA enzyme (Barton *et al*. 1990). Investigations into additives to final GBA-PTD4 preparations will be helpful to yield similar affects on enzyme activity without compromising cellular uptake and therapeutic studies, because the enzyme does appear to be more stable in a heterogeneous preparation.

4.3 Analysis of commercial antibodies for immunoaffinity chromatography

As mentioned previously, an alternative method for purification of GBA-PTD4 from *P. pastoris* media would be beneficial to this project in multiple ways. First of all, the current purification methods fail to separate one endogenous yeast protein from GBA-PTD4 because of the similarity in hydrophobic properties and size. Also, current methods fail to give a high yield of GBA-PTD4 recovery, where a new method may be able to increase the yield, possibly by minimizing the amount of enzyme handling.

Immunoaffinity chromatography (IAC) is one alternate option for the purification of recombinant GBA-PTD4. IAC can be used to purify target proteins by immobilizing antibodies which recognize the target to a stationary phase (Moser and Hage 2010). Once

the antibody has been fixed to the matrix support in a column, the antigen (in crude form) can be passed through the column where the protein of interest will bind specifically to antibody. Elution can be performed in various ways, for example, changes in pH or addition of a chaotropic agent to disrupt antibody/antigen binding are common methods of releasing desired molecules while keeping the column in a state where it can be regenerated. Berg *et al.* (2001) used a single step IAC for the purification of recombinant lysosomal enzyme α-mannosidase expressed in CHO cells with a 60% yield of protein, which was double that from purification using combined methods of ultrafiltration, anion-exchange chromatography and gel filtration chromatography. Additionally, native placental GBA was purified in a single step using IAC with an overall yield of 80% (Aerts *et al*. 1986). Furthermore, about 90% of the active GBA eluted from the column was present in the first 5 ml of eluate, which would decrease the amount of concentration needed for further applications. These past experiments made IAC purification of GBA-PTD4 an attractive option for this project.

To pursue this avenue, we contracted Abmart (Shanghai, China) to produce monoclonal mice antibodies specific to GBA. According to Moser and Hage (2010), both polyclonal and monoclonal antibodies can be used in IAC. With monoclonal antibodies, although the process to make them is tedious, a large amount of antibody can be generated which have well-defined specificity towards to the target protein. Also, by fusing a single antibody producing cell line with a carcinoma or myeloma cell line, a hybridoma cell line can be produced, which can be easily cultured and provides a long-term supply of antibody. Both of the examples of IAC purification mentioned earlier utilized monoclonal antibodies.

Antibodies received from China (as ascites fluid) were all directed against one epitope of GBA-PTD4, and all had a reported titre of 128K against the epitope peptide sequence. We collaborated with Dr. Terry Pearson's lab for the testing of each of the ascites samples. In Figure 3.15 and Figure 3.16 is ELISA data from 5 of the 6 ascites samples sent to us, combined with crude GBA-PTD4 *P. pastoris* medium as well as vector-only *P. pastoris* medium (as a negative control). The titre of each of the samples did not match the report of 128K given by Abmart, as the signal dropped sharply when diluted more than 1/400. This could be because the antibody is now being tested against not only a short epitope but the entire GBA-PTD4 protein. It was encouraging, however, to see some signal through ELISA, and prompted us to further evaluate each of the antibody samples. The negative control ELISA with *P. pastoris* medium devoid of GBA-PTD4 (as seen in Figure 3.1) was as expected, with lower signals than that in the ELISA with the GBA-PTD4 antigen. The less-intense signals seen in the negative control ELISA can be explained as background reactions, as the ascites fluids do not contain pure monoclonal antibody, rather a mixture of mouse antibodies which could react non-specifically with other *P. pastoris* proteins.

The next assay done for the ascites samples was a western blot, seen in Figure 3.17. Ascites samples 503-1 and 426-3 showed no signal at all on the western blot; this was curious because GBA-PTD4 present in the crude medium run on the SDS-PAGE gel would be denatured, and therefore the short sequence of the epitope would be exposed. Since other ascites fluid gave more interesting results, this was not investigated further. Ascites fluid 425-3 had a very high background signal, we predicted that this was due to something in the ascites fluid that reacted with a protein present in the skim milk used for

blocking the membrane during the western blot; the background was not diminished with more extensive washing procedures. Sample 428-4 had a band at approximately the correct size for GBA-PTD4 (Figure 3.17 **c**), as well as a band of higher molecular weight. The higher band may be another form of GBA-PTD4 (perhaps with a different glycosylation pattern or a dimer, since it is approximately twice the size of GBA) or it could be another protein altogether which also reacts with the antibody. Non-specific binding of *P. pastoris* proteins by the monoclonal antibodies would not be completely detrimental to the ultimate application of IAC. Though it would be desirable to have the antibodies specifically bind to GBA-PTD4 for one-step purification, another protein co-purified with GBA-PTD4 could be eliminated through other purification procedures such as GFC or HIC. This made ascites fluid 428-4 a candidate for further analysis. Samples 520-6 and 422-4 also had signals which appeared as a single band. These were slightly larger than expected at approximately 100 kDa. Again, we hypothesized that this may be a different isoform of GBA or perhaps this apparent difference in size was due to the SDS-PAGE gel. In either case, these samples were also candidates for further analysis.

The three candidate ascites fluid samples, 428-4, 422-4 and 520-6, along with the purified monoclonal anti-GBA antibody from Abnova Corporation (Taipei City, Taiwan), were further tested for compatibility with the IAC purification application. The final test of these antibodies would be to see if they could pull the complete, folded GBA-PTD4 protein out of crude *P. pastoris* media. This was accomplished with an immunoprecipitation or "pull down" experiment using magnetic beads. The proteins pulled down using each of the antibodies were run on SDS-PAGE, transferred to a PVDF membrane and probed with their respective antibody; each of the three sample ascites

fluids showed a band that was approximately 67 kDa (Figure 3.18). This band has yet to be confirmed as GBA-PTD4 (i.e. by mass spectrometry), but current efforts are working towards that end. Confirmation of the protein pulled down being our recombinant GBA-PTD4 would prompt us to order the hybridoma cell line for one or all of these three samples, and use them to create an immunoaffinity chromatography column. Interestingly, the pure monoclonal antibody which works so well for western blots failed to pull GBA-PTD4 out of crude *P. pastoris* media. This antibody must bind to a section of the denatured GBA protein which, when folded, is located within the hydrophobic core of the protein. Success in this method of purification will help in the continuation of this research.

4.4 Construction of a GBA- only control cell line

4.4.1 Overview of control construct project

In further investigations with purified GBA-PTD4, the ability of the fusion protein to cross cell membranes will be assessed, first through uptake studies using *in vitro* cultures of human skin fibroblasts obtained from GD patients. For these trials, it would be prudent to include a negative control protein which does not contain a transduction domain; this way, effectiveness in crossing cell membranes can be assessed due only to the PTD4 transduction domain, and any inherent properties that the GBA enzyme has when expressed in *P. pastoris* would be controlled for. To this end, we began to construct a *P. pastoris* cell line which would express human recombinant GBA without a fused transduction domain.

4.4.2 *P. pastoris* transfection

Once necessary cloning steps were taken to insert *GBA* into a pPIC9K expression vector (example in Figure 3.19), the ligation product was linearized and transfected by electroporation into YA208 *P. pastoris* electrocompetent cells in the same way that the *GBA*- PTD4 construct was done previously in our lab.

When inserting our transgene into the *P. pastoris* genome, there were implications for the resulting phenotype of the cell line that we had to take into account. Reviews by Cereghino and Cregg (2000) and Macauley-Patrick *et al*. (2005) describe two possible phenotypes for the yeast concerning methanol utilization, methanol utilization plus (Mut^+) and methanol utilization slow (Mut^S). Although most current research utilizes the Mut^+ phenotype for the expression of heterologous proteins, Mut^S phenotype strains can be optimal for expression systems by producing higher levels of the recombinant protein, as well as requiring a decreased amount of methanol for large scale culture inductions (i.e. fermentation systems). GBA- PTD4 was produced previously in both types, and expression was found to be better in Mut^S cell lines (Goebl 2010). It was predicted that the slower growth rate on methanol frees up more cellular transcriptional and translational equipment for production of the transgene and allows more time for proper post-translational modifications of recombinant GBA-PTD4. Also, a slower growth rate would decrease the amount of cell lysis in each of the cultures, whereas the increased growth rate in Mut^+ cultures would create a higher cell death rate, and therefore increased cell lysis. It was observed that after approximately 48 hrs of induction, increased cell

lysis released more proteolytic enzymes, which lead to increased degradation of GBA-PTD4. Using a Mut^S cell line for expression would decrease the proteolytic degradation due to cell lysis, leading to a longer optimal induction time, although protease inhibitors added to the medium would also help if degradation continued to be a problem. Previous successes in producing GBA-PTD4 in a Mut^S cell line prompted us to hypothesize that similar results would be seen with expression studies of GBA-only control constructs; however we set out to create cell lines of both phenotypes as a comparison to confirm this theory.

The two different phenotypes are created according to the way the transgene is inserted into the genome (Higgins and Cregg 1998). A single gene insertion of the recombinant gene at the 5' *AOXI* region (with homologous region on the pPIC9K expression vector) leads to insertion of the *GBA* gene just upstream of the endogenous *AOXI* gene; because in this instance *AOXI* is still intact and active, these cell lines will have the ability to grow normally on methanol and thus display the Mut^+ phenotype. An example of a gene insertion event is demonstrated in Supplementary Figure 2. Multiple insertions of the transgene are possible, which creates higher expression levels. For this reason, clones can be screened for increased copies of the kanamycin resistance gene which is included in the pPIC9K expression cassette.

Gene replacement can also take place during transfection, where homologous recombination happens at both the 3' *AOXI* region and 5' *AOXI* region. Gene replacement disrupts *AOXI* and these cell lines will not express this protein which is crucial to methanol metabolism. *P. pastoris* has another copy of the alcohol oxidase gene, *AOXII*, which shares 90% homology with *AOXI* and produces a functional enzyme

(Cregg *et al*. 1989). The *AOXII* gene, however, is under a weaker promoter than *AOXI* and consequentially produces 10-20 times less alcohol oxidase enzyme (Macauley-Patrick *et al*. 2005). Cell lines which have undergone a gene replacement of *AOXI* upon transfection will be able to grow on methanol, but because they have to rely on the less productive *AOXII* gene, their growth will be inhibited and therefore they will display the Mut^S phenotype. Multiple insert clones of this phenotype can be produced as well.

Variable linearization of the expression vector can promote either type of transgene integration into the yeast genome (Cereghino and Cregg 2000). A single digestion point with the SacI restriction enzyme promotes single gene replacement at 3' *AOXI* and therefore Mut^+ phenotype of resulting cell lines. The single crossover event happens at high frequencies, and 50-80% of resulting transformants will have this type of integration. The vector can also be digested by BglII, which has two restriction sites present in pPIC9K so as to free the expression cassette from the rest of the vector. This type of digestion is said to promote an increased frequency of gene replacement integration events, although these still occur relatively low frequency of approximately 10-20 % in this integration scenario. We employed both types of vector digestion, in order to obtain both resulting phenotypes. Screening of phenotypes as in Figure 3.21 show the low frequency of Mut^S clones expected as compared to Mut^+ cell lines.

4.4.3 Screening for multiple inserts and Mut^+/Mut^S phenotype

His^+ transformants were all assumed to have at least one copy of the expression cassette containing *GBA* because of their ability to grow on histidine deficient medium.

GS115 *P. pastoris* cell lines are *his4* (histidine dehydrogenase gene) mutants, and therefore cannot produce their own histidine in the absence of the inserted *HIS4* provided by the pPIC9K expression cassette (Cereghino and Cregg 2000). Transformants with multiple copies of the expression cassette have the ability to produce superior levels of expressed recombinant enzyme, and spontaneously occur at low frequencies of approximately 1-10% of transformants (Cereghino and Cregg 2000). Because of the low frequency of clones with 2 or more copies of the transgene, all His^+ transformants were collected by suspension in water to make a homogenous cell mixture. This way, a larger number of cells could be plated on Geneticin®, and allowed us to screen many clones at once. We found that growing transformants on 0.75 mg/ml Geneticin® directly after growth on MD plates as implied by the Invitrogen manual very rarely yielded any clones appearing to have 2 or more copies of the expression cassette. We hypothesized that this may be due to a lag time in expression, and clones with multiple insertions would succumb to cell death before appropriate levels of expression of the kanamycin resistance gene could be obtained. The pPIC9K Invitrogen manual suggests that geneticin not be used as an initial screening method for transformants for this very reason, insinuating that transformants may die due to low expression levels, as expression is under control of the weak kanamycin resistance native bacterial promoter. It stands to reason that the same problem may have been preventing us from finding clones with multiple copy inserts. To correct this problem, clones were first grown on lower concentrations of Geneticin® (0.25- 0.5 mg/ml), and then exposed to a higher concentration of 0.75 mg/ml; this allowed transformants time for appropriate expression of the kanamycin resistance gene

before exposure to a higher concentration of Geneticin®, which resulted in the selection of clones predicted to have more than 2 copies of the expression cassette.

Screening for Mut^+/Mut^S phenotypes was also more difficult than outlined in the Invitrogen manual. Clones which grew well on Geneticin® and were therefore ascertained to have multiple copies of the expression cassette were then grown on both a dextrose and methanol carbon source. Initially, all clones grown on methanol appeared to have slower growth than those with the dextrose carbon source. Although Invitrogen did not describe this phenomenon, it is validated by the fact that even in Mut^+ clones, there would be an initial lag in expression of metabolic enzymes, including alcohol oxidase I, as methanol is the inducer in this system. With growth on dextrose, comparatively, the metabolic enzymes would already be present in high levels as initial growth on both MD and YPD medium utilized dextrose as a carbon source. In spite of the difference in growth rate of all clones on dextrose versus methanol medium, scoring of growth after approximately 48 hrs yielded a few transformants which grew noticeably slower on methanol than other clones, as show in Figure 3.21, and these were categorized phenotypically as Mut^S transformants. We found this categorization, however, slightly ambiguous at times, and it was difficult to assess the reliability of results obtained by this qualitative method.

A second way to confirm Mut^+/Mut^S status is PCR amplification of genomic DNA using primers which anneal to the 5' and 3' *AOXI* sequence. In Mut^+ clones, where endogenous *AOXI* is present along with inserted recombinant DNA, two PCR products can be detected after amplification with these primers. Mut^S clones, on the other hand, have had endogenous *AOXI* replaced by the transgene, and therefore only one product

would be amplified. An example of this type of direct yeast PCR screening can be seen in Figure 3.20.

4.4.4 Trial GBA expression studies

After confirmation of clone phenotype, a trial expression study was done with selected Mut^+ and Mut^S clones to compare production of the GBA enzyme. Figure 3.22 shows a western blot of crude medium from one of each type of cell line, probed with a GBA specific mAb to observe relative protein levels in each. As predicted by previous *P. pastoris* expression studies in our lab (to produce recombinant GBA-PTD4), the Mut^S clone had a higher concentration of GBA in the crude medium, as seen by the more intense band present in that sample on the western blot. Degradation of GBA is evident in the Mut^S clone, which is also in agreement with GBA-PTD4 studies. We used a 48 hr induction period for this trial expression study, as this has been proven optimal in the past (Goebl 2010), with the best protein production and the least degradation. Time point expression studies will be used in the future to confirm this.

One detail to note is that the condition with which expression is carried out is different for Mut^S as opposed to Mut^+. The normal growth rate of Mut^+ clones on methanol obliges us to have a much more diluted cell culture than Mut^S; this provides the cells with enough methanol to maintain metabolic levels. The total culture volume is five times larger in Mut^+ than in Mut^S, which means that a sample of crude medium will contain GBA which is more diluted; in this way, it is possible the assumption that GBA is not being produced at levels equal to that in Mut^S cell strains is incorrect, since it may be

just the dilution that causes a less intense band on the western blot. There are, however, advantages to using a Mut^S strain, such as the decreased amount of methanol needed for fermentor cultures, as previously mentioned. Also, increased concentration of GBA in the crude medium is advantageous during purification steps, where media loading onto the purification column is time consuming. Although further expression analysis with time point studies and RT-PCR should be carried out to confirm these results, I believe that a 48 hr induction of the Mut^S cell line created in this study will be sufficient for large scale production of GBA for purification studies. Further scaling up of enzyme expression will be possible with a fermentor system.

4.5 Future directions and conclusions

Current expression methods for producing GBA-PTD4 in *P. pastoris* are not ideal for semi-preparative or preparative procedures. To generate enough crude medium for one purification run is a tedious process, as multiple shake-flask cultures are grown and induced at the same time, and this process is repeated for a number of weeks. For each culture round, we use six shake-flask cultures, producing approximately 800 ml of crude induction medium with a final OD_{600} anywhere between 10 and 30; we are looking into scaling-up the expression by using a fermentation system. *P. pastoris* is an ideal organism for expression of heterologous proteins in fermentation cultures because the mineral media is economical and well-defined (Cereghino *et al*. 2002). Under optimal conditions provided by a fermentation system, such as control over pH and oxygen levels, culture OD_{600} exceeding 500 has been reported previously. Increased cell density

and therefore increased expression would lend to the efficiency of the production of GBA-PTD4, making further optimization of purification protocols more attainable and increasing final protein yields.

Another future direction we are currently exploring is an alternate method of purification. As mentioned, there is an endogenous *P. pastoris* protein being co-purified with GBA-PTD4 due to the limitations of current purification methods being employed; namely, the un-identified contaminant protein shares similar hydrophobic properties with GBA and is of a similar size, making HIC and GFC purification methods unable to separate it and provide an entirely homogenous preparation. We are exploring immunoaffinity chromatography as another method of purification of GBA-PTD4, either by itself or in tandem with one of the current purification procedures. IAC has been used to purify native GBA in the past with a reported 81% yield (Aerts *et al*. 1986), which would make this a suitable option for purification of a recombinant protein. As discussed, we have obtained six ascites fluid samples which have been analyzed for suitability for IAC, three of which have shown positive results so far. The near future may include ordering hybridoma cell lines producing one or more of these monoclonal antibodies, and further antibody production and trial IAC purification studies.

We have attempted a few cellular uptake studies with human fibroblasts obtained from GD patients previously, though these tests proved to be less than effective in determining PTD4 efficiency for cell membrane translocation. We believe that the low productivity of GBA-PTD4 in shake-flask cultures and the inefficiency of the current purification methods are responsible for non-conclusive data in this area. By the end of the purification method, what little enzyme is collected is unstable and has lost activity

from excessive handling during purification and analysis. Utilizing a fermentation system for high-yield expression and finding a more efficient purification method will enable conclusive data from *in vitro* cellular uptake studies. This also requires the large scale expression and purification of the GBA- only control construct.

This study provides a method for large scale expression and semi-preparative purification of GBA-PTD4 by building on previous expression and purification work completed in this lab. The present purification methods have been optimized to decrease the amount of aggregation of enzyme in the first purification step (HIC), thereby increasing homogeneity of GBA-PTD4 after the final purification step (GFC). During the optimization of the purification procedure, ethylene glycol has proven to be an effective elution agent for our recombinant enzyme. This method produced GBA-PTD4 preparations with only one major contaminating protein species, a large improvement from previous trials both in this study and previously. Future efforts to improve efficiency at both the expression and purification levels will lead to downstream investigations for the determination of the value of GBA-PTD4 as a therapeutic enzyme. Although there is still much work to be accomplished in the entire scope of this project, this study lays a strong foundation for investigations towards the treatment of the neurological symptoms of Gaucher's disease.

Bibliography

Aerts, J.M.F.G., W.E. Donker-Koopman, G.J. Murray, J.A. Barranger, J.M. Tager, and A.W. Schram. 1986. 'A Procedure for the Rapid Purification in High Yield of Human Glucocerebrosidase Using Immunoaffinity Chromatography with Monoclonal Antibodies'. *Analytical Biochemistry* 154 (2): 655–663.

Aerts, Johannes M. F. G., Carla E. M. Hollak, Rolf G. Boot, Johanna E. M. Groener, and Mario Maas. 2006. 'Substrate Reduction Therapy of Glycosphingolipid Storage Disorders'. *Journal of Inherited Metabolic Disease* 29 (2-3) (April): 449–456. doi:10.1007/s10545-006-0272-5.

Alberts, Bruce, Alexander Johnson, Julian Lewis, Martin Raff, Keith Roberts, and Peter Walter. 2002. *Molecular Biology of the Cell*. 4th ed. New York: Garland Science.

Atrian, Sílvia, Eduardo López-Viñas, Paulino Gómez-Puertas, Amparo Chabás, Lluïsa Vilageliu, and Daniel Grinberg. 2008. 'An Evolutionary and Structure-based Docking Model for Glucocerebrosidase–saposin C and Glucocerebrosidase–substrate interactions—Relevance for Gaucher Disease'. *Proteins: Structure, Function, and Bioinformatics* 70 (3) (February 15): 882–891. doi:10.1002/prot.21554.

Ballabh, P., A. Braun, and M. Nedergaard. 2004. 'The Blood-brain Barrier: An Overview:: Structure, Regulation, and Clinical Implications'. *Neurobiology of Disease* 16 (1): 1–13.

Barton, N.W., F.S. Furbish, G.J. Murray, M. Garfield, and R.O. Brady. 1990. 'Therapeutic Response to Intravenous Infusions of Glucocerebrosidase in a Patient with Gaucher Disease'. *Proceedings of the National Academy of Sciences* 87 (5): 1913.

Berg, T, B King, P J Meikle, Nilssen Ø, O K Tollersrud, and J J Hopwood. 2001. 'Purification and Characterization of Recombinant Human Lysosomal Alpha-mannosidase'. *Molecular Genetics and Metabolism* 73 (1) (May): 18–29. doi:10.1006/mgme.2001.3173.

Berg-Fussman, A., M. E. Grace, Y. Ioannou, and G. A. Grabowski. 1993. 'Human Acid Beta-glucosidase. N-glycosylation Site Occupancy and the Effect of Glycosylation on Enzymatic Activity.' *Journal of Biological Chemistry* 268 (20): 14861–14866.

Beutler, Ernest. 2006. 'Lysosomal Storage Diseases: Natural History and Ethical and Economic Aspects'. *Molecular Genetics and Metabolism* 88 (3) (July): 208–215. doi:10.1016/j.ymgme.2006.01.010.

Beutler, Ernest, and Terri Gelbart. 1996. ‘Glucocerebrosidase (Gaucher Disease)’. *Human Mutation* 8 (3) (January 1): 207–213. doi:10.1002/(SICI)1098-1004(1996)8:3<207::AID-HUMU2>3.0.CO;2-6.

Boado, Ruben J. 2007. ‘Blood–brain Barrier Transport of Non-viral Gene and RNAi Therapeutics’. *Pharmaceutical Research* 24 (9) (June 8): 1772–1787. doi:10.1007/s11095-007-9321-5.

Boven, L.A., M. van Meurs, R.G. Boot, A. Mehta, L. Boon, J.M. Aerts, and J.D. Laman. 2004. ‘Gaucher Cells Demonstrate a Distinct Macrophage Phenotype and Resemble Alternatively Activated Macrophages’. *American Journal of Clinical Pathology* 122 (3): 359–369.

Brady, R.O. 2003. ‘Enzyme Replacement Therapy: Conception, Chaos and Culmination’. *Philosophical Transactions of the Royal Society of London. Series B: Biological Sciences* 358 (1433): 915.

Cabrera-Salazar, M.A., S.D. Bercury, R.J. Ziegler, J. Marshall, B.L. Hodges, W.-L. Chuang, J. Pacheco, L. Li, S.H. Cheng, and R.K. Scheule. 2010. ‘Intracerebroventricular Delivery of Glucocerebrosidase Reduces Substrates and Increases Lifespan in a Mouse Model of Neuronopathic Gaucher Disease’. *Experimental Neurology* 225 (2) (October): 436–444. doi:10.1016/j.expneurol.2010.07.023.

Cardoso, Filipa Lourenço, Dora Brites, and Maria Alexandra Brito. 2010. ‘Looking at the Blood–brain Barrier: Molecular Anatomy and Possible Investigation Approaches’. *Brain Research Reviews* 64 (2) (September 24): 328–363. doi:10.1016/j.brainresrev.2010.05.003.

Cereghino, Geoff P.Lin, Joan Lin Cereghino, Christine Ilgen, and James M Cregg. 2002. ‘Production of Recombinant Proteins in Fermenter Cultures of the Yeast Pichia Pastoris’. *Current Opinion in Biotechnology* 13 (4) (August 1): 329–332. doi:10.1016/S0958-1669(02)00330-0.

Cereghino, Joan Lin, and James M Cregg. 2000. ‘Heterologous Protein Expression in the Methylotrophic Yeast Pichia Pastoris’. *FEMS Microbiology Reviews* 24 (1) (January 1): 45–66. doi:10.1111/j.1574-6976.2000.tb00532.x.

Chattopadhyay, A., and KG Harikumar. 1996. ‘Dependence of Critical Micelle Concentration of a Zwitterionic Detergent on Ionic Strength: Implications in Receptor Solubilization’. *FEBS Letters* 391 (1-2): 199–202.

Chen, Y., and L. Liu. 2011. ‘Modern Methods for Delivery of Drugs Across the Blood–brain Barrier’. *Advanced Drug Delivery Reviews*.

Cheng, SH, and AE Smith. 2003. ‘Gene Therapy Progress and Prospects: Gene Therapy of Lysosomal Storage Disorders’. *Gene Therapy* 10 (16): 1275–1281.

Cox, TM. 2001. ‘Gaucher Disease: Understanding the Molecular Pathogenesis of Sphingolipidoses’. *Journal of Inherited Metabolic Disease* 24: 107–123.

Cregg, J M, K R Madden, K J Barringer, G P Thill, and C A Stillman. 1989. ‘Functional Characterization of the Two Alcohol Oxidase Genes from the Yeast Pichia Pastoris.’ *Molecular and Cellular Biology* 9 (3) (March 1): 1316 –1323. doi:10.1128/MCB.9.3.1316.

Cregg, J.M., T.S. Vedvick, and W.C. Raschke. 1993. ‘Recent Advances in the Expression of Foreign Genes in Pichia Pastoris’. *Nature Biotechnology* 11 (8): 905–910.

Dallasta, Linda M., Liubomir A. Pisarov, James E. Esplen, Jonette V. Werley, Ashlee V. Moses, Jay A. Nelson, and Cristian L. Achim. 1999. ‘Blood-Brain Barrier Tight Junction Disruption in Human Immunodeficiency Virus-1 Encephalitis’. *The American Journal of Pathology* 155 (6) (December): 1915–1927.

Daly, Rachel, and Milton T. W Hearn. 2005. ‘Expression of Heterologous Proteins in Pichia Pastoris: a Useful Experimental Tool in Protein Engineering and Production’. *Journal of Molecular Recognition* 18 (2) (March 1): 119–138. doi:10.1002/jmr.687.

Doll, R.F., and F.I. Smith. 1993. ‘Regulation of Expression of the Gene Encoding Human Acid [beta]-glucosidase in Different Cell Types’. *Gene* 127 (2): 255–260.

Duchardt, F., M. Fotin-Mleczek, H. Schwarz, R. Fischer, and R. Brock. 2007. ‘A Comprehensive Model for the Cellular Uptake of Cationic Cell-penetrating Peptides’. *Traffic* 8 (7): 848–866.

Durand, Patrick, Pierre Lehn, Isabelle Callebaut, Sylvie Fabrega, Bernard Henrissat, and Jean-Paul Mornon. 1997. ‘Active-site Motifs of Lysosomal Acid Hydrolases: Invariant Features of Clan GH-A Glycosyl Hydrolases Deduced from Hydrophobic Cluster Analysis’. *Glycobiology* 7 (2) (February 1): 277 –284. doi:10.1093/glycob/7.2.277.

Durocher, Yves, and Michael Butler. 2009. ‘Expression Systems for Therapeutic Glycoprotein Production’. *Current Opinion in Biotechnology* 20 (6) (December): 700–707. doi:10.1016/j.copbio.2009.10.008.

Dvir, Hay, Michal Harel, Andrew A. McCarthy, Lilly Toker, Israel Silman, Anthony H. Futerman, and Joel L. Sussman. 2003. ‘X-ray Structure of Human Acid-β-glucosidase, the Defective Enzyme in Gaucher Disease’. *EMBO Reports* 4 (7) (June 3): 704–709. doi:10.1038/sj.embor.embor873.

ElAli, Ayman, and Dirk M Hermann. 2011. ‘ATP-Binding Cassette Transporters and Their Roles in Protecting the Brain’. *The Neuroscientist* 17 (4) (August 1): 423–436. doi:10.1177/1073858410391270.

Elstein, D., A. Abrahamov, I. Hadas-Halpern, and A. Zimran. 2001. 'Gaucher's Disease'. *Lancet* 358 (9278): 324–327.

Fawell, S, J Seery, Y Daikh, C Moore, L L Chen, B Pepinsky, and J Barsoum. 1994. 'Tat-mediated Delivery of Heterologous Proteins into Cells'. *Proceedings of the National Academy of Sciences* 91 (2) (January 18): 664 –668.

Frankel, Alan D., and Carl O. Pabo. 1988. 'Cellular Uptake of the Tat Protein from Human Immunodeficiency Virus'. *Cell* 55 (6) (December 23): 1189–1193. doi:10.1016/0092-8674(88)90263-2.

Furbish, F S, H E Blair, J. Shiloach, P G Pentchev, and R O Brady. 1977. 'Enzyme Replacement Therapy in Gaucher's Disease: Large-Scale Purification of Glucocerebrosidase Suitable for Human Administration'. *Proceedings of the National Academy of Sciences* 74 (8) (January 8): 3560–3563.

Futerman, A.H., and G. Van Meer. 2004. 'The Cell Biology of Lysosomal Storage Disorders'. *Nature Reviews Molecular Cell Biology* 5 (7): 554–565.

Goebl, April. 2010. 'An Approach to Treat Neurological Gaucher Disease: Expression and Purification of a Human Acid Beta Glucosidase- Protein Transduction Domain Fusion from Pichia Pastoris'. Masters, Victoria, BC: University of Victoria.

Grabowski, G.A., N.W. Barton, G. Pastores, J.M. Dambrosia, T.K. Banerjee, M.A. McKee, C. Parker, R. Schiffmann, S.C. Hill, and R.O. Brady. 1995. 'Enzyme Therapy in Type 1 Gaucher Disease: Comparative Efficacy of Mannose-terminated Glucocerebrosidase from Natural and Recombinant Sources'. *Annals of Internal Medicine* 122 (1): 33–39.

Grabowski, Gregory A., and Ariel Dagan. 1984. 'Human Lysosomal B-glucosidase: Purification by Affinity Chromatography'. *Analytical Biochemistry* 141 (1) (August 15): 267–279. doi:10.1016/0003-2697(84)90456-1.

Green, M., and P.M. Loewenstein. 1988. 'Autonomous Functional Domains of Chemically Synthesized Human Immunodeficiency Virus Tat Trans-activator Protein'. *Cell* 55 (6): 1179–1188.

Guggenbuhl, P., B. Grosbois, and G. Chalès. 2008. 'Gaucher Disease'. *Joint Bone Spine* 75 (2): 116–124.

Hamilton, S.R., and T.U. Gerngross. 2007. 'Glycosylation Engineering in Yeast: The Advent of Fully Humanized Yeast'. *Current Opinion in Biotechnology* 18 (5): 387–392.

He, G S, and G A Grabowski. 1992. 'Gaucher Disease: A G+1----A+1 IVS2 Splice Donor Site Mutation Causing Exon 2 Skipping in the Acid Beta-glucosidase mRNA.' *American Journal of Human Genetics* 51 (4) (October): 810–820.

Higgins, D.R., and J.M. Cregg. 1998. 'Introduction to Pichia Pastoris'. *Methods in Molecular Biology-clifton Then Totowa-* 103: 1–16.

Ho, A., S.R. Schwarze, S.J. Mermelstein, G. Waksman, and S.F. Dowdy. 2001. 'Synthetic Protein Transduction Domains: Enhanced Transduction Potential in Vitro and in Vivo'. *Cancer Research* 61 (2): 474.

Hollak, C.E.M., S. Vom Dahl, J.M.F.G. Aerts, N. Belmatoug, B. Bembi, Y. Cohen, T. Collin-Histed, et al. 2010. 'Force Majeure: Therapeutic Measures in Response to Restricted Supply of Imiglucerase (Cerezyme) for Patients with Gaucher Disease'. *Blood Cells, Molecules, and Diseases* 44 (1): 41–47.

Hruska, Kathleen S, Mary E LaMarca, C. Ronald Scott, and Ellen Sidransky. 2008. 'Gaucher Disease: Mutation and Polymorphism Spectrum in the Glucocerebrosidase Gene (GBA)'. *Human Mutation* 29 (5) (May 1): 567–583. doi:10.1002/humu.20676.

Im, M J, R P Riek, and R M Graham. 1990. 'A Novel Guanine Nucleotide-Binding Protein Coupled to the Alpha 1-Adrenergic Receptor. II. Purification, Characterization, and Reconstitution.' *Journal of Biological Chemistry* 265 (31) (May 11): 18952–18960.

Jiang, L., L. He, and M. Fountoulakis. 2004. 'Comparison of Protein Precipitation Methods for Sample Preparation Prior to Proteomic Analysis'. *Journal of Chromatography A* 1023 (2): 317–320.

Jmoudiak, Marina, and Anthony H Futerman. 2005. 'Gaucher Disease: Pathological Mechanisms and Modern Management'. *British Journal of Haematology* 129 (2) (April 1): 178–188. doi:10.1111/j.1365-2141.2004.05351.x.

Johnson, William, Robert Desnick, Donlin Long, Harvey Sharp, William Krivit, B. Brady, and Roscoe Brady. 1973. 'Intravenous Injection of Purified Hexosaminidase A into a Patient with Tay-Sachs Disease'. *Birth Defects: Original Article Series* 9 (2): 120–124.

Kaye, Edward M, M. David Ullman, Edward R Wilson, and John A Barranger. 1986. 'Type 2 and Type 3 Gaucher Disease: A Morphological and Biochemical Study'. *Annals of Neurology* 20 (2) (August 1): 223–230. doi:10.1002/ana.410200208.

Kitatani, K., J. Idkowiak-Baldys, and Y.A. Hannun. 2008. 'The Sphingolipid Salvage Pathway in Ceramide Metabolism and Signaling'. *Cellular Signalling* 20 (6): 1010–1018.

Koltun, Elena, Steven Richards, Vicky Chan, Jason Nachtigall, Hongwang Du, Kevin Noson, Adam Galan, et al. 2011. 'Discovery of a New Class of Glucosylceramide Synthase Inhibitors'. *Bioorganic & Medicinal Chemistry Letters* 21 (22) (November): 6773–6777. doi:10.1016/j.bmcl.2011.09.037.

Macauley-Patrick, S., M.L. Fazenda, B. McNeil, and L.M. Harvey. 2005. 'Heterologous Protein Production Using the Pichia Pastoris Expression System'. *Yeast* 22 (4): 249–270.

Mann, Giovanni E, David L Yudilevich, and Luis Sobrevia. 2003. 'Regulation of Amino Acid and Glucose Transporters in Endothelial and Smooth Muscle Cells'. *Physiological Reviews* 83 (1) (January 1): 183–252. doi:10.1152/physrev.00022.2002.

Mao, Rong, John F. O'Brien, Subramanya Rao, Eric Schmitt, Benjamin Roa, Gerald L. Feldman, W.Christine Spence, and Karen Snow. 2001. 'Identification of a 55-bp Deletion in the Glucocerebrosidase Gene in Gaucher Disease: Phenotypic Presentation and Implications for Mutation Detection Assays'. *Molecular Genetics and Metabolism* 72 (3) (March): 248–253. doi:10.1006/mgme.2000.3141.

Mattanovich, Diethard, Alexandra Graf, Johannes Stadlmann, Martin Dragosits, Andreas Redl, Michael Maurer, Martin Kleinheinz, Michael Sauer, Friedrich Altmann, and Brigitte Gasser. 2009. 'Genome, Secretome and Glucose Transport Highlight Unique Features of the Protein Production Host Pichia Pastoris'. *Microbial Cell Factories* 8 (1) (June 2): 29. doi:10.1186/1475-2859-8-29.

Moser, Annette C, and David S Hage. 2010. 'Immunoaffinity Chromatography: An Introduction to Applications and Recent Developments'. *Bioanalysis* 2 (4) (April): 769–790. doi:10.4155/bio.10.31.

Moyses, C. 2003. 'Substrate Reduction Therapy: Clinical Evaluation in Type 1 Gaucher Disease'. *Philosophical Transactions of the Royal Society of London. Series B: Biological Sciences* 358 (1433): 955–960.

Nemethy, George., and Ashoka. Ray. 1971. 'Micelle Formation by Nonionic Detergents in Water-ethylene Glycol Mixtures'. *J. Phys. Chem.* 75 (6): 809–815. doi:10.1021/j100676a015.

Ohashi, T, C M Hong, S Weiler, J M Tomich, J M Aerts, J M Tager, and J A Barranger. 1991. 'Characterization of Human Glucocerebrosidase from Different Mutant Alleles.' *Journal of Biological Chemistry* 266 (6) (February 25): 3661 –3667.

Pardridge, William M. 2006. 'Molecular Trojan Horses for Blood–brain Barrier Drug Delivery'. *Current Opinion in Pharmacology* 6 (5) (October): 494–500. doi:10.1016/j.coph.2006.06.001.

Park, J., J. Ryu, K. Kim, H.J. Lee, J.H. Bahn, K. Han, E.Y. Choi, K.S. Lee, H.Y. Kwon, and S.Y. Choi. 2002. 'Mutational Analysis of a Human Immunodeficiency Virus Type 1 Tat Protein Transduction Domain Which Is Required for Delivery of an Exogenous Protein into Mammalian Cells'. *Journal of General Virology* 83 (5): 1173.

Pastores, G.M. 2010. ‘Neuropathic Gaucher Disease’. *WMW Wiener Medizinische Wochenschrift* 160 (23): 605–608.

Pastores, G.M., and N.L. Barnett. 2003. ‘Substrate Reduction Therapy: Miglustat as a Remedy for Symptomatic Patients with Gaucher Disease Type 1’. *Expert Opinion on Investigational Drugs* 12 (2): 273–281.

Pelled, Dori, Selena Trajkovic-Bodennec, Emyr Lloyd-Evans, Ellen Sidransky, Raphael Schiffmann, and Anthony H. Futerman. 2005. ‘Enhanced Calcium Release in the Acute Neuronopathic Form of Gaucher Disease’. *Neurobiology of Disease* 18 (1) (February): 83–88. doi:10.1016/j.nbd.2004.09.004.

Phenix, Christopher P., Brian P. Rempel, Karen Colobong, Doris J. Doudet, Michael J. Adam, Lorne A. Clarke, and Stephen G. Withers. 2010. ‘Imaging of Enzyme Replacement Therapy Using PET’. *Proceedings of the National Academy of Sciences* 107 (24) (June 15): 10842 –10847. doi:10.1073/pnas.1003247107.

Queiroz, J.A., C.T. Tomaz, and J.M.S. Cabral. 2001. ‘Hydrophobic Interaction Chromatography of Proteins’. *Journal of Biotechnology* 87 (2) (May 4): 143–159. doi:10.1016/S0168-1656(01)00237-1.

Rahim, Ahad A., Andrew M. S. Wong, Klemens Hoefer, Suzanne M. K. Buckley, Citra N. Mattar, Seng H. Cheng, Jerry K. Y. Chan, Jonathan D. Cooper, and Simon N. Waddington. 2011. ‘Intravenous Administration of AAV2/9 to the Fetal and Neonatal Mouse Leads to Differential Targeting of CNS Cell Types and Extensive Transduction of the Nervous System’. *The FASEB Journal* 25 (10) (October 1): 3505 –3518. doi:10.1096/fj.11-182311.

Ray, Ashoka. 1969. ‘Micelle Formation in Pure Ethylene Glycol’. *J. Am. Chem. Soc.* 91 (23): 6511–6512. doi:10.1021/ja01051a069.

Roettger, Belinda F., and Michael R. Ladisch. 1989. ‘Hydrophobic Interaction Chromatography’. *Biotechnology Advances* 7 (1): 15–29. doi:10.1016/0734-9750(89)90901-4.

Sands, M.S., and B.L. Davidson. 2006. ‘Gene Therapy for Lysosomal Storage Diseases’. *Molecular Therapy* 13 (5): 839–849.

Sato, Y, and E Beutler. 1993. ‘Binding, Internalization, and Degradation of Mannose-terminated Glucocerebrosidase by Macrophages.’ *Journal of Clinical Investigation* 91 (May 1): 1909–1917. doi:10.1172/JCI116409.

Schueler, U., C. Kaneski, G. Murray, K. Sandhoff, and RO Brady. 2002. ‘Uptake of Mannose-terminal Glucocerebrosidase in Cultured Human Cholinergic and Dopaminergic Neuron Cell Lines’. *Neurochemical Research* 27 (4): 325–330.

Schwarze, Steven R., Alan Ho, Adamina Vocero-Akbani, and Steven F. Dowdy. 1999. 'In Vivo Protein Transduction: Delivery of a Biologically Active Protein into the Mouse'. *Science* 285 (5433): 1569 –1572. doi:10.1126/science.285.5433.1569.

Sethuraman, N., and T.A. Stadheim. 2006. 'Challenges in Therapeutic Glycoprotein Production'. *Current Opinion in Biotechnology* 17 (4): 341–346.

Shukla, Abhinav A, Joshua Peterson, Laura Sorge, Patsy Lewis, Shannon Thomas, and Steve Waugh. 2002. 'Preparative Purification of a Recombinant Protein by Hydrophobic Interaction Chromatography: Modulation of Selectivity by the Use of Chaotropic Additives'. *Biotechnology Progress* 18 (3) (January 1): 556–564. doi:10.1021/bp020038a.

Simon, Melissa J, Shan Gao, Woo Hyeun Kang, Scott Banta, and Barclay Morrison III. 2009. 'TAT-mediated Intracellular Protein Delivery to Primary Brain Cells Is Dependent on Glycosaminoglycan Expression'. *Biotechnology and Bioengineering* 104 (1) (September 1): 10–19. doi:10.1002/bit.22377.

Sinclair, Graham. 2001. 'Mutation Analysis,heterologous Expression, and Characterization of Human Glucocerebrosidase'. PhD, Victoria, BC: University of Victoria.

Tsuji, S, B M Martin, J A Barranger, B K Stubblefield, M E LaMarca, and E I Ginns. 1988. 'Genetic Heterogeneity in Type 1 Gaucher Disease: Multiple Genotypes in Ashkenazic and non-Ashkenazic Individuals'. *Proceedings of the National Academy of Sciences* 85 (7) (April 1): 2349 –2352.

Vervecken, W., V. Kaigorodov, N. Callewaert, S. Geysens, K. De Vusser, and R. Contreras. 2004. 'In Vivo Synthesis of Mammalian-like, Hybrid-type N-glycans in Pichia Pastoris'. *Applied and Environmental Microbiology* 70 (5): 2639–2646.

Weinreb, Neal J, Joel Charrow, Hans C Andersson, Paige Kaplan, Edwin H Kolodny, Pramod Mistry, Gregory Pastores, et al. 2002. 'Effectiveness of Enzyme Replacement Therapy in 1028 Patients with Type 1 Gaucher Disease After 2 to 5 Years of Treatment: a Report from the Gaucher Registry'. *The American Journal of Medicine* 113 (2) (August 1): 112–119. doi:10.1016/S0002-9343(02)01150-6.

Wetlaufer, D.B., and M.R. Koenigbauer. 1986. 'Surfactant-mediated Protein Hydrophobic-interaction Chromatography'. *Journal of Chromatography A* 359 (0): 55–60. doi:10.1016/0021-9673(86)80061-9.

Wraith, JE. 2006. 'Limitations of Enzyme Replacement Therapy: Current and Future'. *Journal of Inherited Metabolic Disease* 29 (2): 442–447.

You-Hai Xu, Li Jia, Brian Quinn, Matthew Zamzow, Keith Stringer, Bruce Aronow, Ying Sun, Wujuan Zhang, Kenneth D. R. Setchell, and Gregory A. Grabowski. 2011. 'Global Gene Expression Profile Progression in Gaucher Disease Mouse Models'. *BMC Genomics* 12 (1) (January): 1–23. doi:10.1186/1471-2164-12-20.

Zhang, Yun, and William M Pardridge. 2005. 'Delivery of β-Galactosidase to Mouse Brain via the Blood-Brain Barrier Transferrin Receptor'. *Journal of Pharmacology and Experimental Therapeutics* 313 (3) (June 1): 1075–1081. doi:10.1124/jpet.104.082974.

Zheng, Wei, Janak Padia, Daniel J. Urban, Ajit Jadhav, Ozlem Goker-Alpan, Anton Simeonov, Ehud Goldin, et al. 2007. 'Three Classes of Glucocerebrosidase Inhibitors Identified by Quantitative High-throughput Screening Are Chaperone Leads for Gaucher Disease'. *Proceedings of the National Academy of Sciences* 104 (32): 13192 –13197. doi:10.1073/pnas.0705637104.

Zuckerman, Shachar, Amnon Lahad, Amir Shmueli, Ari Zimran, Leah Peleg, Avi Orr-Urtreger, Ephrat Levy-Lahad, and Michal Sagi. 2007. 'Carrier Screening for Gaucher Disease'. *JAMA: The Journal of the American Medical Association* 298 (11): 1281 –1290. doi:10.1001/jama.298.11.1281.

Appendix:
Supplementary Figures and Tables

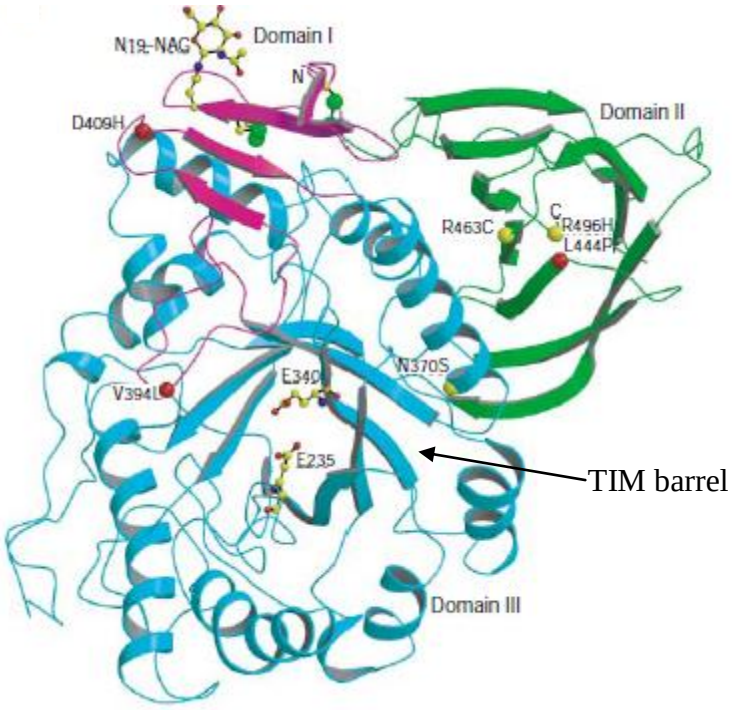

Supplementary Figure 1. Model of predicted structure of GBA.

Catalytic Domain III is shown in blue where Domains I and II are magenta and green, respectively. Ball and stick models of catalytic glutamic acid residues E340 and E235 are shown and TIM barrel structure of Domain III indicated. One N-glycosylation site is shown as a ball and stick model. Red and yellow balls indicate residues which are common mutation sites. Figure was adapted from Dvir *et al*. (2003).

Supplementary Table 1. Sequences and orientation for vector specific primers used for construction of a GBA only *P. pastoris* cell line.

5' *AOXI*/ 3' *AOXI* primer pair as well as α secretion signal are specific to the pPIC9K vector which M13 Fwd/ M13 Rvs primer pair is specific to the pGEM-T vector.

Primer name	Primer Sequence	Orientation
5' *AOXI*	**5'-** GACTGGTTCCAATTGACAAGC	Sense
3' *AOXI*	**5'-** GCAAATGGCATTCTGACATCC	Anti-sense
α secretion signal	**5'-** TACTATTGCCAGCATTGCTGC	Sense
M13 Fwd	**5'-** GTAAAACGACGGCCAGTG	Sense
M13 Rvs	**5'-** GGAAACAGCTATGACCATG	Anti- sense

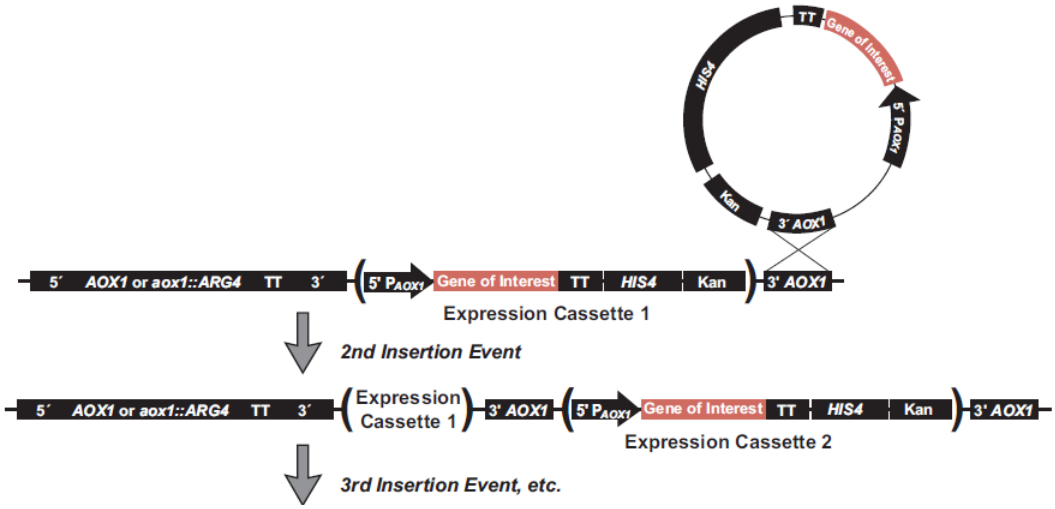

Supplementary Figure 2. Schematic representation of transgene integration into *P. pastoris* genome.

Integration is an example of homologous recombinantion at 3' *AOXI* site (single crossover event) which would produce a Mut^{+} clone, in contrast to a gene replacement which would produce a Mut^{S} clone. The GBA-only construct created in this work inserted the gene of interest at the 5' *AOXI* locus, as opposed to the 3'locus. Diagram also shows multiple insertion events, which create cell lines with multiple copies of the expression cassette, and therefore enhanced expression of recombinant protein. The indicated gene of interest in the case of this study would be *GBA*. This diagram was adapted from the pPIC9K manual (Invitrogen).